THE ADAPTIVE OPTIMISATION OF A WATER GAS SHIFT REACTOR

BY

ANDREW JOSEPH KISIEL, B.Sc. (Eng) (Chem Eng), A.C.G.I.

A thesis submitted for the
Degree of Doctor of Philosophy in the
Faculty of Engineering of the University
of London

Department of Chemical Engineering
Imperial College of Science and Technology
London, S.W. 7

October 1965

SUMMARY

Maximum seeking control systems have been widely discussed in recent years, but much of the work reported has been either on the theoretical analysis of idealised systems or on the performance of optimisers working on computer simulations. Relatively few experimental studies of optimiser performance on actual plant in the chemical or process industries have been reported. The present study investigates the performance of an on-line optimiser which seeks to reach and maintain by a sinusoidal perturbation method the best steady operating conditions of a small experimental water gas shift reactor.

The determination of the best settings of optimiser parameters was assisted by developing a mathematical model for the process. This was performed by finding experimentally the overall dynamic response of the process and fitting a two stage exponential model plus delay to these results. The description of the dynamics was then superimposed onto the steady state kinetic model, using a technique developed by Box and Jenkins. The kinetic model derived by Moe was found to be the most satisfactory of those considered, but in the simulation a simpler model due to Mars was used. The parameters in the models were fitted by the method of non-linear least squares.

The obtained mathematical model was used successfully to predict on-line results. Initially several objective functions were considered and the effect of the optimiser parameters on these objectives was investigated. The size of the problem was then reduced by fixing the

objective function as the loss in profit over a period of 20 minutes. The optimisation was performed with respect to the amplitude of the input perturbation signal and the gain of the feed-back signal while the frequency and phase shift of the input, as well as the constant of the high pass filter, were kept at fixed values.

ACKNOWLEDGEMENTS

I would like to express my gratitude and thanks to Dr. D. W. T. Rippin and Professor G. M. Jenkins for their constant advice, help and encouragement throughout the research and writing of the thesis. My thanks are also due to Professor K. G. Denbigh and Professor G. A. Barnard for making the project possible, by instigating the mutual cooperation between the Departments of Chemical Engineering and Statistics and to the Department of Industrial and Scientific Research for supporting the research. Esso Petroleum Co. Ltd. were most generous with their studentship and I would like to thank them very much for it.

I am indebted to the Chemical Engineering Department Workshops for help with the construction of the apparatus and in particular to Mr. B. Lucas and Mr. J. Bradman. Also I would like to thank Mr. R. J. Price for helping me construct and test the apparatus.

Finally I would like to acknowledge the great deal of work which my wife, Brigitte, has put into the production and typing of the thesis and the ever cheerful and encouraging face which she has presented during the many setbacks in the research.

To My Parents

NUMBERING SYSTEM

The numbers in the brackets refer to bibliography listed on pages 159 et seq.

Chapters and sections are numbered. For example 4.2. refers to chapter 4 section 2.

Tables and figures are also numbered separately for each chapter, an exception being chapter 2.

The equations are numbered separately for each chapter and section e.g. 3.2.5. refers to the 5th equation in section 2 of chapter 3.

LIST OF CONTENTS

CHAPTER I

CHAPTER II

CHAPTER IV

CHAPTER V

LIST OF DIAGRAMS

LIST OF TABLES

LIST OF SYMBOLS

a	Amplitude of the sinusoidal perturbation signal Constant used in the objective function - defined by 4.1.1.
a_i	Scaling factor for standardizing the variables - defined by 1.1.2. General constant
a_{ij}	Coefficient in the relationship between canonical and process variables defined by 1.4.5.
A, $A(K)$	Arrhenius constant in the rate constant expression
$A(KT)$	Arrhenius constant in the equilibrium constant expression
A_i	Cross-sectional area of the inside of the reactor
b	Constant used in the objective function - defined by 4.1.1.
b_i	General constant
B	Constant defined by 3.1.19.
B'	Constant defined by 3.1.22.
C, C_p	Value at time p of the objective function being optimized
C', C'_p	Value at time p of C after passing through the high pass filter
C_i	Molar concentration of gas i measured at time t and distance x along the reactor
$(C_i)_{in}$	Molar concentration of gas i in the inlet gas into the reactor
$(C_{CO})_{eq}$	Molar concentration of carbon monoxide which would occur if all the gas entering the reactor reacted to equilibrium
d	Internal diameter of the reactor
d_p	Mean particle diameter of the catalyst
D	Differential operator

E, $E(K)$	Activation energy for the forward reaction
$E(KT)$	Activation energy in the equilibrium constant expression
$F_{p,q,}(\alpha)$	"F" statistic at the α significance level with p and q degrees of freedom
g, $G_j(\omega)$	Gain of the system resulting from dynamics; j refers to the order of the term
G_T	Total volumetric flow rate of dry gases and steam at the exit from the reactor; measured at temperature T_1
$(G_i)_{in}$	Volumetric flow rate of gas i at the inlet to the reactor; measured at temperature T_1
$(G_{CO})_{eq}$	Volume of carbon monoxide which is removed by the reaction in unit time, if equilibrium conditions are reached with a given composition of entry gas; measured at temperature T_1
k, k_i	Rate constant for the forward reaction
k_o	Steady state value of k
$k(T)$	Rate constant for the forward reaction
K_T	Equilibrium constant at temperature T; defined by 3.2.8.
$L(p)$	Transfer function of the system
m_i	Coefficients in the relationship between canonical and process variables; defined by 1.1.7.
n	Number of perturbation cycles over which integration is performed
$n(t)$	Level of noise in the system at time t
N	Number of experimental points to which constants are fitted

p	Discrete time Number of parameters estimated
p'	Number of experimental points used to estimate the reproducibility of the experiments i.e. $= 2$
P_i	Partial pressure of component i at distance x along the reactor
P_T	Total pressure of gas at the inlet to the reactor
$(P_i)_{in}$	Partial pressure of component i at the inlet to the reactor
$(P_{CO})_{eq}$	Partial pressure of carbon monoxide which would occur if all the gas reacted to equilibrium
r	Reaction rate per unit reactor volume
R	Gas constant
S	Conversion of carbon monoxide to carbon dioxide and hydrogen, expressed as a percentage of the inlet flow of carbon monoxide
S'	Value of S after passing through the high pass filter
$S.S.$	Sum of squares of the discrepancies between observed and predicted values
$S.S._{min}$	Minimum value of S.S.
t	Continuous time
Δt	Sampling interval
T_a	Temperature in the reactor Period of the perturbation signal introduced into the system
T_l	Temperature at which the gas flows are measured i.e. room temperature
T_i, T'_i	Time constants used to describe the dynamics of the process
$T(i\omega)$	Frequency response function of the system
$T(p)$	Transfer function of the system

u	Linear velocity of the gases passing through the reactor; measured at the temperature in the reactor
u_o	Steady state value of u
W, W_{in}	Volumetric flow rate of steam at the inlet to the reactor; measured at temperature T_1
x	Distance measured along the length of the reactor
x_i	Level of a quantitative variable
x_o	Length of the reactor
$\bar{x}_i$	Coordinates of the local maximum of the response surface for a general second order relationship
X, X_t	Level of a general independent variable at time t
X_i	Level of a canonical variable
X_o	Steady state value of variable X_t
$X(t)$	Level of a general independent variable at time t
y	Number of litres of carbon monoxide converted per hour at distance x along the reactor
$y(t)$	Observed value of the response at time t
$y'(t)$	Value of $y(t)$ after passing through the high pass filter
Y, $Y(t)$	General dependent variable
z	Value of y at the exit from the reactor

α — Level of significance in the "F" test
Proportion of the total gas flow in the reactor, flowing inside the area whose diameter is $(d - 2 d_p)$

β_i — Coefficient of x_i in the general first order relationship

β_{ij} — Coefficient of $x_i x_j$ in the general second order relationship

β'_{ii} — Coefficient of a canonical variable

γ_o — Proportional control constant

γ_1 — Integral control constant

γ_{-1} — Derivative control constant

δ , δ_i — Amplitude of the sinusoidal perturbation signal

η , η_t — Real value of the objective function at time t

η_o — Steady state value of η_t

η_s — Value of η_t at the centre of a factorial design

$\eta(max)$ — Value of η_t at the origin of the canonical variable system

Θ — Expression defined by 3.3.7.

Θ_i — Angle corresponding to the delay in the system due to finite time of passage; i = 1 conversion, i = 2 steam flow rate

Θ_t — Level of X_t which corresponds to the maximum value of the response η_t

λ — Expression defined by 3.3.6. - Compensation for delay between steam and conversion signals

λ_h — Phase shift angle due to the high pass filter

λ_i — Constants used in the canonical transformation

μ Expression defined by 3.3.5.

$\mu_i(\omega)$ Gain of the useless component for a system which has transfer at the maximum

$\nu_i(\omega)$ Gain of the useful component for a system which has transfer at the maximum

ν_i Gain due to the dynamics of the system; i = 1 conversion i = 2 steam flow rate

ν_h Gain due to the high pass filter

π_{ij} Constants defined by the inverse transformation of 1.4.5.

σ^2 Variance of the experimental results

τ Constant of high pass filter

τ' Time delay between an independent variable X and the dependent variable Y

$\phi_i'(\omega)$ Phase shift angle used in the correlator signal for a system which has transfer at the maximum

$\phi_j(\omega)$ Phase shift angle resulting from the system dynamics - j refers to the order of the term

χ^2 Distribution of the sum of squares of a normal population

ψ Phase shift applied to the input signal before correlating with the output signal

ω Frequency of the sinusoidal signal

SUFFICES

CO	Carbon monoxide
CO_2	Carbon dioxide
H_2	Hydrogen
H_2O	Steam
N_2	Nitrogen
eq	Under equilibrium conditions
in	At the inlet to the reactor
o	At steady state
p, p-j	At time p, p-j
t	At time t

CHAPTER I

1.1. Static Optimisation

Box and Wilson can probably be called the originators of the ideas concerning optimisation of chemical processes. In 1951 (1) they published a method of maximising (or minimising) an objective function in the presence of error without a prior detailed knowledge of the relevant response surface. In large scale experimentation the error, or noise, is due to such causes as variation of the quality of feed stock, inlet stream flow variations and catalyst decay. They assumed that the experimenter is concerned with elucidating certain aspects of a functional relationship.

$$\eta = \phi (x_1, x_2 - - - - - - x_k) \qquad 1.1.1.$$

connecting a response, η, such as yield, with levels $x_1, - - - - - x_k$ of a group of k quantitative variables, or "factors", like temperature, concentration of reactants, pressure of the reaction. For simplicity of analysis these are "standardised" variables, in which the origin is taken to be the centre of the design and the units are fixed by the amounts the natural variables are changed in the design i.e.

$$x_i = \frac{T_i - T_s}{a_i} \qquad 1.1.2.$$

where T_i is the measured operating variable

T_s is the mean value of the operating variable in the design

a_i is equal to $T_i - T_s$ when $x_i = 1$

The skill of the experimenter enters into the choice of the range, a_i, so that the contribution to the response, η, from each of the factors x_i, is of the same order of magnitude. A large error in "a_i" can result in considerable

inefficiency of the design. Further, as is pointed out by Box (4), x_i may be a non-linear transformation, e.g. when the experimenter suspects a logarithmic dependence of the objective function on say the time of reaction, he may adopt the following form of the standardised variable, in order to linearise the relationship

$$x_i = \frac{2\,(\log_{10} T_i - \log_{10} T_s)}{\log_{10} a} + 1 \qquad 1.1.3.$$

The response is initially approximated by a first order relationship i.e.

$$\eta = \beta_0 + \beta_1 x_1 + \beta_2 x_2 \text{ - - - - - - - - - - } \beta_k x_k \qquad 1.1.4.$$

This is very reasonable if the current operating conditions are distant from the optimum, for in such a case the magnitude of the slope of the response surface is usually much greater than the size of the second order effects. A two level factorial or fractional factorial (2) experiment is then performed on the process, in order to determine the direction of steepest ascent of the response surface, about the given experimental point. The constants β_i are fitted by the method of least squares. Further experiments are conducted in this direction of steepest ascent, until the point corresponding to the maximum or minimum value of the response, η, is found. Centred at this point another factorial layout of experiments is performed and the direction of the new optimum slope is determined.

By inserting extra points in the factorial design it is possible to keep a rough check on the size of the curvature. When the calculated slope is no longer large compared with the neglected second order terms, the design is augmented by adding extra points, so as to allow the extraction of all the coefficients in the second order approximation of the form:

$$\eta = \beta_0 + \sum_{i=1}^{k} \beta_i x_i + \sum_{i=1}^{k} \sum_{j=1}^{k} \beta_{ij} x_i x_j \quad i \neq j \qquad 1.1.5.$$

The position of the points used to amplify the factorial design is determined by considerations of rotatability, namely that the response, η, is estimated with the same accuracy in all directions. Further progress towards the optimum is thus made and if necessary third and fourth order relationships for η can later be fitted. This, however, is seldom required, the only exception which has been quoted in the literature is concerned with some work on the flooding capacity of pulse columns (3).

The above approach represented a big breakthrough as far as industrial methods of optimisation were concerned. Prior to this time, the best operating conditions for industrial plants were found using the "one factor at the time" method which in general failed to find the most economic operating conditions for ridge shaped response surfaces. This was a major disadvantage, because a large number of chemical processes have ridge shaped response surfaces. The reason for this, which is discussed in Box's paper of 1954 (4), is that factors like temperature, concentration, pressure etc. are only regarded as natural because they can be measured conveniently. More fundamental variables, not directly measurable but in terms of which the system could be more realistically described e.g. frequency of a particular type of molecular collision, will often be a function of two or more natural variables. For this reason it is possible that several combinations of the natural variables could correspond to the optimum level of a fundamental variable.

The quickest approach to an optimum value on a response surface is obtained, when the contours of the surface are spherical, for in this case the radial direction will lead directly to the optimum. In general, however, the

response surface is not spherical and in this case the direction of quickest ascent towards the optimum is best found by a canonical transformation of the response contours. This is a linear transformation, which shifts the origin of the system to the centre of the design and rotates the coordinate axes so that they lie along the axes of the contours, representing the local topography of the response surface, i.e. the general second order equation 1.1.5. is changed to

$$\eta - \eta_s = \sum_{i=1}^{k} \beta_{ii} X_i^2 \qquad 1.1.6.$$

where η_s is the value of the response corresponding to the centre of the design and

$$X_i = \sum_{i=1}^{k} m_i x_i \qquad 1.1.7.$$

where m_i are constants.

Box in his 1954 (4) and 1955 (5) papers discusses the necessity to replicate, in order to average out the noise. Further, he points out, that knowledge of the local geography of the surface can be used to improve the effectiveness of the control of the process and should thus be acquired from the experiments. These two points characterise the statistical methods of steepest ascent. The rewards for careful design of experiments, which incorporates all the available knowledge of the system, are stressed. It is emphasized that the results obtained from the experiments should yield both the best operating conditions and at least a partial explanation of the mechanism of the process.

A useful summary of the statistical methods used for the design and analysis of the experiments in the above papers was given by Hunter (6). Another very useful paper dealing with the design and properties of fractional factorial experiments was published by Box and Hunter in 1961 (2).

The application of the above methods to industrial problems has begun to be widely used under the name "Evolutionary Operation" or "EVOP" and it has met with considerable success, especially in the U.S.A. (7). It introduced the idea that industrial processes should be run so as to generate not only the desired product but also information about how that product can be improved economically. Thus in his 1957 paper Box (8) made detailed suggestions on how plant operators could take an active part in the continuous experimentation on a plant, in the course of its normal running routine. The calculation procedures were basically simple, so that personnel without a specialised statistical knowledge could perform them. An elaboration of the method was given in a further paper in 1959 (9).

There is however a fundamental difference between EVOP and the planned experimentation which has so far been discussed. In EVOP only three or four variables are considered at any one time and the incremental changes made are small - of the same order of magnitude as the noise. Thus, in order to obtain significant effects, it is necessary to employ a considerable amount of replication, which averages out the effects of the noise. The drawback of this procedure is, that it slows down the approach to the optimum.

1.2. Dynamic Optimisation

Successful application of Evolutionary Operation depends on the assumption that the uncontrollable variables in the system either remain constant or else vary sufficiently slowly with time, so that the changes can be followed. EVOP is thus very effective for batch type processes. Now, it often happens that the uncontrolled variables in a process e.g. quality of feed stock, flow rates etc., change appreciably with time. Furthermore,

these changes occur faster than the time taken to attain optimum conditions by static methods. Because of this, a control strategy is required which not only reaches the optimum conditions of the process, but also is able to follow the movement in the position of the optimum.

The first of the commercial schemes to account partially for the above situation was the "Quarie" controller (10). This introduced step changes into one independent variable at a time and noted the effect on the sign of the slope of the objective function. If this was positive - it is assumed that the function is being maximised - then another step change was introduced in the same direction as the last, otherwise the direction of the change was reversed. The advantage of this scheme was its simplicity and that it was automatic, but it did not take into account the dynamics of the process i.e. one had to wait for steady state to be established before making the next change. Also, as only one variable at a time was changed, the Quarie controller was unable to detect ridge type response surfaces.

In 1951, Draper and Li (11) summarized the ideas on optimisation available at the time. They considered the following four types of control.

1. Drive Reversal Technique. The control variable was changed at a constant rate. Hence the local slope of the response surface was proportional to the rate of change of the objective function and this could readily be calculated. The direction of movement of the control variable was altered, when the slope changed sign and increased in magnitude to a certain predetermined limit.

2. The control variable was changed at a rate proportional to the slope of the response surface. The slope was determined by dividing the derivative of the objective function with respect to time by the derivative of the control

variable with respect to time. The method had the advantage that more time was spent at points nearer the optimum value than in the previous set up. However in the absence of noise the optimum would be approached exponentially because at the turning point the slope of the response curve is zero. Thus a combination of the two methods was suggested as a good form of control, with rate proportional to slope away from the optimum and constant rate control near the turning point.

3. Peak Holding Control. The independent variable was changed at a constant rate and a discriminating device was used. This stored the largest value of the objective function occurring since the start of a cycle in the given direction. When the optimum was reached the difference between the current value of the objective function and the optimum value started to increase. The direction was changed when the integral of the error was greater than some specified value - the integral of the error, rather than the error, was taken, as thereby the sensitivity of the process towards changes away from the optimum was increased. When the direction was reversed, the optimum was taken as the current value of the objective function. The method has an advantage for noisy systems, as no differentiation is required - in fact small pulses increase the speed of switching and thereby improve the performance. Draper and Li applied the method very successfully to the control of an internal combustion engine.

4. The Use of a Perturbation Signal. Here the independent variable was perturbed using a sinusoidal forcing function. An estimate of the local slope of the response curve was obtained by correlating the output signal with a phase shifted input. The set point of the control variable was then

altered in proportion to this slope. Again the method switched to constant rate control near the optimum, as otherwise the approach would have been exponential.

Draper and Li's optimisation principles were not followed up in industry possibly because the idea of perturbing the actual process contradicted the classical thinking of control engineers. At that time prime importance was attached to the attainment of steady conditions of operation. Increased knowledge concerning the properties of stable systems, improved instrumentation and the success of Evolutionary Operation created a more receptive atmosphere for the paper by Box and Chanmugan (12), which first appeared as a Princeton report in 1961. In this the authors suggested, as a natural extension of static optimisation studies, what had to a certain extent been said by Draper and Li ten years earlier. The whole theory however was set out in a far more elegant way and in a form more readily applicable to an industrial process. The input signal was perturbed sinusoidally, the objective function was correlated with a suitably phase shifted input signal and then integrated over a whole number of cycles. This, as in the case of Draper and Li, gave an estimate of the local slope or "sensitivity" of the response surface. The control variable was then adjusted by an amount proportional to this slope. The exponential approach to the optimum was overcome by feeding back only a portion of the slope together with a portion of the sum of all previous slopes i.e. effectively proportional and integral control. The big difference between the two papers was one of emphasis. Draper and Li were concerned with reaching an optimum and then controlling the system at the found <u>static</u> level. Box and Chanmugan on the other hand were more interested

in the problem of keeping close to the optimum value of an objective function, despite any noise or drift which might cause this to move around. For this reason the dynamics of the process were investigated in detail. The control philosophy, which was called Adaptive Optimisation, was illustrated by the chemical reaction,

$$N_1 \xrightarrow{k_1} N_2 \xrightarrow{k_2} N_3$$

performed in an isothermal, ideally stirred, continuous flow tank reactor.

So far practical experience with an adaptive optimisation procedure of the type described above is small. Two known working projects on the subject are those at the University of Wisconsin* and our own at Imperial College, London. A brief account of the Imperial College project was given by Jenkins (13) and in this the extension of the control strategy to two and more variables was discussed.

Adaptive optimisation is primarily concerned with problems in which the input to a given system varies in some fashion, but only the effect of these variations on the objective function, as opposed to the disturbances themselves, is measureable. Examples of this are the variation of feed composition into a crude oil distillation column or catalyst degeneration in a reactor. However in a wide range of industrial processes, the disturbances although uncontrollable, can be measured and in such cases feed forward control is more efficient than the feed back control of adaptive optimisation. The philosophy of feed forward control is to programme a mathematical model of the process on an analogue or digital computer and at fixed intervals of time to feed into the computer the input conditions to the process. The computer then chooses on some basis, e.g. look up tables - Whiting project of the American Oil

*) Chemical Engineering Department, University of Wisconsin, Madison, Wisconsin, U.S.A.

Company, Indiana (14) - or dynamic programming (15) the optimum adjustments to be made to the process control variables. These adjustments are implemented either automatically or by plant personnel. Feed forward control has a big advantage over feed back control, as adjustments in the controlled variables are made to compensate for the disturbances before they are transmitted through the process. The effectiveness of this compensation depends on the efficiency of the programmed mathematical model of the process. This in general is obtained in form from theoretical considerations, with constants fitted to satisfy the practical results. The constants are then updated either continuously or on a semi-continuous basis. Often, however, several of the disturbances cannot be measured, due to the limitations of the available instruments and thus a mixture of feed forward and feed back control would seem to be optimal. The feed back control compensates both for the immeasurable disturbances and the inadequacy of the model and can be of the form investigated in this thesis.

1.3. General Control Strategy for One Variable

Introduction

Evolutionary operation is performed on a continuous chemical process by treating the process as if it were producing separate batches of product. After each change in the levels of the variables has been made, a period of time is allowed for the process to settle down before measuring performance. As a result, the need to consider the dynamics of the process is avoided (12). The theory which is now discussed and which was originated by Box and Chanmugan, considers an extension of evolutionary operation. It thus assumes initially, that the process is perturbed sinusoidally at a sufficiently low frequency for

the dynamic effects to be neglected. Later the dynamics of the process are taken into account.

Quasi Steady State

Suppose that the objective function, η_t, of a process is only dependent on a single process variable, X_t, all other conditions being maintained constant. Also suppose that the objective function is being maximized - the theory applies equally well if it were minimized. Assume further that the dependence of η_t on X_t can be approximated by a quadratic expression

$$\eta_t = \eta_t(\max) - \tfrac{1}{2}\beta_{11}(X_t - \theta_t)^2 \qquad 1.3.1.$$

where θ_t is the position of X_t corresponding to a maximum in η_t at time t.

$\eta_t(\max)$ is the maximum value of the objective function at time t.

β_{11} is the local curvature of the response surface.

Let cosinusoidal perturbations of amplitude, δ, and frequency, ω, be introduced about a set point, X_o, so that

$$X_t = X_o + \delta \cos \omega t \qquad 1.3.2.$$

The response is given by

$$\eta_t = \eta_t(\max) + \beta_{11}(X_o - \theta_t)\delta \cos \omega t - \tfrac{1}{4}\beta_{11}\delta^2(1 + \cos 2\omega t) - \tfrac{1}{2}\beta_{11}(X_o - \theta_t)^2$$

$$= \eta_o - \beta_{11}\delta^2 + \beta_{11}(X_o - \theta_t)\delta \cos \omega t - \tfrac{1}{4}\beta_{11}\delta^2 \cos 2\omega t \qquad 1.3.3.$$

where η_o is the steady state yield when $X_t = X_o$ i.e.

$$\eta_o = \eta_t(\max) - \tfrac{1}{2}\beta_{11}(X_o - \theta_t)^2$$

The output, η_t, as given by 1.3.3. is seen to contain a fundamental term, at the same frequency as the input perturbation, whose amplitude is proportional to the slope at $X_t = X_o$ i.e.

$$\left(\frac{d\eta_t}{dX_t}\right)_{X_t = X_o} = -\beta_{11}(X_o - \theta_t) \qquad 1.3.4.$$

The d.c. component, $\eta_o - \frac{1}{4}\beta_{11}\delta^2$, is made up of the steady state component, η_o, biassed by a loss $\frac{1}{4}\beta_{11}\delta^2$, due to the perturbation.

If β_{11} were known from preliminary calibrations, then we could estimate from the amplitude of the fundamental in 1.3.3., the distance which X_o is away from its optimum value i.e. $(X_o - \theta_t)$. In practice η_t is contaminated with a noise $n(t)$, so that $(X_o - \theta_t)$, is subject to an uncertainty. Thus it would not be sensible to feed back the whole estimate of $(X_o - \theta_t)$, but only a certain proportion of it. As is discussed later, this proportion depends on the properties of the noise in the system.

The second harmonic contains information concerning the curvature, β_{11}, and this could thus be estimated continuously. However the magnitude of this term is much smaller than that at the fundamental frequency. Also the term is contaminated by random variations in the process as well as the contributions from higher harmonics, due to lack of fit of a second order equation, and so the estimate of β_{11} would be unreliable. In any case it would still be necessary to decide what proportion of the slope to feed back and so β_{11} is included in the control parameters. The second harmonic term thus contributes to the noise $n(t)$ in the estimation of $(X_o - \theta_t)$.

Dynamic Considerations

As the frequency, ω, of the perturbations in the input, X_t, is increased, it becomes necessary to take account of the dynamic behaviour of the process. It is clear, that for a fixed amplitude of the perturbation signal, the system will follow the higher frequencies with increasingly greater difficulty, until for frequencies beyond a certain value, no detectable change in the response will be obtained. Also, due to the dynamics and the finite time of passage through the process, changes in the output signal will tend to lag behind the changes in the input. 1.3.3. thus becomes

$$\eta_t = \eta_o - \tfrac{1}{4}\delta^2 G_o(\omega) + \delta_1 G_1(\omega)\cos\left\{\omega t + \phi_1(\omega)\right\} - \\ - \delta^2 G_2(\omega)\cos\left\{2\omega t + \phi_2(\omega)\right\} \qquad 1.3.5.$$

where $G_i(\omega)$ are the gains of the system

and $\phi_i(\omega)$ are the phase shift angles

In 1.3.5. the d.c. component $\eta_o - 1/2\,\delta^2 G_o(\omega)$ now depends on the frequency, ω, which represents the loss encountered due to the perturbation. Also, it is convenient to combine the phase and amplitude information in the complex quantity

$$T(i\omega) = G_j(\omega)\, e^{i\phi_j(\omega)} \qquad 1.3.6.$$

which at the fundamental frequency is called the frequency response function, or transfer function when regarded as a function of $p = i\omega$. The gains and phase shift angles can in general be determined from the differential equations describing the given process. When the differential equations are not known, the gains are obtained by calibrating the process.

The form of the frequency response function of the system determines its dynamic behaviour. If the frequency response, L(p) takes the form

$$L(p) = \frac{\text{const}}{\sum_{i=0}^{n} a_i p^i}$$

the process gain at the fundamental frequency is proportional to the steady state slope. Thus if the system output signal is correlated with the phase shifted input and integrated, the result will always be proportional to the local slope of the response curve. Another case arises if the frequency response function is

$$L(p) = \frac{\text{const} \sum_{j=0}^{k} b_j p^j}{\sum_{i=0}^{n} a_i p^i}$$

Here the process gain is proportional to the steady state slope plus a term which is a function of the frequency ω . Thus if this is correlated with the phase shifted input signal and integrated, the result contains the steady state slope, but this is biassed by a frequency dependent term. The former term has been named (12), the <u>useful component</u> while the latter the <u>useless component</u> for it contains no information concerning the required slope of the response curve.

The examples derived below illustrate the two cases just discussed. In them theoretical gains and phase shift angles are calculated for first and second order systems.

First Order System

Consider an ideal, stirred tank reactor of unit volume in which substance A decomposes to substance B at a rate proportional to the concentration of A. Let the flow rate of A into the reactor be X_t and the rate constant for the reaction be k. Then by a material balance on A

$$\frac{d\eta_t}{dt} = X_t (1 - \eta_t) - k\eta_t \qquad 1.3.7.$$

where η_t is the concentration of A in the output at time t.

At steady state, i.e. $\frac{d\eta_t}{dt} = 0$, the response, η_o, is $\eta_o = \frac{X_o}{X_o + k}$ which has a slope given by

$$\left\{\frac{d\eta_t}{dX_t}\right\}_{X_t = X_o} = \frac{k}{(X_o + k)^2} = \frac{1 - \eta_o}{X_o + k} \qquad 1.3.8.$$

It should be noted that there is no natural maximum in the concentration, η_t, because the system tends to its maximum value of unity as $X_o \longrightarrow \infty$

For small perturbations in X_t about its steady state value X_o, 1.3.7. can be linearized and thus the transfer function of the system becomes

$$T(p) = \frac{1 - \eta_o}{X_o + k + p}$$

From this the gains and phase shifts as applied to 1.3.5. can be shown to be

$$G_1(\omega) = \frac{1 - \eta_o}{\sqrt{(X_o + k)^2 + \omega^2}} = \frac{\left\{\frac{d\eta_t}{dX_t}\right\} X_t = X_o}{\sqrt{1 + \omega^2/(X_o + k)^2}} \qquad 1.3.9.$$

$$G_o(\omega) = G_2(\omega) = 0 \qquad \phi_2(\omega) = 0 \qquad \phi_1(\omega) = \tan^{-1} \frac{-\omega}{X_o + k}$$

Hence the dynamic response of 1.3.7. to a sinusoidal perturbation of the input variable X_t is given by

$$\eta_t = \eta_o + \delta \frac{\left(\frac{d\eta_t}{dX_t}\right)_{X_t = X_o}}{\sqrt{1 + \omega^2/(X_o + k)^2}} \cos(\omega t + \phi_1(\omega)) \qquad 1.3.10.$$

From this it can be seen that as the frequency of perturbation becomes large $G_1(\omega) \longrightarrow o$ i.e. the input perturbations cease to have an effect on the output. In quasi steady state the slope of the response surface can be obtained by multiplying η_t in 1.3.3. by a correlator signal cos ωt and integrating i.e.

$$\text{slope} = \frac{2}{T}\int_{t-T}^{t} \eta_u \cos \omega u \; du = -\beta_{11}(X_o - \theta_t)$$

If T, is an integral number of cycles, i.e. $\frac{2\pi n}{\omega}$, all the other harmonics are eliminated by the integration and an average value of the slope over the period T is obtained. The choice of the number of cycles, n, over which the integration should be performed, is a problem which is discussed later.

For the dynamic system considered, it can be seen by inspection of 1.3.10. that the correlator signal should be $\cos\left\{\omega t + \phi_1(\omega)\right\}$ and the attenuated slope is thus given by

$$\frac{1}{\sqrt{1 + \omega^2/(X_o + k)^2}} \left(\frac{d\eta_t}{dX_t}\right)_{X_t = X_o} = \frac{2}{T}\int_{t-T}^{t} \eta_u \cos\left\{\omega u + \phi_1(\omega)\right\} du \qquad 1.3.11.$$

The output from this integrator is always proportional to the slope and hence it can be used as an estimate of the distance which the operating point is from the maximum. In this case the amplitude of the signal at the fundamental frequency is called the "useful component."

Second Order System

In general, the fundamental frequency may contain, in addition to the "useful" component, another component not related to the slope and called the "useless" component. This is illustrated below.

The yield of the intermediate product B in the reaction $A \xrightarrow{k_1} B \xrightarrow{k_2} C$ is given by the following differential equation - the derivation of this is given in the Box and Chanmugan paper (12)

$$(D + X_t + k_1)\ (D + X_t + k_2)\ \eta_t = k_1 X_t \qquad 1.3.12.$$

The corresponding transfer function is

$$T(p) = \frac{\left\{\frac{d\eta_t}{dX_t}\right\} X_t = X_o - p\,\eta_o\, a_1\, a_2}{(1 + p\,a_1)\ (1 + p\,a_2)} \qquad 1.3.13.$$

where $\left\{\frac{d\eta_t}{dX_t}\right\}_{X_t = X_o}$ is the slope of the process function at $X_t = X_o$

η_o is the steady state response

$$a_i = \frac{1}{k_i + X_o} \qquad 1.3.14.$$

For cosinusoidal perturbations in X_t of the form

$$X_t = X_o + \delta \cos\omega t$$

the objective function is

$$\eta_t = \eta_o + \delta\, G_1(\omega)\ \cos\left\{\omega t + \phi_1(\omega)\right\} \qquad 1.3.15.$$

where $G_1(\omega)$ is the gain of the system given by

$$G_1(\omega) = \left\{ \frac{\left\{\frac{d\eta_t}{dX_t}\right\}^2_{X_t = X_o} + \omega^2 \eta_o^2\, a_1^2\, a_2^2}{(1 + \omega^2 a_1^2)\ (1 + \omega^2 a_2^2)} \right\}^{1/2} \qquad 1.3.16.$$

and the phase shift is

$$\phi(\omega) = \tan^{-1} \frac{\omega\left\{\eta_o a_1 a_2 (1 - \omega^2 a_1 a_2) + \left(\frac{d\eta_t}{d X_t}\right)_{X_t=X_o} (a_1 + a_2)\right\}}{\left(\frac{d\eta_t}{d X_t}\right)_{X_t=X_o} (1 - \omega^2 a_1 a_2) - \eta_o \omega^2 a_1 a_2 (a_1 + a_2)} \qquad 1.3.17.$$

If in 1.3.15 η_t is correlated with $\cos(\omega t + \phi_1(\omega))$, the resulting quantity is not proportional to the slope $\left(\frac{d\eta_t}{d X_t}\right)_{X_t=X_o}$, because of the influence of $\omega^2 \eta_o a_1^2 a_2^2$. However, if instead of expressing the output in terms of $\cos(\omega t + \phi_1(\omega))$, it is written in terms of $\cos(\omega t + \phi_1'(\omega))$ and $\sin(\omega t + \phi_1'(\omega))$, where the angle $\phi_1'(\omega)$ is so chosen that the amplitude of $\cos(\omega t + \phi_1'(\omega))$ is directly proportional to $\left(\frac{d\eta_t}{d X_t}\right)_{X_t=X_o}$, we may correlate η_t with $\cos(\omega t + \phi_1'(\omega))$ and thus obtain directly a quantity which is proportional to $\left(\frac{d\eta_t}{d X_t}\right)_{X_t=X_o}$. More specifically

$$\eta_2 = \eta_o + \delta \nu_1(\omega) \left\{\frac{d\eta_t}{d X_t}\right\}_{X_t=X_o} \cos(\omega t + \phi_1'(\omega)) + \delta \mu_1(\omega) \sin(\omega t + \phi_1'(\omega)) \qquad 1.3.18.$$

where $$\phi_1'(\omega) = \tan^{-1} - \frac{\omega(a_1 + a_2)}{1 - \omega^2 a_1 a_2} \qquad 1.3.19$$

$$\nu_1(\omega) = \frac{1}{(1 + \omega^2 a_1^2)^{1/2} (1 + \omega^2 a_2^2)^{1/2}} \qquad 1.3.20$$

and $$\mu_1(\omega) = \frac{\eta_o a_1 a_2}{(1 + \omega^2 a_1^2)^{1/2} (1 + \omega^2 a_2^2)^{1/2}} \qquad 1.3.21.$$

Relations 1.3.19., 1.3.2o. and 1.3.21. are obtained by equating the coefficients of $\cos\omega t$ and $\sin\omega t$ in 1.3.15. and 1.3.18. The $\cos(\omega t + \phi_1'(\omega))$ term is known as the "useful" component, for it is proportional to the slope and $\nu_1(\omega)$ is the gain of the useful component. The $\sin(\omega t + \phi_1'(\omega))$ contains no useful information about the steady state slope and is thus called the "useless" component.

For some systems it is not possible to find an angle $\phi_1'(\omega)$, such that the slope of the response surface can be isolated, but it is usually possible to find some $\phi_1'(\omega)$ for which the amplitude of the useful component is less biassed than for any other estimate. Further, the appropriate angle $\phi_1'(\omega)$ is itself a function of the operating position on the response surface. Box and Chanmugan (12) found however that $\phi_1'(\omega)$ varies only slowly with X_o and so they suggested that in the interest of simplicity, a constant value corresponding to some "average" optimum conditions should be used. As the mechanism of an industrial process is seldom known very exactly, the value of the compromise phase shift is best found by experimental calibration. In fact in 1.3.18. only the $\sin(\omega t + \phi_1'(\omega))$ term is present at the maximum and thus the required phase shift is one which cancels out this term i.e. an angle 9o degrees out of phase with it.

The Control Loop for One Variable

A diagram of the control loop is shown in figure 1 and typical outputs from the various stages of the control loop in figure 2. The observed objective function, y(t), is made up of the real response, η_t, and a noise term n(t). The latter arises from uncontrollable variations in the process

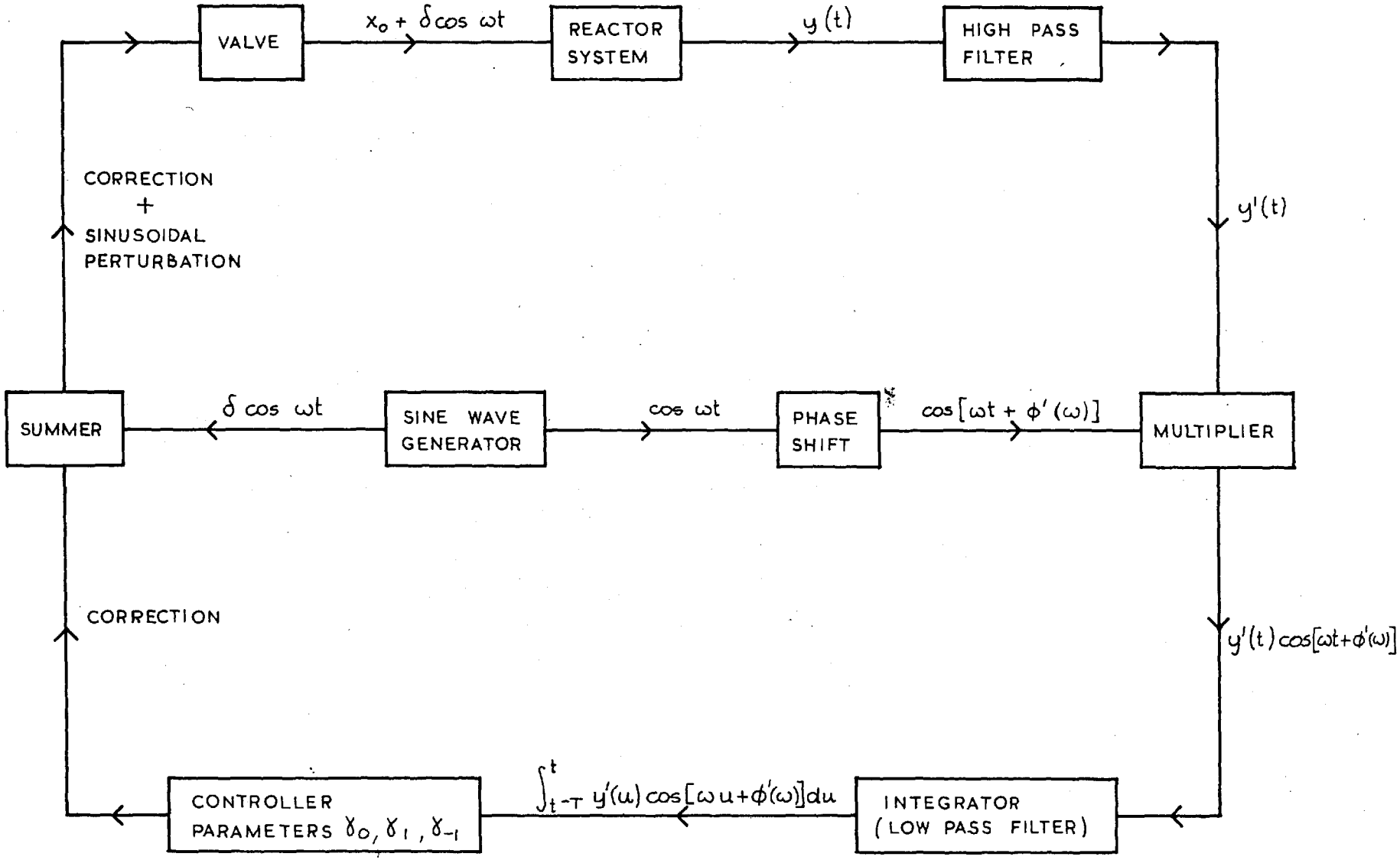

CONTROL LOOP FOR ONE VARIABLE

FIG. 1.

TYPICAL OUTPUT FROM VARIOUS STAGES OF THE CONTROL LOOP

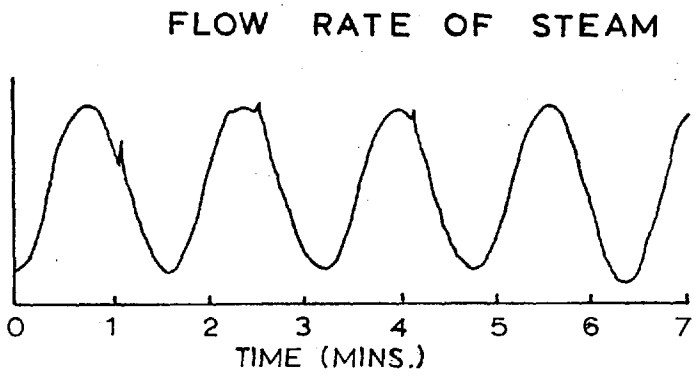

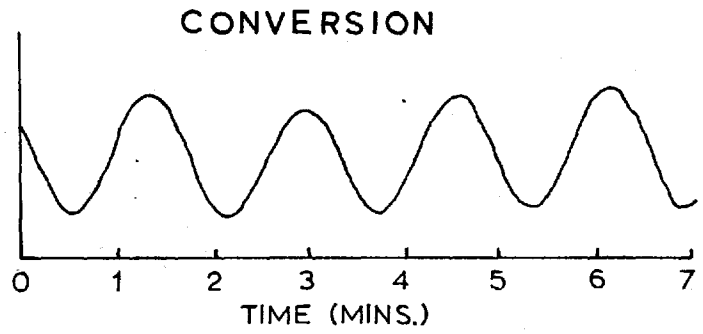

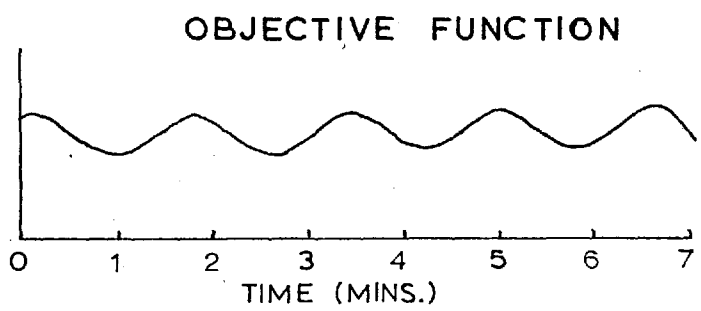

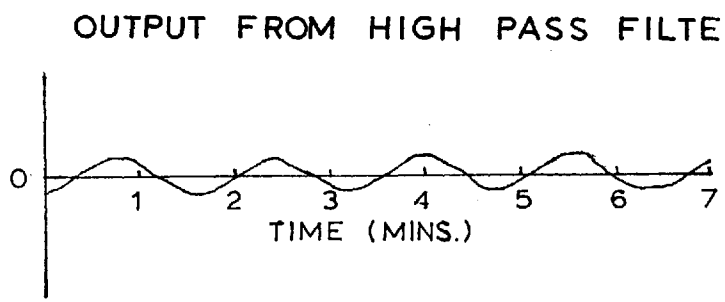

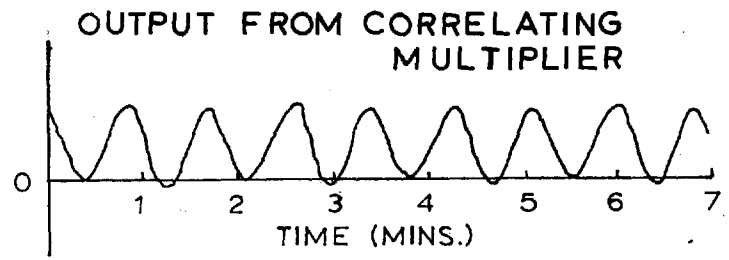

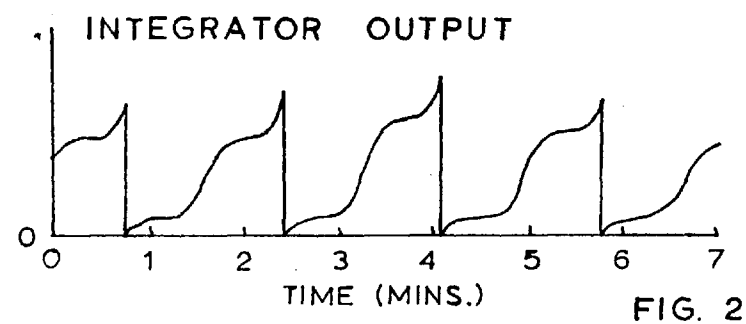

FIG. 2

itself together with the measurement errors.

The d.c. component in $y(t)$, which represents the steady state part of the response, is removed by a high pass filter. The time constant of this filter is a quantity which has to be optimized, for if it is too large, the filter will not be able to follow the changes occurring in the process. On the other hand, if it is too small, the filter will attenuate the sinusoidal variations put into the system. Now the break off point of a high pass filter occurs approximately at a frequency given by $1/T$ cycles/sec, where T is the time constant. Thus the time constant (T) is initially chosen so that $1/T$ is slightly less than the perturbation frequency.

The output, $y'(t)$, from the high pass filter is multiplied by a phase shifted correlator signal, $\cos(\omega t + \phi'(\omega))$, coming from a sine wave generating device. The phase shift angle, $\phi'(\omega)$, is obtained in the way indicated in the last section. As the result of the correlation, the signal now contains the desired slope of the response surface modulated by contributions from second and higher harmonics as well as noise. There are basically two ways of feeding this information into the controller.

a) The amplitude modulated term can be removed by forming

$$\frac{2}{T}\int_{t-T}^{t} y'(u) \cos(\omega u + \phi'(\omega)) \, du \qquad 1.3.22.$$

where T is the interval corresponding to the integral number of periods, n, of frequency, ω, i.e. $T = \frac{2\pi n}{\omega}$

b) $y'(t) \cos(\omega t + \phi'(\omega))$ may be fed directly into the controller. The integrator in 1.3.22. acts as a low pass filter, which attenuates from the multiplier output all terms except the d.c. level. A disadvantage of this method of control is that by integrating over a complete period or periods, the

controller is unable to detect real changes occurring in the process, as quickly as otherwise. Some filtering of the second harmonic and noise is however essential, otherwise the controller follows the sizeable perturbations about the slope and also the noise. This results in large losses both during the ascent to the optimum and also while attempting to follow the movements of the optimum. This point is discussed in more detail later.

The controller consists of conventional analogue equipment - Electronic Associates TR 10 Computer - producing a mixture of proportional, integral and derivative control, characterized by the parameters γ_0, γ_1 and γ_{-1}. A detailed diagram of the analogue equipment used, is given in figure 10.

1.4. General Control Strategy for Two Variables

Introduction

The theory described so far has dealt with the case of the response, η, depending on one process variable. In general, however, the response depends on several process variables and the section below outlines a general method for treating this situation. For the sake of convenience the case of two variables is considered.

Steady State

As in the case of one variable, it is assumed that the steady state response may be approximated by a quadratic polynomial. For two variables this takes the form

$$\eta(x_1,x_2) = \beta_0 + \beta_1 x_1 + \beta_2 x_2 + \beta_{11} x_1^2 + \beta_{22} x_2^2 + \beta_{12} x_1 x_2 \qquad 1.4.1.$$

If the control strategy were based on partial derivatives

$$\frac{\partial \eta}{\partial x_i} = \beta_i + 2\beta_{ii} x_i + \beta_{ij} x_j \qquad i,j = 1,2;\ i \neq j \qquad 1.4.2.$$

a quick approach to the optimum would be achieved, if the response contours were circular. However, in general, the contours are elongated, in which case the most rapid direction of ascent is along and perpendicular to the axes of the response surface. This direction can be found by a canonical transformation i.e. moving the origin to the local maximum of the surface ($\bar{x}_1$, $\bar{x}_2$) and rotating the coordinate axes to correspond with those of the response surface. The resultant canonical variables (X_1, X_2) are related to the standardized process variables (see 1.1.2.) by the linear transformation

$$X_1 = \lambda_1(x_1 - \bar{x}_1) + \lambda_2(x_2 - \bar{x}_2)$$

$$X_2 = \lambda_2(x_1 - \bar{x}_1) - \lambda_1(x_2 - \bar{x}_2) \qquad 1.4.3.$$

where λ_1 and λ_2 are constants.

The response surface in this case can be expressed by

$$\eta = \eta\,(\max) - 1/2\,\beta'_{11}\,X_1^2 - 1/2\beta'_{22}\,X_2^2 \qquad 1.4.4.$$

where $\eta\,(\max)$ is the value of the response at the centre of the design, and β'_{11}, β'_{22} are constants whose sign and magnitude determine the shape of the response contours (4).

In 1.4.3. the standardized variables x_1 and x_2 have scaling constants a_1 and a_2 associated with them (see 1.1.2.). However it is only the ratio a_1/a_2 which influences the relative values of X_1 and X_2. Thus if 1.4.3. is rewritten in the form

$$X_1 = a_{11}\,(x_1 - \bar{x}_1) + a_{12}\,(x_2 - \bar{x}_2)$$

$$X_2 = a_{21}\,(x_1 - \bar{x}_1) + a_{22}\,(x_2 - \bar{x}_2) \qquad 1.4.5.$$

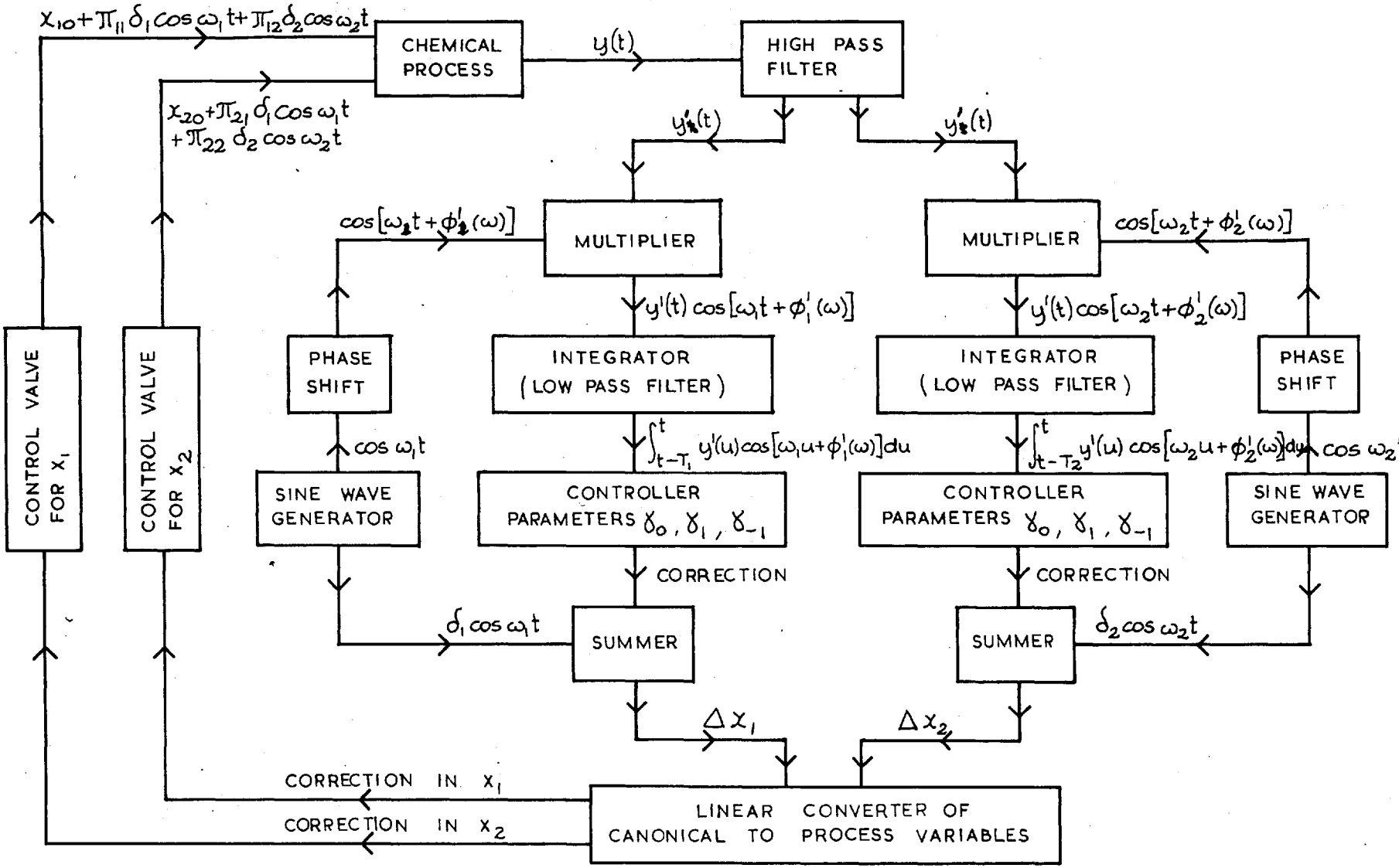

CONTROL LOOP FOR TWO VARIABLES

FIG. 3.

then the scale and direction of the axes $X_1 = X_2 = 0$ relative to those of x_1 and x_2 can be altered at will by changing the three independent ratios of the constants a_{ij}.

Dynamic Considerations

As the position of the maximum response tends to change with time, it is convenient to rewrite 1.4.4. in the form

$$\eta_t = \eta_t(\max) - 1/2\,\beta'_{11}(X_{1t} - \theta_{1t})^2 - 1/2\,\beta'_{22}(X_{2t} - \theta_{2t})^2 \qquad 1.4.6.$$

where θ_{it} is the position of X_i, corresponding to a maximum in η_t at time t, referred to the canonical axes.

If perturbations

$$X_{1t} = \bar{X}_{1t} + \delta_1 \cos \omega_1 t$$

$$X_{2t} = \bar{X}_{2t} + \delta_2 \cos \omega_2 t \qquad 1.4.7.$$

are then introduced into the canonical variables, corrections, proportional to the distances $(X_{1t} - \theta_{1t})$ and $(X_{2t} - \theta_{2t})$, can be fed back in a way similar to that for one variable. A schematic diagram of this is shown in figure 3.

The advantages of working with canonical variables are basically two-fold

a) If the system is a ridge, the advance will be along its axis and thus the optimum will be reached in the most efficient manner. This is because for a ridge system one of the constants, β_{ii}, is large relative to the other and thus any offset from the ridge is very quickly compensated.

b) Independent control can be exercised over the canonical variables,

whereas the process variables themselves would be coupled. It may be seen that the perturbations in the process variables are

$$\Delta x_1 = \pi_{11}\ \delta_1 \cos \omega_1 t + \pi_{12}\ \delta_2 \cos \omega_2 t$$

$$\Delta x_2 = \pi_{21}\ \delta_1 \cos \omega_1 t + \pi_{22}\ \delta_2 \cos \omega_2 t \qquad 1.4.8.$$

where π_{ij} are constants, which can be obtained from the inverse transformation of 1.4.5.

They are thus made up of a mixture of cosine waves, the mixing proportions being such that the net effect is to produce a cosine wave along and at right angles to the ridge. Had the process variables been perturbed sinusoidally, the output would have contained the sum and difference frequencies due to coupling. The canonical variables may thus be thought of as a device for mixing the two perturbation frequencies in such a way that these interaction terms are eliminated.

The Control Loop for Two Variables

A diagram of the control loop in two variables is shown in figure 3. The control strategy and considerations in the choice of constants are the same here as in the case of one variable.

The objective function is fed into a high pass filter and then is split into two identical signals. Each signal is correlated with the phase shifted cosine at one of the perturbation frequencies and can be integrated so as to remove the harmonic frequency terms. The result is then fed into a controller, similar to that for one variable, and into a summer where the perturbation

signal is added. The outputs from the two summers, which represent the corrections in the canonical variables, are then converted back into corrections in terms of the process variables and these are fed into the devices controlling x_1 and x_2.

CHAPTER II

The Water Gas Shift Reaction

Introduction

In the last chapter the basic ideas of adaptive optimisation were summarized. In what follows, the process to which these ideas are applied is discussed. The apparatus used is then described, followed by the control system.

2.1. The Choice of Reaction to Optimize

The purpose of this work is to study the effectiveness and properties of the control ideas described in the last chapter, when these are applied to a physical system. For this reason the reaction to be optimized has to have a continuously measurable optimum with respect to at least two independent variables. This optimum can be either a natural one like yield or percentage conversion or else an artificially created one like cost. Further, there should be other process parameters, besides those used for control purposes, which can be varied in a controlled manner, so as to generate fluctuation in the system. Finally the conditions under which the reaction is performed should be realisable in a university laboratory.

Surprisingly few reactions satisfy all the above criteria, especially when one requires that the reaction should have a natural optimum in two variables. The water gas shift reaction

$$CO + H_2O \rightleftharpoons CO_2 + H_2$$

does however seem to be a good choice. It has been often investigated because

of its great industrial importance as an intermediate stage which produces hydrogen in the manufacture of ammonia and methanol and is further practicable to operate under pilot scale conditions in a university laboratory. Since the reaction is exothermic and reversible there is an optimum temperature of operation for a fixed inlet composition. Also, when the temperature is fixed, there is an optimum flow rate of steam for any dry gas flow. This occurs because an increase in the steam flow rate increases the amount of carbon monoxide converted to hydrogen and carbon dioxide. However, the time of contact of gases with the catalyst decreases, resulting in less conversion occurring and thus a turning point.

2.2. Survey of the Water Gas Shift Reaction

The water gas shift reaction

$$CO + H_2O \rightleftharpoons CO_2 + H_2 + \text{heat}$$

has been studied by a large number of workers, but so far no universally accepted description of its kinetics has been produced. This is principally due to difficulties in reproducibility of results e.g. diffusion and heat transfer properties, catalyst size and proportion of promoters used with the basic iron oxide catalyst. Further, the results obtained are fitted to several possible reaction mechanisms and the model showing the best fit on the basis of some criterion, such as variance, is accepted. This does introduce ambiguous interpretation, particularly as the criterion of best fit also varies. Stelling and Krusenstierna (17) surveyed the approaches available, starting with the various adsorption isotherms and concluded that the same rate equation can in principle be derived irrespective of the choice of the isotherm. They also suggested a standard procedure for the investigation of reaction kinetics and illustrated this with some preliminary work on the

water gas shift reaction, using an unpromoted iron oxide catalyst at 390° C. On the basis of these experiments they proposed a rate equation of the form

$$r = k(T)\ P_{CO} \left(\frac{P_{H_2O}}{P_{CO_2}} \right)^n$$

where $k(T)$ is the rate constant at temperature $T\ ^{\circ}K$ and P_i is the partial pressure of component i.

Stelling and Krusenstierna advocated the use of "one variable at a time" type of experimentation, which has been shown by Box and Wilson (1) to be a less effective procedure than a statistically designed experiment of the factorial type. Hulburt and Srinivasan (18) performed a half replicate 2^5 factorial experiment on the water gas shift reaction and then fitted constants to several possible rate equations. The form of the equation which gave the smallest variance was adopted but the experimental procedure was stated not to have been sufficiently refined for any great confidence in the results.

Bohlbro (19) found that the reaction rate was best described by the expression

$$r = k(T)\ \frac{P_{CO}^{0.90}\ P_{H_2O}^{0.25}}{P_{CO_2}^{0.60}}$$

which in form agrees with Stelling and Krusenstierna's proposal. The reactor used was a differential type i.e. low conversions, containing 3 gms of commercial iron oxide-chromium oxide catalyst. The catalyst size was 2 mm's and it was concluded that below 380° C the reaction was not mass transfer limited. At higher temperatures the diffusion effects were satisfactorily

corrected for, by means of the effectiveness factor, calculated by Hoogschagen's method (20). It was also pointed out that above 380° C there exists a danger of reducing the catalyst to iron if the partial pressure of water falls below a certain limit. The iron then catalyses the reaction

$$2\,CO \longrightarrow CO_2 + C$$

Bohlbro found an activation energy of 27.4 kcals/mole for the shift reaction.

Mars (21), also using a commercial iron oxide–chromium oxide catalyst assumed that the reaction rate is first order with respect to the displacement of CO from its equilibrium concentration i.e.

$$r = k(T)\ (P_{CO} - P_{CO_{eq}})$$

where $P_{CO_{eq}}$ is the partial pressure of carbon monoxide if the inlet gas mixture reacts to equilibrium.

Mars' results agreed with those of Stelling and Krusenstierna in so far as the rate is proportional to P_{CO} and is lowered by P_{CO_2}. The experiments were performed in a differential reactor, 8 mm diameter, containing 1.4 gms of 500 to 700 μ catalyst. The reactor was immersed in a fluidized bed of carborundum powder (200 μ). The effectiveness factor (20) was used to correct for mass transfer limitations with diffusivity calculations based on Knudsen type model i.e. the gas mean free path was assumed to be much larger than the pore diameter. The results of the laboratory experiments were used to predict the temperature profiles in industrial adiabatic shift reactors and the predictions were found to lie within the range of measured results. The exception was that at high temperatures the slopes of the calculated curves decreased insufficiently. Using Mars' rate constant results, an activation energy of 28.5 kcals/mole was obtained.

Moe (22) found experimentally that the Mars type rate equation did not account satisfactorily for the dependence of conversion on the steam to gas ratio. He thus proposed that the shift reaction should be considered as being reversible, with the rate being first order with respect to each reactant i.e.

$$r = k(T) \left\{ (A - x)\ (B - x) - \frac{(C + x)\ (D + x)}{K_T} \right\}$$

where A, B are initial concentrations of the reactants

C, D are initial concentrations of the products

x = conversion

K_T = equilibrium constant

$k(T)$ = reaction rate constant

Moe's results when fitted to a Mars type rate equation resulted in an activation energy of about 33.9 kcals/mole.

Moe was interested in producing a rate equation, which could be used with confidence in the design calculations of shift reactors. His practical results do show an improvement over Mars' model in that at a given temperature, the rate constant, k, showed less sensitivity to the inlet gas composition. However, due to experimental error, the results are not really conclusive. Also, no results are given for the performance of predicted and actual adiabatic reactors. The paper does consider very clearly several of the factors needed for the design of an industrial shift reactor.

Mars's kinetic model has been used for the purpose of simulating the process on a digital computer. The relative simplicity of the model was an advantage and as we lacked experience, there was no reason to suppose that the more complex model of Moe was necessary. Further, other workers (23), (28)

have found Mars' rate equation satisfactory.

2.3. The Choice of Gas Composition

The purpose of the water gas shift reaction is to convert carbon monoxide to carbon dioxide and hydrogen by reacting it with steam over a catalyst. The hydrogen is then used in the manufacture of methanol or ammonia. In the old processes the feed gas for the reaction came from the water gas reactors, where the gas was produced by passing steam and air over heated coke. Recently, however, industry has tended to use steam reforming i.e. cracking of light hydrocarbons, or partial oxidation of heavy hydrocarbon oils with air or oxygen to produce the source gas for the shift converters. The cracking or partial oxidation of natural gas has been used in places where natural gas is readily available.

The source of gas largely determines the inlet gas composition for the shift converters. Thus a typical inlet gas from water gas reactors* is

CO	32%	CO_2	8%
H_2	37%	N_2, A, CH_4	22%

The gas then passes through a water saturating tower operated at about 85° C.

A typical exit gas from the partial oxidation process contains

CO	45%	CO_2	4.5%
H_2	49%	N_2, A, CH_4	1.5%

The steam is introduced by passing through a water saturating tower and further injecting superheated steam.

*) Nitrogen Engineering Corporation

A typical exit gas from the steam reforming process contains

CO	12.2%	CO_2	8 %
H_2	57.2%	N_2, A, CH_4	22.6%

The steam is present here as excess from the reforming stage.

On the project since the reacting gases were only available from cylinders, the overall scale of the apparatus was chosen so that standard cylinders of gases gave about a week's operation. Thus the flow rate of dry gases was calculated to be about 50 litres/hr.

The flow rates of the individual gases were chosen primarily to enable convenient operation. The carbon monoxide flow rate, which for computational purposes was assumed constant, was required to be as large as possible, so as to minimize rotameter control errors in conversion. However, it was expected that the range of investigation would be up to 10:1 ratio of steam to carbon monoxide and the dry gas collected approximately twice its own flow of steam. Hence the flow rate of carbon monoxide was fixed at 10 l/hr. In order to simplify the experiments, no carbon dioxide was fed into the system.

The hydrogen flow rate was chosen so that the density of the dry gas mixture was the same as that of steam. In this way measurement errors in the steam flow rate were reduced, as density corrections could be neglected. Thus the hydrogen flow rate was fixed at 19 l/hr and the flow rate of the inert carrier gas, nitrogen, was taken as 21 l/hr.

The approximate composition of the inlet gas used in experiments was thus

CO	20%	CO_2	-
H_2	38%	N_2	42%

The composition does not correspond exactly to any encountered in industry. However, the ratio of hydrogen to carbon monoxide has a value lying between that from the reforming and that from the oxidation processes.

2.4. The Apparatus Used

Figures 4 to 9 show the layout and details of the apparatus used.

Preparation of the Gases for the Reactor

The reacting gases: carbon monoxide, carbon dioxide, hydrogen and the inert nitrogen were obtained from cylinders and after being metered with Rotameters*, they were fed into a mixing chamber. For the purpose of stabilizing the flow two o.oo8 inch orifices were inserted into each gas line and a further one was placed in the line joining the mixing chamber to the saturator. The mixing chamber itself was a vertically mounted tube 12" long and 1" diameter tightly packed with sand - 550 μ nominal diameter. Flow through the mixer was from bottom to top. Small amounts of other gases, such as sulphur compounds, which act as catalyst poisons, could have been added at this stage, were it desired to study the effectiveness of the control system in maintaining optimum conditions in the face of catalyst degeneration.

The remaining reactant, steam, was introduced by partially saturating part of the dry gas with water at 98° C, this temperature being controlled to better than 1/20th of 1° C. This special technique was made necessary by the small scale of the project and the need to introduce accurately liquid quantities of the order of 50 ccs/hr. A pneumatically operated Annin** valve

*) The Rotameter Manufacturing Co. Ltd., 330 Purley Way, Croydon, Surrey

**) Gloucester Controls Ltd., Eastern Avenue, Gloucester

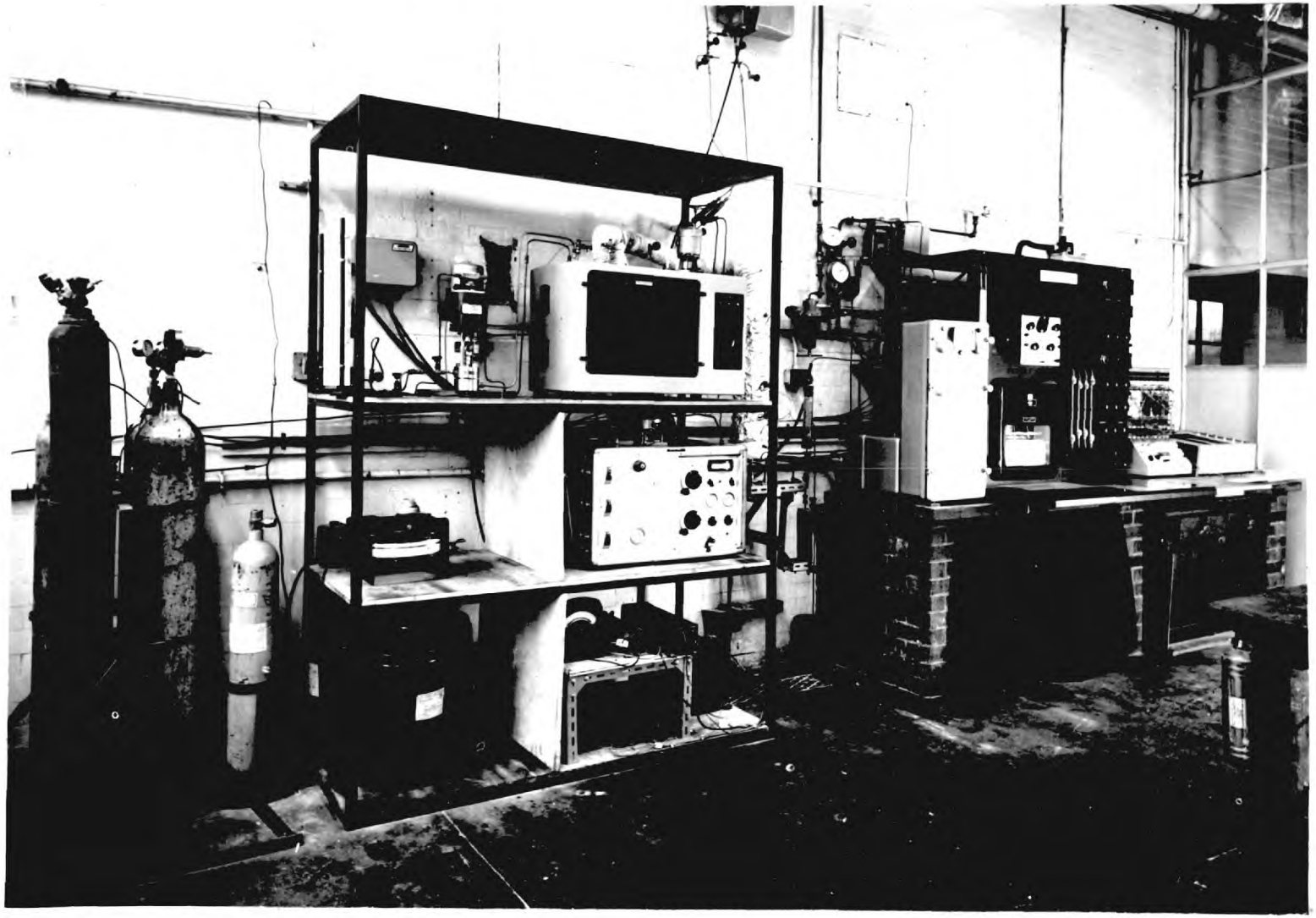

GENERAL VIEW OF THE EQUIPMENT

FIG.4

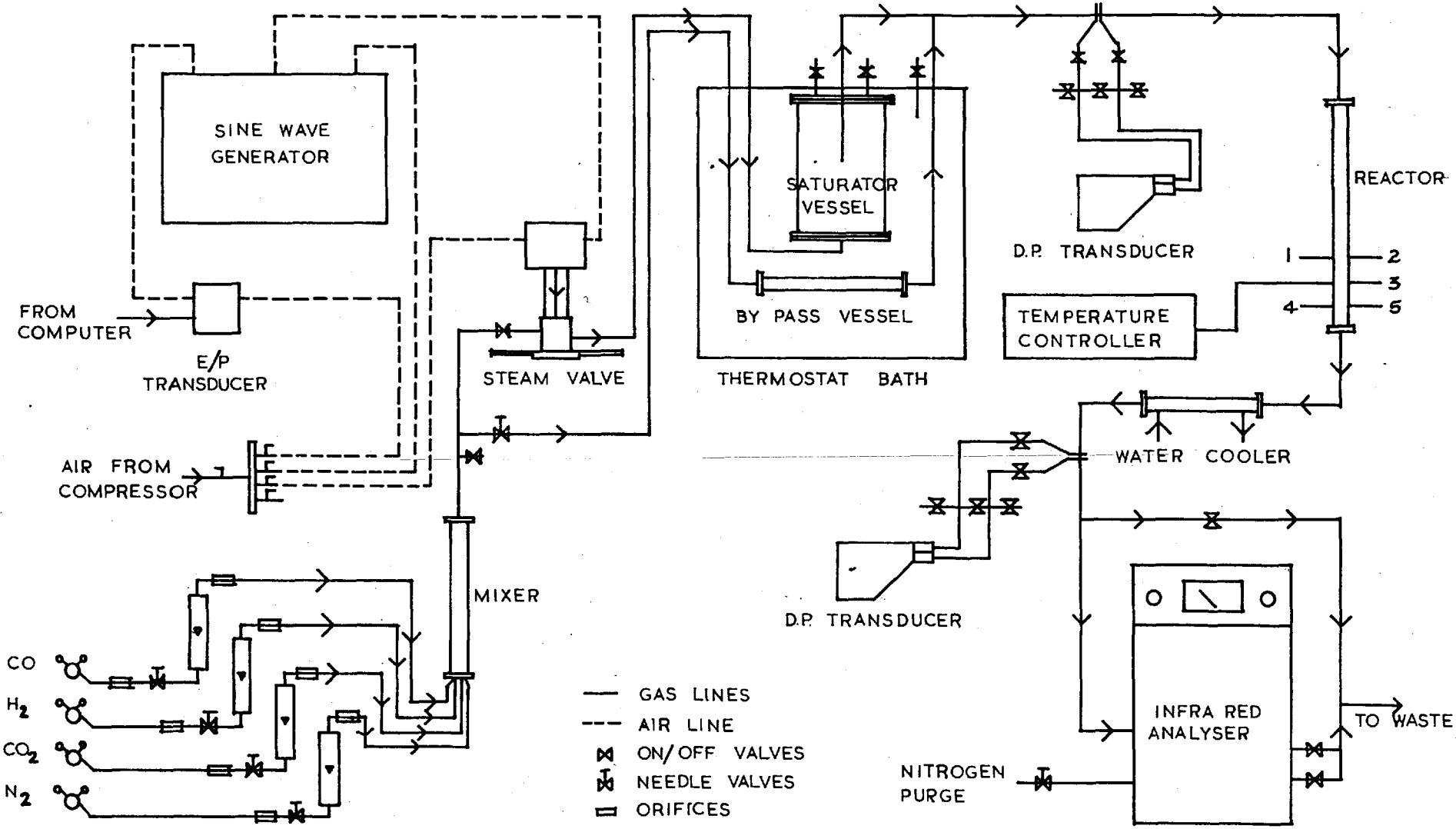

BLOCK LAYOUT OF APPARATUS

FIG. 5.

controlled the flow of gas entering the saturator and as this gas picked up a fixed proportion of steam, the valve effectively controlled the flow rate of steam introduced into the reactor. The rest of the gas was sent through a by-pass circuit, which contained a needle valve for making the resistance in the two circuits equal and also a cylindrical vessel - 620 ccs volume. The purpose of this vessel was to make the time of passage through the two parts of the system approximately the same. If this is not the case, the volume of dry gas going through the reactor varies and this in turn introduces a bias into the dependence of the conversion on the sinusoidal perturbations of the steam flow rate.

The flow rate of the steam was measured with an Evershed* differential pressure transducer (ER 315/1/C) placed across an orifice plate in the saturator exit line. The steam was prevented from condensing out by heating this line with electrical heating wire (175 watts) to about 200° C at the orifice. As the dry gas density was approximately the same as that of the steam, no density adjustments were necessary. The accuracy of this method of measurement was dependent on whether the times of passage in the by-pass and saturator circuits were approximately the same and experimentally this was found to be the case. A constant flow corresponding to the dry gas flow rate was subtracted from the continuous, total flow signal, to give the steam flow rate.

The minimum size of the saturator vessel was calculated by Mr. R. J. Price. Initially it was designed to ensure 100% saturation and thus two vessels were used with about 95% saturation taking place in the first one. However, with the method of measurement finally adopted, 100% saturation was no longer essential and thus only the first one of the vessels was employed.

*) Evershed and Vignoles Ltd., Acton Lane Works, London W. 4

The vessel height of 12 ins was chosen on the basis of the largest height which could conveniently be immersed in the available standard constant temperature bath*. The diameter - 8 ins - was such that the vessel could operate for at least 10 hours without a significant change in the level of water. The inlet gas stream entered the saturator at the bottom and was broken up into bubbles by a 453 μ copper gauze fixed across the saturator cross-section.

The exit gases from the saturator system, after passing through the orifice plate, which measured the steam flow rate, were fed into an electrically heated tubular reactor.

The Reactor and Associated Equipment

The main considerations in the design of the reactor were as follows:

1) The reactor diameter should be small enough to avoid significant radial temperature gradients.

2) The $\frac{\text{reactor diameter}}{\text{particle diameter}}$ ratio should be large enough to approximate to plug flow and also to minimize radial diffusion effects.

3) The $\frac{\text{reactor length}}{\text{particle diameter}}$ ratio should be greater than 300 to eliminate the influence of axial diffusion.

4) For a given reactor diameter a small $\frac{\text{reactor diameter}}{\text{particle diameter}}$ ratio is desirable to avoid an excessive pressure drop across the reactor.

The compromises in the reactor design were made empirically using as an indication some criteria given by Rietema (23). In fact the designed reactor satisfied all the above conditions except 2) and this was compensated in the manner described in section 3.5.

*) Townson and Mercer, Beddington Lane, Croydon, Surrey

STEAM CONTROL VALVE AND SATURATOR FIG.6

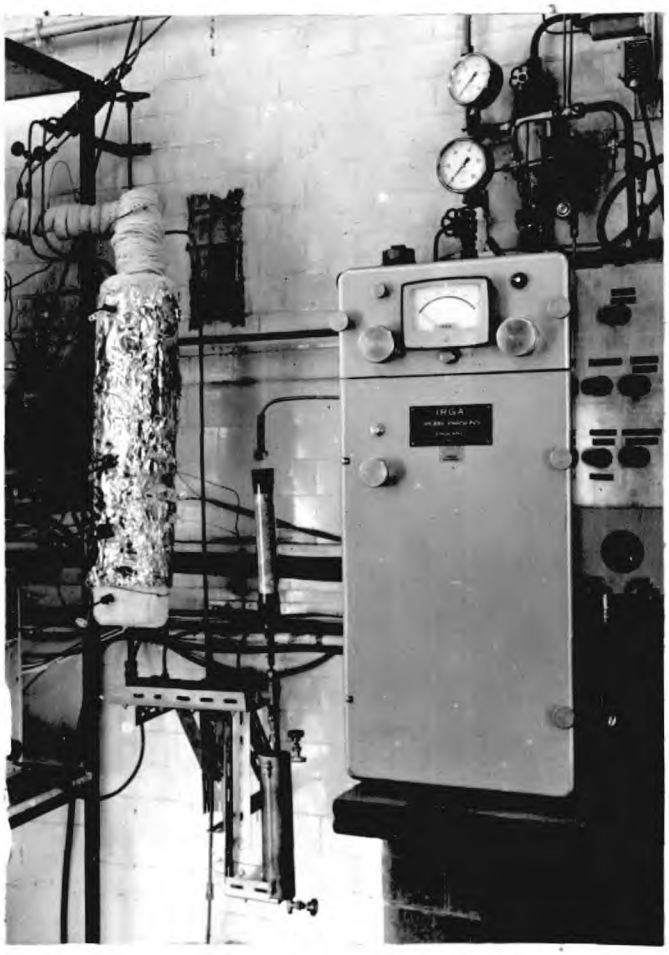

REACTOR AND INFRA RED ANALYSER FIG.7

The reactor consisted of a vertical 1 inch I.D. copper tube packed with 40 ccs of I.C.I. high temperature shift catalyst. The catalyst was ground down from industrial sized pellets and the sieve fraction 599 to 699 microns was used. The volume was chosen to allow near equilibrium operation. The gases entered the reactor tube at the top and passed through a 14" preheating section containing coarse sand - 1003 to 1204 μ - before entering the catalyst bed. A half inch length of fine sand - 599 to 699 μ - was packed on either side of the catalyst to stabilize flow conditions and on the downstream side there was a further 5 inches of coarse sand. The reactor bed was supported on a 600 μ copper gauze.

A nichrome strip heater was wound on the outside of the reactor tube and was electrically insulated from the tube and lagging with 0.003 inch thick mica. The lagging consisted of a layer of $\frac{1}{4}$" asbestos rope and a section of 2 inch thick magnesia. A 50 watt heating tape and a sheet aluminium foil were wound around the magnesia to minimize heat losses. The heater was wourd in 3 parallel sections:

a) preheater	400 watts
b) reactor i.e. catalyst	350 watts
c) end effects	250 watts

The maximum power into each section is shown and the actual power was adjustable by a resistor in series with each circuit. Further, the overall power being supplied, was controlled with a variac. The controller was a simple on/off type, but by adjusting the power input to be 5 - 10% larger than the power needed to compensate for heat losses, the temperature in the reactor was controlled to an accuracy better than 2^{o} C. The temperature indication was obtained with five 0.062 inch chromel-alumel thermocouples

spaced as follows: one each at centre of the bed at entry, middle and exit from the catalyst and one each at reactor wall, in the middle and at the exit from the catalyst. The signal for the controller was obtained from a thermocouple placed at the centre of the bed at entry to the catalyst.

Measurement of the Outlet Gases from the Reactor

The reaction products were cooled to a maximum temperature of 25° C, in a short counter-current water condenser and after passing through a drying tower containing silica gel, they were introduced into an infra red analyser. The chemical removal of water was found to be necessary because even water in concentrations of saturation vapour pressure at 25° C caused appreciable errors, by forming a film of condensate on the walls of the analysis tube. An orifice plate was fitted into the line connecting the condenser to the analyser and an Evershed* differential pressure transducer (ER 315/1/C) placed across it, gave an electrical signal corresponding to the gas flow rate.

The method of measurement by infra red absorption was chosen because it provided a convenient way of obtaining relatively cheaply a continuous signal corresponding to the concentration of carbon monoxide in the presence of hydrogen, nitrogen, carbon dioxide and water. The Grubb Parsons** instrument had two ranges (0 - 2%, 0 - 20% carbon monoxide) and was provided with a carbon dioxide filter which removed all the effect of this gas on the readings.

The output signal from the analyser, together with the analyser gas flow signal were fed into a PACE TR 10*** general purpose analogue computer, which

*) Evershed and Vignoles Ltd., Acton Works, London W 4
**) Grubb Parsons Co. Ltd., Walkergate, Newcastle-on-Tyne 6
***) Electronic Associates Ltd., Burgess Hill, Sussex

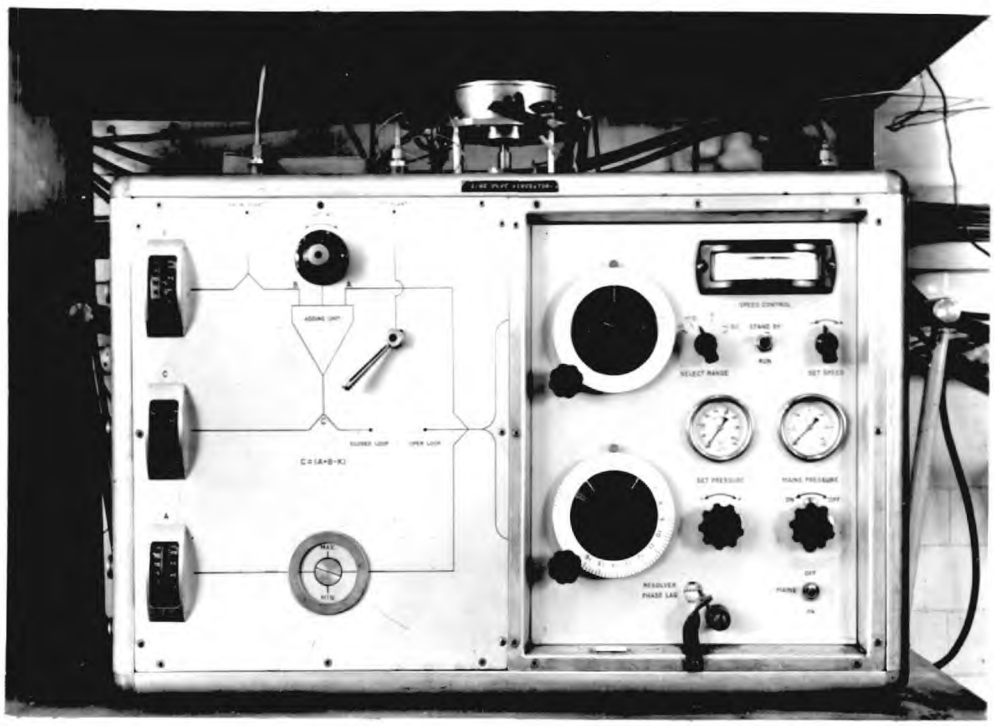

SINE WAVE GENERATOR FIG.8

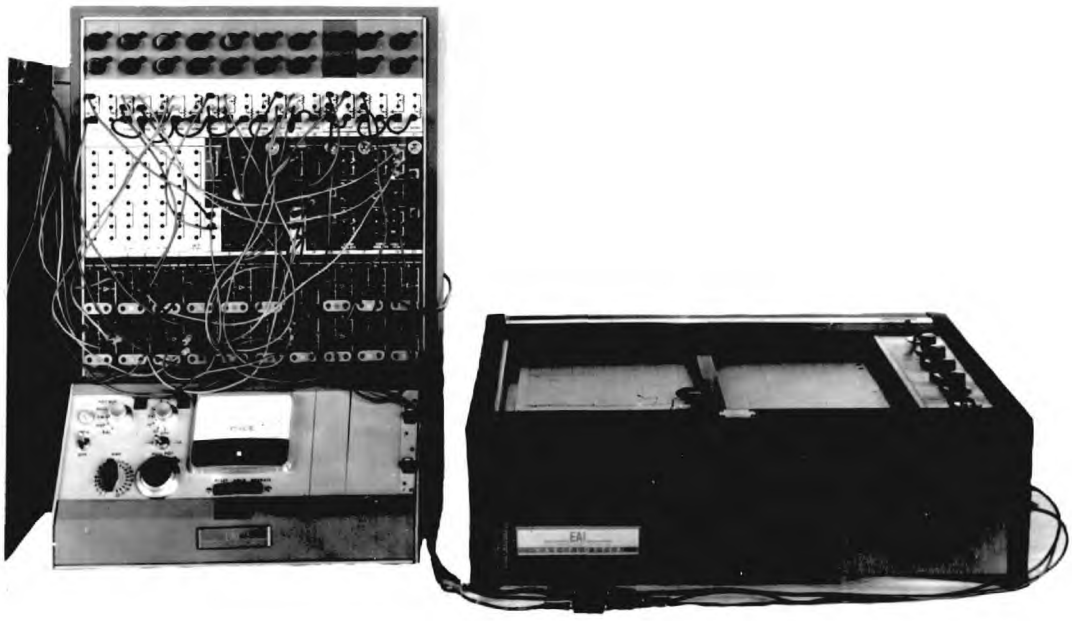

COMPUTER AND X–Y PLOTTER FIG.9

PATCHING DIAGRAM FOR THE ANALOGUE COMPUTER

FIG.10.

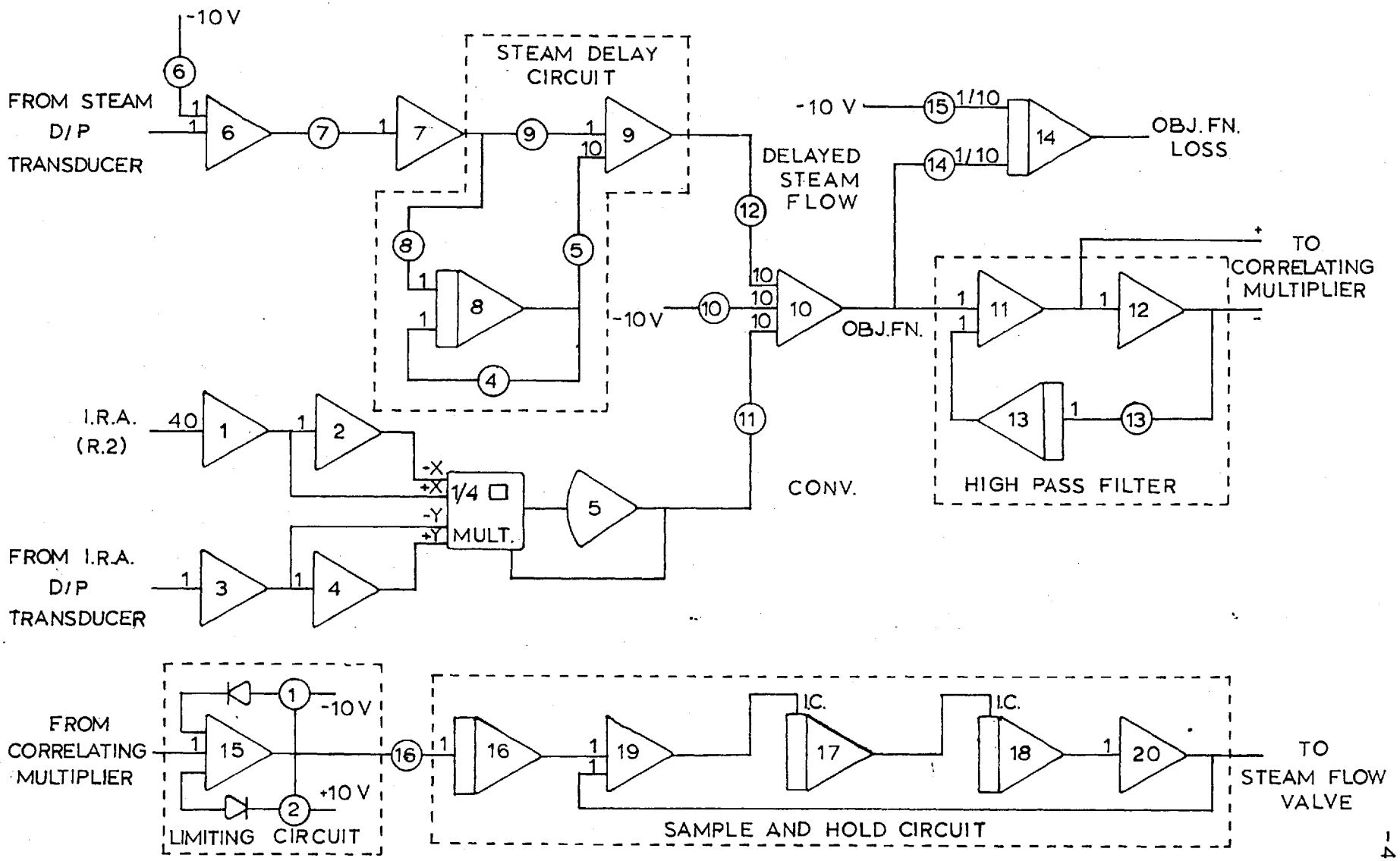

was used to calculate the amount of carbon monoxide removed by the reaction as well as the objective function. The latter is discussed in the next chapter.

2.5. The Analogue Circuit Used

Figure 1o shows the way in which the analogue circuit was patched up on the computer.

Steam Flow

The transducer in the exit line from the saturating vessel measured the total flow of gas and the signal produced was in the range 0 - 10 volts. Calibration showed that 1 volt corresponded to 14.3 l/hr of gas and this was taken into consideration by pot 7. The dry gas flow was subtracted from the total flow in amplifier 6 and so the output from amplifier 7 was the true flow of steam with 1 v equivalent to 10 l/hr. To obtain an equivalence in time between conversion and the steam flow for use in the objective function - discussed in chapter 4 - the steam flow was delayed in the circuit shown. The relevant transfer function was

$$T(p) = - \frac{p - 2/\tau}{p + 2/\tau}$$

and this was simulated by using amplifier 9 and integrator 8 as well as pot 4 which corresponded to $2/\tau$, the time constant of the circuit. Pots 5, 8 and 9 were needed for scaling the signal and pot 12 was the constant used in setting up the objective function.

Conversion

The signal from the analyser was amplified by 40 because the instrument gave a maximum output of 0.5 v for a 0 - 20% range in carbon monoxide

concentration. In fact the concentration range of interest was only 0 - 10%. The variation of concentration was not completely linear throughout the signal range but this effect was neglected - the maximum error thus introduced was 0.1% on the 0 - 10% concentration range. The flow of dry gas into the analyser was measured with another differential pressure transducer and the output of this was calibrated. The two signals were then multiplied on a quarter square multiplier which needed the positive and negative signals as inputs (amps 1, 2, 3, 4) and amplifier 5 in the output. The setting of pot 11 was derived from the calibrations of the transducer and analyser, the inlet flow of carbon monoxide and also the constant used in the objective function. In fact the signal from pot 11 corresponded to (1 - conversion), the output from amplifier 5 being the flow of carbon monoxide leaving the reactor.

Objective Function

The objective function (C) which is described in chapter 4, is

$$C = 0.3 \ (S - 0.4 \ W - 53.3)$$

and this was computed on amplifier 10. Pot 10 corresponded to 0.3 (100 - 53.3) = 14 v. The 100 comes from the percentage conversion i.e. 100 (1 - output from amp 5). An estimate of the maximum value of the objective function was set up on pot 15 and output of amplifier 10 was subtracted from this and the result integrated to give the cumulative loss as an output of integrator 14. In order to prevent overloading when the amplifier reached 10 volts the signal was scaled by a factor of 1/20 and also as a spare comparator was available, the integrator was automatically reset when the signal reached 10 volts. This is not shown in the diagram.

High Pass Filter and Correlating Multiplier

The objective function signal was passed through a high pass filter whose transfer function is

$$T(p) = \frac{pT}{1 + pT}$$

and this was set up by means of amplifiers 11 and 12 and the feed back integrator 13. Pot 13 specified the reciprocal of the filter constant. The outputs from amps 11 and 12 were fed to the two terminals of a sine/cos potentiometer connected to a servo-motor driven shaft on the sine wave generator. The other two quadrants of the potentiometer were earthed and thus a signal corresponding to the product of the filtered objective function and a sine wave was obtained on the wiper of the potentiometer. This signal was fed into amplifier 15.

The Integration Circuit

Amplifier 15 had its output limited by two diodes. The purpose of this is described in chapter 4. The output went through pot 16 which specified the gain of the loop and then into the sample and hold circuit. Here the signal was integrated by integrator 16 and after summation with the current valve position, was fed into the initial condition of integrator 17. A micro switch closed by a magnet fixed to the shaft of the sine wave generator, activated a comparator once every cycle. When this occurred, integrator 17, was put into the operate mode and integrators 16 and 18 were reset. When the comparator switched again after a short time - this being a fixed proportion of the cycle due to the finite size of both the switch and magnet - integrators 16 and 18 were changed to the operate mode. As amplifier 18 had no input signal except

the initial condition, it held the valve setting until it was reset again. Amplifier 20 was required for sign changing purposes and the output from it went to the electro-pneumatic transducer. Here the 0 - 10 volt electrical signal was converted into a 3 - 15 psi pneumatic signal and this was then fed to the summing unit on the sine wave generator where the sine perturbation was added. The resulting signal was fed back into the steam controlling valve.

CHAPTER III

Steady State Model

3.1. Introduction

Suppose that the reactor can be assumed isothermal, that there are negligible variations in the linear velocity along the length of the reactor, i.e. incompressible gas, and that both mass and heat diffusion effects can be considered small i.e. plug flow assumption

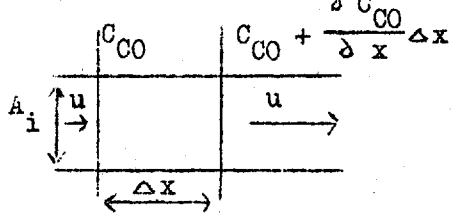

Under these conditions, a carbon monoxide material balance over a differential section of the reactor yields

$$u A_i C_{CO} = u A_i \left(C_{CO} + \frac{\partial C_{CO}}{\partial x}\Delta x\right) + \frac{\partial C_{CO}}{\partial t} A_i \Delta x + A_i \Delta x\, r$$

where C_{CO} = the number of moles of carbon monoxide per unit volume of gas at time t and distance x along the reactor

r = the molar rate of formation of carbon monoxide per unit reactor volume

u = linear velocity of gas through the reactor under the operating conditions

The above equation simplifies to

$$u \frac{\partial C_{CO}}{\partial x} + \frac{\partial C_{CO}}{\partial t} = -r \qquad 3.1.1.$$

This is a partial differential equation, which can be solved by using a

standard method for reducing a first order P.D.E. into two ordinary differential equations (29) i.e.

$$\frac{dx}{u} = \frac{dt}{1} = \frac{d\,C_{CO}}{-r} \qquad 3.1.2.$$

A digital computer programme was developed for solving 3.1.1. using Mars' (21) expression for the reaction rate. However the reactor only contributes a portion to the total dynamics of the process i.e. the saturator, condenser and analyser have dynamic lags of the same order as the reactor. For this reason it was decided that it is unprofitable to pursue the solution of the P.D.E. 3.1.1. In principle differential equations for all the main parts of the process could be set up from theoretical considerations, and from these equations, the overall dynamic behaviour could be obtained. To do this would involve a great deal of estimation of the various process parameters, like heat transfer coefficients, compressibilities of gases etc. and even then, in order to solve the resulting equations, simplifications would probably have to be made. Thus for obtaining a dynamic description of the process, it was decided to calibrate the system in a way described in chapter 4. However if equation 3.1.1. was reduced to steady state, the resulting ordinary first order differential equation was expected to predict realistically the steady state response surface. This is so, because for a given set of inlet gas flow rates, the conversion only depends on the operating conditions in the reactor.

At steady state 3.1.1. reduces to

$$u\,\frac{d\,C_{CO}}{d\,x} = -r \qquad 3.1.3.$$

Different expressions used for the reaction rate, r, in 3.1.3. will yield a number of different response surfaces for the objective function chosen.

Initially Mars' (21) kinetic model is considered, followed by two other kinetic models. The fitting of the models to the practical results and a discussion of the results are given in sections 3.6. and 3.7. at the end of the chapter.

3.2. Mars' Kinetic Model

Mars (21) considered the rate of the water gas shift reaction to be first order with respect to the displacement of the carbon monoxide concentration from its equilibrium value i.e.

$$r = k\,(C_{CO} - (C_{CO})_{eq}) \qquad 3.2.1.$$

where k = rate constant in units of time^{-1}

$(C_{CO})_{eq}$ = the molar concentration of carbon monoxide which would occur if all the gas entering the reactor, reacted to equilibrium

substituting 3.2.1. into 3.1.3.

$$u\,\frac{d\,C_{CO}}{d\,x} = -k\,(C_{CO} - (C_{CO})_{eq}) \qquad 3.2.2.$$

Now $(C_{CO})_{eq}$ is a function only of the inlet composition of the gases and the temperature at a given point in the reactor and at steady state both these remain constant. Thus 3.2.2. can be integrated to

$$C_{CO} = (C_{CO})_{eq} + (\,(C_{CO})_{in} - (C_{CO})_{eq})\,e^{-k\,x_o/u} \qquad 3.2.3.$$

where $(C_{CO})_{in}$ = molar concentration of carbon monoxide at entry to the reactor

and x_o = total length of the reactor

The objective function, S, chosen, is the conversion of carbon monoxide to carbon dioxide and hydrogen, expressed as a percentage of the inlet flow of

carbon monoxide, i.e.

$$S = \frac{(G_{CO})_{in} - G_T C_{CO} \frac{RT}{P_T}}{(G_{CO})_{in}} \quad 100\% \qquad 3.2.4.$$

where $(G_{CO})_{in}$ = the volumetric flow rate of carbon monoxide at entry to the reactor

G_T = total volumetric flow rate of dry gases and steam at distance x along the reactor

As no volume change occurs as a result of the reaction, G_T is constant for all values of x.

In the experiments the quantities measured are: the temperature in the reactor, the inlet gas flow rates, the rate of flow of gas entering the analyser and the concentration of carbon monoxide in this gas. Thus 3.2.3. is now transformed so that the conversion, S, in 3.2.4. is expressed in terms of the measured quantities.

From the gas laws, the molar concentration of carbon monoxide is given by

$$(C_{CO})_{in} = \frac{(P_{CO})_{in}}{RT} = \frac{(G_{CO})_{in}}{G_T} \frac{P_T}{RT} \qquad 3.2.5.$$

$$\text{also } (C_{CO})_{eq} = \frac{(G_{CO})_{in} - (G_{CO})_{eq}}{G_T} \frac{P_T}{RT} \qquad 3.2.6.$$

where $(G_{CO})_{eq}$ = the volume of carbon monoxide which is removed by the reaction in unit time, if equilibrium conditions are reached with a given composition of entry gas

P_T = total pressure in the reactor

R = gas constant

Substituting 3.2.6., 3.2.5. and 3.2.3. into 3.2.4.

$$S = \frac{(G_{CO})_{eq}}{(G_{CO})_{in}} \left(1 - e^{-kx_o/u} \right) \qquad 3.2.7.$$

This states that the conversion, S, is given by the conversion which would occur if the inlet gases reacted to equilibrium at the given reactor temperature, with a correction term to allow for the fact that equilibrium conditions have not been established. The term x_o/u is the time of passage of the gas through the reactor.

An expression for $(G_{CO})_{eq}$ can be obtained from the definition of thermodynamic equilibrium constant for the forward reaction, K_T, i.e.

$$K_T = \frac{\left((G_{CO_2})_{in} + (G_{CO})_{eq} \right) \left((G_{H_2})_{in} + (G_{CO})_{eq} \right)}{\left((G_{CO})_{in} - (G_{CO})_{eq} \right) \left(W_{in} - (G_{CO})_{eq} \right)} \qquad 3.2.8.$$

where W_{in} = volumetric flow rate of steam at entry to the reactor

The dependence of K_T on temperature is obtained from free energy data (25) and is given by

$$K_T = \exp \left\{ \frac{4934.9}{T} + 2.7212 \left(\frac{T}{1000}\right) - 0.77054 \left(\frac{T}{1000}\right)^2 + 0.09687 \left(\frac{T}{1000}\right)^3 - 0.73569 \ln T - 1.603405 \right\} \qquad 3.2.9.$$

where T = temperature measured in ^oK

In the temperature range of interest i.e. 350 - 460° C this can be approximated to an accuracy better than 1% (21) by

$$K_T = 0.01171 \exp (9220/RT)$$
$$= \exp (9220/RT - 4.45) \qquad 3.2.10.$$

For an isothermal reactor operating under steady state conditions, K_T is constant

and thus an explicit expression for $(G_{CO})_{eq}$ can be obtained from 3.2.8.

$$(G_{CO})_{eq} = \frac{\left\{ (G_{CO})_{in} + W_{in} \right\} K_T + (G_{CO_2})_{in} + (G_{H_2})_{in} - \sqrt{B}}{2 (K_T - 1)} \qquad 3.2.11.$$

where $$B = \left\{ \left\{ (G_{CO})_{in} + W_{in} \right\} K_T + (G_{CO_2})_{in} + (G_{H_2})_{in} \right\}^2 - 4(K_T - 1) \left\{ (G_{CO})_{in} W_{in} K_T - (G_{CO_2})_{in} (G_{H_2})_{in} \right\}$$

3.3. Moe's Kinetic Model

Moe (22) considered the shift reaction to be reversible and the rate to be first order with respect to each reactant, i.e.

$$r = k \left(C_{CO} C_{H_2O} - \frac{C_{CO_2} C_{H_2}}{K_T} \right) \qquad 3.3.1.$$

where C_i = molar concentration of gas i at time t and distance x along the reactor

k = rate constant in units time^{-1} vol^{-1} mole.

Substituting 3.3.1. into 3.1.3.

$$u \frac{dC_{CO}}{dx} = - k \left(C_{CO} C_{H_2O} - \frac{C_{CO_2} C_{H_2}}{K_T} \right) \qquad 3.3.2.$$

Let y be the number of litres of carbon monoxide converted per hr, at distance x along the reactor.

Thus

$$C_i = \frac{(G_i)_{in} \pm y}{G_T} \quad \frac{P_T}{RT} \qquad 3.3.3.$$

where $(G_i)_{in}$ = flow rate of gas i at entry to the reactor

$(G_{H_2O})_{in}$ is written as W_{in}

The sign is negative for the reactants CO and H_2O and positive for the products CO_2 and H_2.

Substituting 3.3.3. into 3.3.2.

$$-u\frac{dy}{dx} = -k\left\{\left\{(G_{CO})_{in} - y\right\}\left\{W_{in} - y\right\} - \frac{\left\{(G_{CO_2})_{in} + y\right\}\left\{(G_{H_2})_{in} + y\right\}}{K_T}\right\}\frac{P_T}{G_T\ RT}$$

i.e.

$$-\frac{P_T}{K_T\ G_T\ RT}\quad\frac{kx_o}{u} = \int_o^z \frac{dy}{-y^2(K_T-1)+y\left\{\left\{(G_{CO})_{in}+W_{in}\right\}K_T+(G_{CO_2})_{in}+(G_{H_2})_{in}\right\}-\left\{(G_{CO})_{in}W_{in}K_T-(G_{CO_2})_{in}(G_{H_2})_{in}\right\}}$$

3.3.4.

where z = number of litres of carbon monoxide converted at the exit, x_o, from the reactor

For simplicity of notation, let

$$\mu = K_T - 1 \qquad 3.3.5.$$

$$\lambda = \left((G_{CO})_{in} + W_{in} \right) K_T + (G_{CO_2})_{in} + (G_{H_2})_{in} \qquad 3.3.6.$$

$$\theta = (G_{CO})_{in} W_{in} K_T - (G_{CO_2})_{in} (G_{H_2})_{in} \qquad 3.3.7.$$

Substituting the above three equations into 3.3.4.

$$-\frac{P_T}{K_T G_T RT} \frac{kx_o}{u} = \int_o^z \frac{dy}{-y^2\mu + y\lambda - \theta}$$

$$= \frac{1}{\sqrt{\lambda^2 - 4\mu\theta}} \ln \left\{ \frac{-2\mu z + \lambda - \sqrt{\lambda^2 - 4\mu\theta}}{-2\mu z + \lambda + \sqrt{\lambda^2 - 4\mu\theta}} \Big/ \frac{\lambda - \sqrt{\lambda^2 - 4\mu\theta}}{\lambda + \sqrt{\lambda^2 - 4\mu\theta}} \right\}$$

Hence

$$\frac{-2\mu z + \lambda - \sqrt{\lambda^2 - 4\mu\theta}}{-2\mu z + \lambda + \sqrt{\lambda^2 - 4\mu\theta}} =$$

$$\frac{\lambda - \sqrt{\lambda^2 - 4\mu\theta}}{\lambda + \sqrt{\lambda^2 - 4\mu\theta}} \exp\left\{ -\frac{\sqrt{\lambda^2 - 4\mu\theta}}{G_T K_T} \frac{P_T}{RT} \frac{kx_o}{u} \right\} = \beta' \qquad 3.3.8.$$

$$z = \frac{1}{2\mu} \left\{ \lambda - \frac{1+\beta'}{1-\beta'} \sqrt{\lambda^2 - 4\mu\theta} \right\} \qquad 3.3.9.$$

The percentage conversion, S, for Moe's kinetic model is thus given by

$$S = \frac{z}{(G_{CO})_{in}} 100\%$$

$$= \frac{100}{(G_{CO})_{in} 2\mu} \left\{ \lambda - \frac{(1+\beta')}{(1-\beta')} \sqrt{\lambda^2 - 4\mu\theta} \right\} \qquad 3.3.10.$$

where z is obtained from 3.3.9.

3.3.10. is similar in form to the result 3.2.7. obtained from Mars' kinetic model. In factif 3.2.7. is rewritten using quantities defined by 3.3.5., 3.3.6. and 3.3.7.

$$S = \frac{100}{(G_{CO})_{in}\, 2\mu} \left\{ \lambda - \sqrt{\lambda^2 - 4\mu\theta} \right\} \left\{ 1 - e^{-kx_o/u} \right\} \qquad 3.3.11.$$

In 3.3.10., β' is the term which corrects for the fact that the system is not at equilibrium. Under equilibrium conditions $\beta' \rightarrow o$ and so does $e^{-kx_o/u}$, in which case Mars' and Moe's kinetic models yield identical results, as they should.

3.4. Log Kinetic Model

Consider the reaction rate to be first order with respect to the displacement of carbon monoxide concentration from its equilibrium value, but corrected by the ratios of the other gas concentrations to their equilibrium values i.e.

$$r = k \left\{ C_{CO} - \frac{(C_{CO})_{eq}\ \dfrac{(C_{H_2O})_{eq}}{C_{H_2O}}}{\dfrac{(C_{CO_2})_{eq}}{C_{CO_2}}\ \dfrac{(C_{H_2})_{eq}}{C_{H_2}}} \right\}$$

$$= kC_{CO} \left\{ 1 - \frac{C_{CO_2}\, C_{H_2}}{C_{CO}\, C_{H_2O}\, K_T} \right\} \qquad 3.4.1.$$

This in some sense is an intermediate between Mars' and Moe's models and thus could be of interest. At equilibrium the results predicted should be the same as those for the other two models.

Using the same notation and procedure as in 3.3.

$$-u\frac{dy}{dx}\frac{P_T}{RT\,G_T} = -k\left\{\left\{(G_{CO})_{in}-y\right\} - \frac{\left\{(G_{CO_2})_{in}+y\right\}\left\{(G_{H_2})_{in}+y\right\}}{K_T\,(W-y)}\right\}\frac{P_T}{RT\,G_T}$$

or

$$-\frac{1}{K_T}\frac{kx_o}{u} =$$

$$\int_o^z \frac{(W-y)\,dy}{-y^2(K_T-1)+\left\{\left\{(G_{CO})_{in}+W_{in}\right\}K_T+(G_{CO_2})_{in}+(G_{H_2})_{in}\right\}y-\left\{(G_{CO})_{in}W_{in}K_T-(G_{CO_2})_{in}(G_{H_2})_{in}\right\}}$$

$$= \int_o^z \frac{(W-y)\,dy}{-y^2\mu+y\lambda-\theta} \qquad 3.4.2.$$

$$-\frac{2(K_T-1)}{K_T}\frac{kx_o}{u} = \int_o^z \frac{d\,(y^2\mu-y\lambda+\theta)}{y^2\mu-y\lambda+\theta} + \int_o^z \frac{(\lambda-2\mu W)\,dy}{y^2\mu-y\lambda+\theta}$$

$$= \left\{\ln\,(y^2-y\lambda+\theta)\right\}_o^z + \frac{2\mu W-\lambda}{\sqrt{\lambda^2-4\mu\theta}}\left\{\ln\frac{-2\mu y+\lambda-\sqrt{\lambda^2-4\mu\theta}}{-2\mu y+\lambda+\sqrt{\lambda^2-4\mu\theta}}\right\}_o^z$$

let

$$\frac{2\mu W-\lambda}{\sqrt{\lambda^2-4\mu\theta}} = \psi \qquad 3.4.3.$$

$$(z^2\mu-z\lambda+\theta)\left\{\frac{-2\mu z+\lambda-\sqrt{\lambda^2-4\mu\theta}}{-2\mu z+\lambda+\sqrt{\lambda^2-4\mu\theta}}\right\}^{\psi} =$$

$$\theta\left\{\frac{\lambda-\sqrt{\lambda^2-4\mu\theta}}{\lambda+\sqrt{\lambda^2-4\mu\theta}}\right\}^{\psi}\exp\left\{-2\frac{(K_T-1)}{K_T}\frac{kx_o}{u}\right\} \qquad 3.4.4.$$

3.4.4. is an implicit function for z, which can be readily solved on a digital computer by using the Newton - Raphson interpolation technique.

As in section 3.3. the conversion, S, is given by

$$S = \frac{z}{(G_{CO})_{in}} \quad 100\ \% \qquad 3.4.5.$$

At equilibrium, 3.4.5. yields the same expression for conversion as that derived from Mars' (3.3.11.) and Moe's (3.3.10.) kinetic models.

3.5. Correction for Plug Flow Assumption

In the kinetic models derived in the last three sections, plug flow has been assumed to occur in the reactor. In order for this assumption to apply, the catalyst particles with which the actual reactor was packed, would have had to be very small and this was impracticable for reasons of the resulting large pressure drop. Thus a correction has been applied to the kinetic models to account for the deviations from plug flow. The derivation of this correction is shown below.

It is assumed that the velocity in the outermost layer of the packing, one particle diameter thick is twice the velocity in the interior (24).

Let d = internal diameter of the reactor

d_p = mean particle diameter of the catalyst

Thus the shaded area

$$= \frac{\pi d^2}{4} - \frac{\pi}{4} (d - 2\,dp)^2$$

$$= \pi\, dp\, (d - dp)$$

and the residual area

$$= \frac{\pi}{4} (d - 2\,dp)^2$$

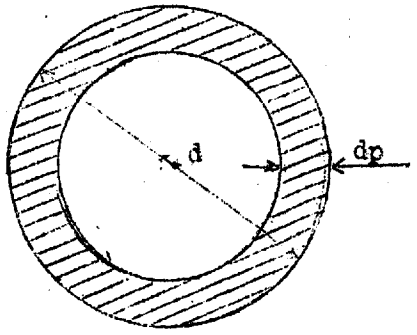

Further, let G_T = total gas flow rate passing through the reactor measured at the reaction temperature

and α = proportion of the total flow, flowing in the inner area of the reactor.

As the velocity in the shaded area is twice the velocity in the inner area then

$$\frac{(1-\alpha)\,G_T}{\pi\, dp\,(d-dp)} = \frac{2\alpha\, G_T}{\frac{\pi}{4}(d-2\,dp)^2}$$

$$\alpha = \frac{(d-2\,dp)^2}{2\,d^2-(d-2\,dp)^2} \qquad 3.5.1.$$

The deviation from plug flow alters the mean time of passage of the gas through the reactor. Thus the gas flow is considered in two parts so as to separate the effect of the gas travelling at the centre of the reactor from that travelling near the wall. The terms containing the time of passage through the reactor, for the three models considered, are all of the form $\exp(-\phi x_o/u)$ where ϕ is independent of the time of passage. Thus the effect on conversion of the time of passage of the gas travelling in the central portion of the reactor is

$$a_1 = \exp\left\{ -\phi x_o \Big/ \frac{\alpha\, G_T}{\frac{\pi}{4}(d-2\,dp)^2} \right\}$$

but the average velocity, u, is

$$u = \frac{G_T}{\frac{\pi}{4} d^2}$$

$$a_1 = \exp\left\{ -\frac{\phi x_o}{u} \left\{ 2 - \left(1 - 2\frac{dp}{d}\right)^2 \right\} \right\} \qquad 3.5.2.$$

The time of passage in the outer portion of the reactor is half that in the

centre, thus the effect a_2 is

$$a_2 = \exp\left\{ - \frac{\phi x_o}{u} \frac{1}{2} \left\{ 2 - \left(1 - 2 \frac{dp}{d} \right)^2 \right\} \right\} \qquad 3.5.3.$$

In the computer programmes, conversions for each of the models, are calculated in two parts on the basis of 3.5.2. and 3.5.3. and the total conversion, S, is obtained from

$$S = \alpha S\ (a_1) + (1 - \alpha)\ S\ (a_2) \qquad 3.5.4.$$

where $S\ (a_i)$ = conversion calculated with the time of passage term given by a_i.

In the reactor used

inside diameter, (d) = 25.4 mm

mean catalyst particle diameter (dp) = 0.65 mm

thus from 3.5.1. α = 0.82

i.e. 18% of the gas flowing through the reactor travels at twice the velocity at the centre.

Further

$$a_1 = \exp\ (-1.10\ \phi x_o/u)$$
$$a_2 = \exp\ (-0.55\ \phi x_o/u) \qquad 3.5.5.$$

TABLE 3.1.

PREDICTION ERRORS OF CONSTANT COMPOSITION DATA
USING MARS, MOE AND LOG MODELS

RUN NO	TEMP (°K)	STEAM FLOW (L/HR)	OBS CONV (%)	ERRORS IN PREDICTION (CONV (OBS) - CONV (MODEL))					
				MARS' MODEL		MOE'S MODEL		LOG MODEL	
				K (T) TRUE	K (T) BEST	K (T) TRUE	K (T) BEST	K (T) TRUE	K (T) BEST
22	362	10.4	60.0	- 8.6	- 7.0	1.1	1.3	- 10.7	- 8.3
29	362	13.6	72.1	- 4.5	- 2.9	4.5	4.8	- 6.3	- 4.2
28	361	17.9	78.0	- 4.1	- 2.8	3.5	3.7	- 6.1	- 4.4
24	361	20.8	79.1	- 5.2	- 4.0	1.1	1.3	- 7.0	- 5.6
20	362	27.2	83.7	- 3.2	- 2.3	0.5	0.7	- 4.7	- 3.7
30	362	32.2	86.4	- 1.5	- 0.8	0.5	0.7	- 2.8	- 2.0
23	362	36.6	86.1	- 2.1	- 1.4	- 1.2	- 1.1	- 3.3	- 2.6
21	362	39.4	86.3	- 1.7	- 1.1	- 1.5	- 1.4	- 2.8	- 2.2
25	363	52.3	87.2	- 1.0	- 0.5	- 3.3	- 3.2	- 1.8	- 1.3
19	363	62.5	87.7	0.6	0.9	- 3.5	- 3.4	- 0.1	0.3
27	365	72.7	88.7	1.7	2.1	- 3.5	- 3.4	1.3	1.6
31	362	75.0	87.7	3.0	3.3	- 3.5	- 3.4	2.6	2.9
26	365	89.5	89.0	3.9	4.2	- 3.5	- 3.4	3.7	3.9
6	389	9.5	62.3	- 0.6	1.2	0.7	1.3	- 4.4	- 4.4
14	387	11.1	66.3	- 2.2	- 0.3	- 0.7	- 0.1	- 2.4	- 0.4
5	389	12.7	73.6	1.1	2.9	2.3	2.9	1.0	3.4
15	387	16.6	80.0	- 0.1	1.6	1.2	1.8	- 0.2	2.0
12	387	21.1	85.0	0.1	1.6	1.0	1.5	0.0	1.9
11	389	22.4	88.0	2.2	3.6	2.9	3.4	2.1	4.0
17	390	24.2	85.3	- 1.6	- 0.3	- 1.0	- 0.6	- 1.7	0.0
4	387	27.0	86.6	- 2.0	- 0.8	- 1.4	- 1.0	- 2.1	- 0.6
16	388	32.4	88.8	- 1.9	- 0.9	- 1.5	- 1.2	- 2.0	- 0.7
8	389	37.0	89.9	- 2.0	- 1.1	- 1.7	- 1.4	- 2.2	- 1.0
3	388	43.6	92.1	- 1.0	- 0.3	- 0.9	- 0.7	- 1.3	- 0.3
10	388	50.6	92.9	- 1.1	- 0.5	- 1.2	- 0.9	- 1.4	- 0.5
7	389	58.0	93.9	- 0.7	- 0.2	- 0.9	- 0.7	- 1.1	- 0.3
18	390	62.2	94.2	- 0.7	- 0.2	- 1.0	- 0.8	- 1.1	- 0.4
13	390	66.1	94.7	- 0.4	0.1	- 0.8	- 0.6	- 0.8	- 0.1
2	388	68.1	94.6	- 0.5	- 0.1	- 1.0	- 0.8	- 0.9	- 0.3
1	389	80.5	95.3	- 0.2	0.2	- 0.9	- 0.8	- 1.6	- 0.1
9	389	119.0	95.1	- 0.1	0.1	- 2.0	- 2.0	- 0.5	- 0.2
42	411	12.2	65.2	- 2.7	- 0.7	- 2.6	- 1.9	- 2.8	- 1.5
38	407	13.2	67.6	- 3.4	- 1.5	- 3.3	- 2.5	- 3.4	- 0.9
44	410	17.2	77.0	- 0.7	1.1	- 0.6	0.1	- 0.7	1.7
43	412	20.9	81.2	- 0.6	1.1	- 0.6	0.1	- 0.6	1.6
39	406	22.9	82.8	- 1.4	0.1	- 1.3	- 0.8	- 1.4	0.6
37	405	27.7	84.4	- 2.9	- 1.7	- 2.9	- 2.4	- 3.0	- 1.2
45	410	31.2	86.6	- 1.9	- 0.7	- 1.8	- 1.4	- 1.9	- 0.3
34	407	35.5	87.5	- 2.8	- 1.7	- 2.8	- 2.4	- 2.8	- 1.4
40	411	36.5	88.7	- 1.6	- 0.5	- 1.6	- 1.1	- 1.6	- 0.2

RUN NO	TEMP (°K)	STEAM FLOW (L/HR)	OBS CONV (%)	ERRORS IN PREDICTION (CONV (OBS) - CONV (MODEL))					
				MARS' MODEL		MOE'S MODEL		LOG MODEL	
				K (T) TRUE	K (T) BEST	K (T) TRUE	K (T) BEST	K (T) TRUE	K (T) BEST
36	408	40.5	89.8	- 1.7	- 0.8	- 1.7	- 1.4	- 1.7	- 0.5
33	406	47.2	91.4	- 1.5	- 0.7	- 1.5	- 1.2	- 1.5	- 0.5
46	411	47.9	92.1	- 0.6	0.2	- 0.6	- 0.3	- 0.6	0.5
41	410	56.7	92.7	- 1.3	- 0.6	- 1.3	- 1.0	- 1.3	- 0.4
47	413	65.8	94.0	- 0.7	- 0.1	- 0.7	- 0.5	- 0.7	0.1
32	404	74.8	95.2	- 0.5	0.0	- 0.5	- 0.4	- 0.6	0.1
35	407	84.6	95.5	- 0.6	- 0.1	- 0.7	- 0.5	- 0.7	- 0.1
54	425	12.1	67.3	1.8	3.8	1.8	2.6	0.6	0.6
60	425	12.5	64.6	- 2.0	0.0	- 2.0	- 1.1	- 2.1	- 2.1
62	422	17.5	76.5	0.2	2.1	0.2	1.0	0.2	2.6
53	426	18.7	78.5	1.1	2.9	1.1	1.8	1.1	3.5
61	422	24.5	83.5	0.0	1.6	0.0	0.7	0.0	2.1
55	423	30.7	85.6	- 1.4	- 0.1	- 1.4	- 0.9	- 1.4	0.4
51	423	32.5	85.9	- 1.9	- 0.6	- 1.9	- 1.4	- 1.9	- 0.2
48	427	38.6	88.7	- 0.8	0.3	- 0.8	- 0.4	- 0.8	0.7
59	424	45.6	92.1	0.6	1.6	0.6	1.0	0.6	1.9
52	424	47.8	90.8	- 1.1	- 0.2	- 1.1	- 0.7	- 1.1	0.1
58	426	53.2	91.7	- 0.9	- 0.1	- 0.9	- 0.6	- 0.9	0.2
49	428	56.2	92.1	- 0.8	0.0	- 0.8	- 0.5	- 0.8	0.3
50	428	66.8	93.3	- 0.8	- 0.1	- 0.8	- 0.5	- 0.8	0.1
63	425	74.8	94.2	- 0.7	- 0.1	- 0.7	- 0.5	- 0.7	0.1
56	428	88.6	95.1	- 0.5	0.0	- 0.5	- 0.3	- 0.5	0.2
57	432	104.9	95.9	- 0.3	0.2	- 0.3	- 0.1	- 0.3	0.3
71	448	13.8	66.9	0.8	3.0	0.8	1.8	0.8	0.2
69	446	19.7	74.7	- 1.2	0.8	- 1.2	- 0.3	- 1.2	1.4
70	444	25.5	82.0	0.4	2.1	0.4	1.1	0.4	2.6
75	444	26.2	80.0	- 2.2	- 0.4	- 2.2	- 1.4	- 2.2	0.1
66	444	36.8	85.2	- 2.3	- 1.0	- 2.3	- 1.7	- 2.3	- 0.6
65	445	43.4	88.0	- 1.4	- 0.2	- 1.4	- 0.9	- 1.4	0.2
72	444	44.2	88.8	- 0.8	0.3	- 0.8	- 0.3	- 0.8	0.7
74	444	52.0	89.9	- 1.4	- 0.3	- 1.4	- 0.9	- 1.4	0.0
68	446	59.5	91.2	- 1.1	- 0.2	- 1.1	- 0.7	- 1.1	0.1
64	447	71.1	92.7	- 0.8	- 0.1	- 0.8	- 0.5	- 0.8	0.2
67	447	87.6	94.0	- 0.8	- 0.1	- 0.8	- 0.5	- 0.8	0.1
73	446	107.8	95.5	- 0.3	0.2	- 0.3	- 0.1	- 0.3	0.3

	MARS MODEL	MOE'S MODEL	LOG MODEL
RATE CONSTANT	$\exp(34.00 - \frac{30750}{RT})$	$\exp(37.00 - \frac{28500}{RT})$	$\exp(34.00 - \frac{30200}{RT})$
BEST EQUILIB EXPRESSION	$\exp(\frac{9200}{RT} - 4.55)$	$\exp(\frac{9300}{RT} - 4.55)$	$\exp(\frac{9150}{RT} - 4.55)$
S.S. OF DISCREPANCIES USING TRUE EQUILIB CONSTANT	308	225	458
S.S. OF DISCREPANCIES USING BEST EQUILIB EXPRESSION	217	202	306

Steady State Calibrations

These were performed in two separate parts. In one case the dry gas composition was fixed and the response curve of conversion was investigated on a grid of values of steam flow rate and temperature. The gas composition was that used later in the optimisation runs and the purpose was to find a kinetic model to use in simulation studies of the process. The other set of experiments was performed in order to test the adequacy of the various models under widely differing conditions of gas composition and temperature. For this reason a factorially designed experiment was run and analysed.

3.6. Constant Composition Data

The gas flow rates were fixed at

Carbon monoxide	9.0	l/hr
Carbon dioxide	-	
Hydrogen	23.8	l/hr
Nitrogen	21.2	l/hr

The steam flow was varied from about 10 to 100 l/hr. As the process took several hours to settle down to a steady state after a change in temperature, the procedure was to keep the temperature constant and alter the steam flow so that the response surface is defined as closely as possible. Thus the experiments were not randomised. The results obtained are shown in Table 3.1.; the column "Run No" shows the order in which the experiments were performed. Mars', Moe's and Log kinetic models derived earlier in the chapter were fitted to the 75 experimental results by using the log likelihood function technique (26). In this, one minimizes the sum of squares of the discrepancies between the

actual results obtained and the results predicted by a particular choice of the fitted parameters. The contours of the sum of the discrepancies are then prepared as the dependent variable with the fitted constants as axes. In the models the constants adjusted were the activation energy, E (k), and the modified Arrhenius constant, A'(k); i.e. the rate constant, k, is

$$k = A(k) \exp (- E(k) / RT)$$

$$= \exp (A'(k) - E (k) / RT) \qquad 3.6.1.$$

The use of the rate constant for fitting a given model to satisfy practical results is very reasonable, because the Arrhenius constant describes the activity of a given catalyst and this in general is not a reproducible quantity. The reasons for this are that the catalyst activity is a function of such effects as radial diffusion of gas in the reactor, pore size and configuration of catalyst particles. Further the activation energy, although theoretically constant, varies considerably in its estimate from one experimentor to another (19, 21, 22, 23).

A typical contour diagram is shown in figure 3.1. The shape of the contours was found to be virtually the same for the three models considered and thus only the diagram for Mars' model is shown. As can be noticed from the caption in figure 3.1. the thermodynamic expression for the equilibrium constant was not used, but this is unimportant because the point of interest is that the contours are parallel lines about a minimum value which is a straight line. At combinations of small values of E (k) and large ones of A' (k) the sums of squares of deviations tend to a constant value which is the same for each of the three models. This is because all models consider deviations from equilibrium conversion and once the rate of reaction becomes sufficiently

large the system is at equilibrium. In this case any change in the parameters $A'(k)$ and $E(k)$ does not affect the sum of square of deviations. Cuts through the contours at constant values of $A'(k)$ and $E(k)$ are shown in figures 3.3. and 3.4. The contours in those figures were obtained by using the thermodynamic expression for the equilibrium constant. For Mars' model the best value of the activation energy is 30750 cals/mole ^{o}K when $A'(k) = 34.00$ but due to the shape of figure 3.1. there are an infinite number of optimum combinations of $A'(k)$ and $E(k)$.

The fact that the minimum contour lies on what effectively is a ridge means that $E(k)$ and $A'(k)$ are correlated. Closer examination shows that in the range of temperatures considered, values of $E(k)$ and $A'(k)$ lying on the minimum line give approximately the same values for the rate constant, k, at any given temperature, irrespective of the temperature of operation. The reason for this is the very limited range of temperature in which it is practicable to operate the reaction. Above about 460^{o} C the reverse reaction starts to predominate while at temperatures much lower than 360^{o} C there is danger of carbon being deposited on the catalyst due to the reaction.

$$2\ CO \longrightarrow CO_2 + C$$

In the range 360^{o} C to 450^{o} C the variations in the reciprocal temperature only amount to $\pm$ 6.6 % of the mean value. The temperature is thus virtually constant and so the effect ($A'(k) - E(k) / RT$) can be obtained by an infinite number of combinations of $A'(k)$ and $E(k)$. This often occurs in rate constant determinations and tends to be ignored. It may at least partially account for the large discrepancies in the values of the activation energy quoted in literature.

LACK OF FIT AS A FUNCTION OF
THE RATE CONSTANT PARAMETERS
EQUILIBRIUM EXPRESSION GIVEN BY 3.6.3
A(KT) = 4.55 E(KT) = 9200

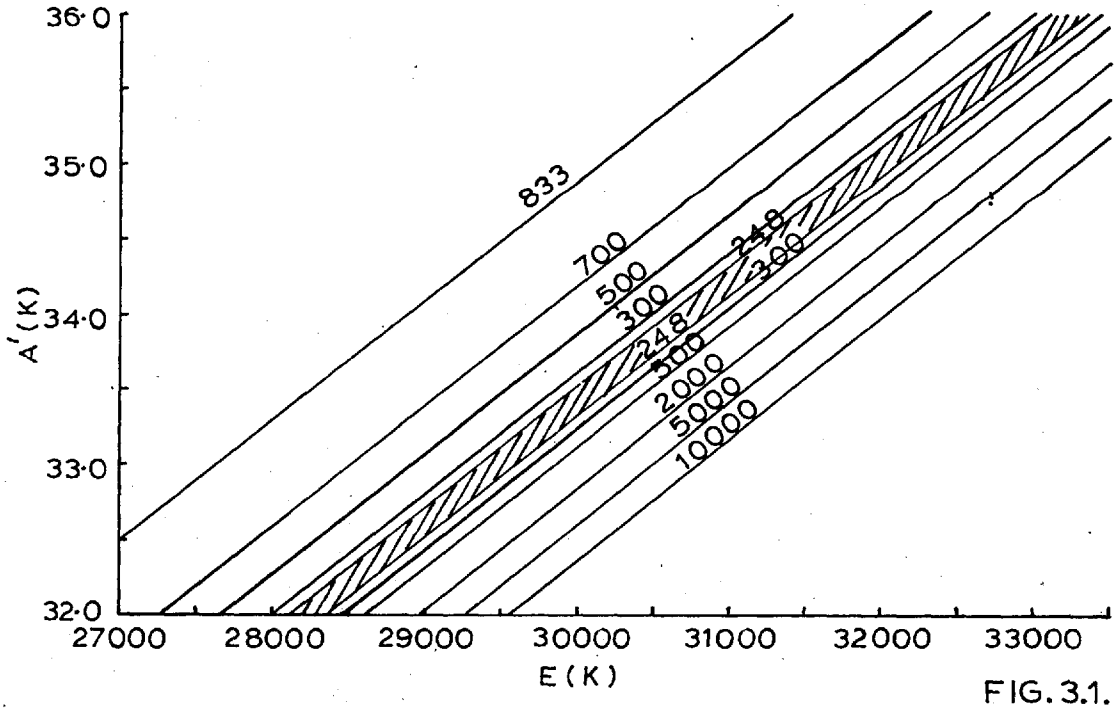

FIG. 3.1.

LACK OF FIT AS A FUNCTION OF THE
EQUILIBRIUM CONSTANT PARAMETERS
A(K) = 34.0 E(K) = 30750

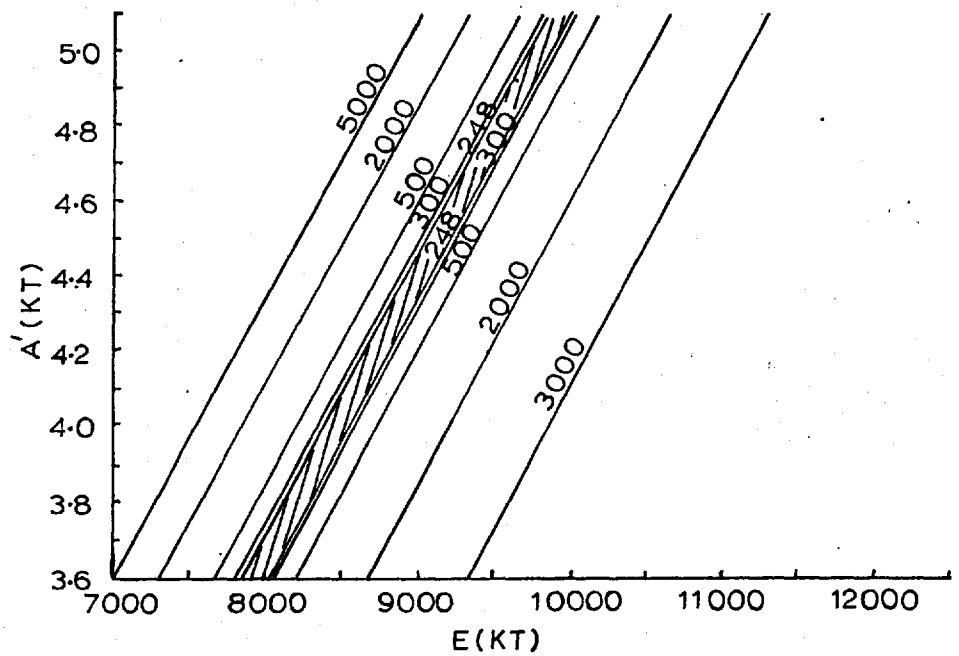

FIG. 3.2.

MARS' KINETIC MODEL

THERMODYNAMIC VALUE OF EQUILIBRIUM CONSTANT

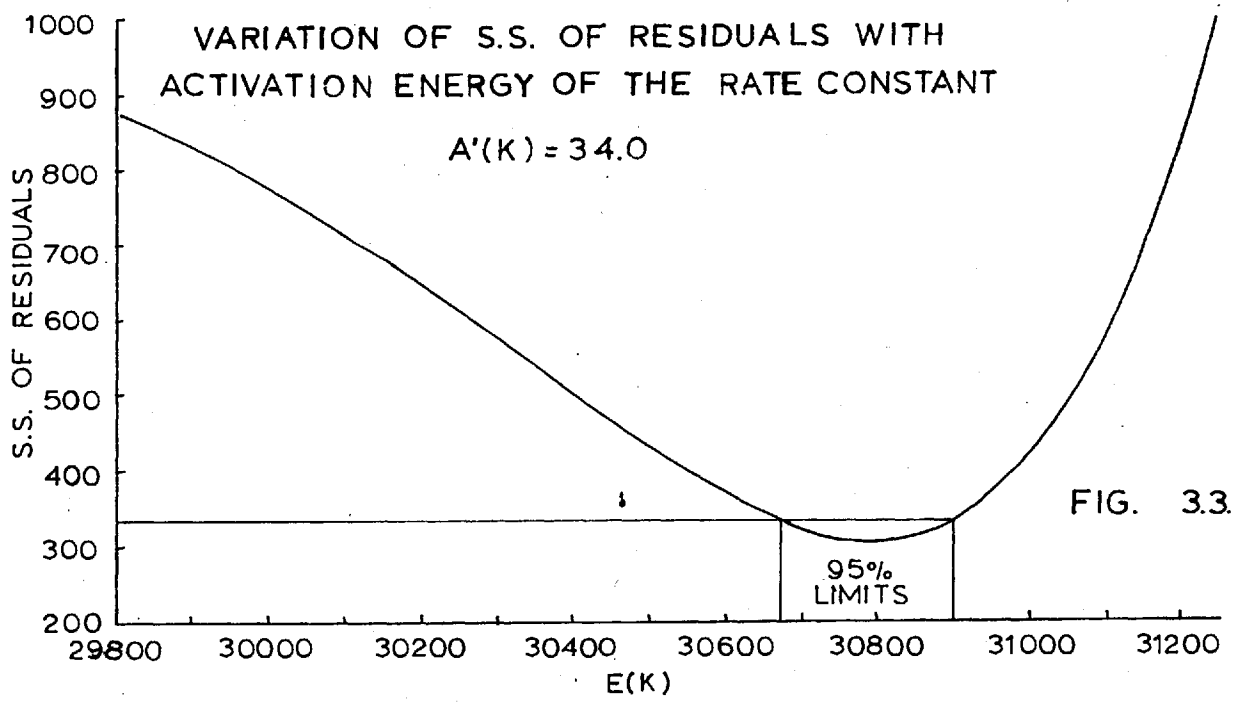

FIG. 3.3.

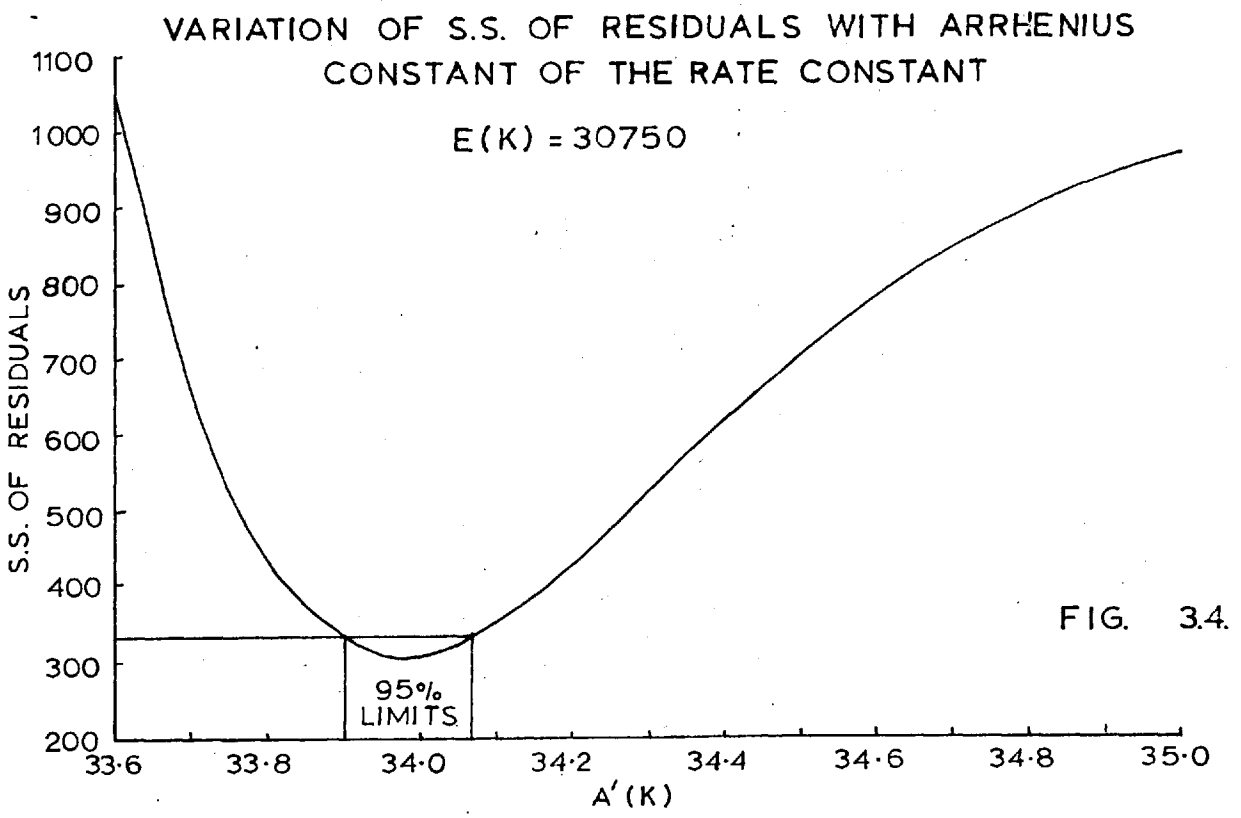

FIG. 3.4.

The accuracy with which the parameters are estimated can be obtained approximately from

$$S.S. = S.S._{min} \left\{ 1 + \frac{p}{N - p} F_{p,\ N-p}(o.95) \right\} \qquad 3.6.2.$$

where p = number of parameters estimated i.e. 2

N = number of results considered i.e. 75

$S.S.$ = sum of squares of discrepancies between the observed and predicted results.

$F_{p,\ N-p}(o.95)$ = value of the F statistic at 95% significance level with p and N-p degrees of freedom

= 3.13 when $p = 2$ and $N = 75$

The approximation is due to the assumption that the sum of squares of the residuals after the predicted results have been subtracted from the observed ones, is normally distributed. The "F" statistic is itself a ratio of two χ^2 distributions each χ^2 being the distribution of the squares of a normal population.

From 3.6.2. the sum of squares corresponding to the 95% confidence limits can be found. A line at this level is then drawn parallel to the relevant parameter axis and the values of parameters at the intercepts of this line with the S.S. curve yields the confidence limits. This is illustrated in figures 3.3. and 3.4.

Using the thermodynamic expression for the equilibrium constant the best

fits for the three models are listed below;

TABLE 3.2.

Model	E (k)	A'(k)	S.S. of Deviations	Confidence Limits	
				E (k)	A'(k)
Mars	30750	34.00	308	30670 - 30900	33.90 - 34.06
Moe	28500	37.00	225	28400 - 28600	36.92 - 37.05
Log	30200	34.00	458	30090 - 30380	33.89 - 34.10

The resulting errors in prediction for the individual observations are shown in table 3.1. (columns 5, 7 and 9).

The adequacy of the models is again determined by means of the "F" test. The assumption here is that the model describes exactly the actual reaction mechanism. If this is so, the ratio

$$\frac{\text{variance estimated from the sum of squares of the discrepancies between predicted and observed results}}{\text{variance due to lack of reproducibility of results}}$$

is distributed as the "F" statistic with $N - p$ and p' degrees of freedom, where p' is the number of results used to estimate the denominator.

Although no runs were truly replicated, an estimate of the reproducibility of results was obtained by interpolation of closely lying results. These were arbitrarily assumed as any steam flow readings measured at the same temperature and differing by less than 3 l/hr. On the basis of 20 such readings an estimate of 6^2 was found to be 3.26. Thus from the sums of squares of discrepancies and 6^2, the value of $F_{73,20}$ could be found for each model. This is shown in table 3.3.

TABLE 5.3.

Model	S.S. min	$F_{73,\ 20}$
Mars	308	1.30
Moe	225	0.94
Log	458	1.92

From tables (32) $F_{73,\ 20}\ (\ 0.90\ ) = 1.67$ $F_{73,\ 20}\ (\ 0.95\ ) = 1.94$

From these it can be seen that both Mars' and Moe's kinetic models give significant predictions of the reaction, whereas the prediction of the Log model although significant is not as good. The level of significance, however, is determined to a large extent by the accuracy of the estimate of σ^2. The lack of replicated results does make this value somewhat suspect. But in any case the results indicate that Mars' and Moe's models predict the conversion fairly well.

A question of interest is whether there is any significant difference between the three models. On the surface it would seem that the answer is "no" for Mars' and Moe's models and "yes" for the Log model. A formal way of deciding, is by using yet again the "F" test. The hypothesis is that if the value of the ratio of the sums of squares of discrepancies using any two different models is less than a given "F" value, then the discrepancies could have originated from the same normal distribution. The relevant statistic is $F_{73,\ 73}$ because the χ^2 for each model has 73 degrees of freedom, two degrees of freedom being lost in the estimation of the two constants for each model.

The values of the relevant ratios are shown below;

$$\frac{\text{Mars}}{\text{Moe}} = 1.37 \qquad \frac{\text{Log}}{\text{Mars}} = 1.49 \qquad \frac{\text{Log}}{\text{Moe}} = 2.04$$

From Davies (32)

$$F_{73,73}\ (0.90) = 1.37 \qquad F_{73,73}\ (0.95) = 1.50 \qquad F_{73,73}\ (0.99) = 1.77$$

Thus it follows that Mars'and Moe's models are distinguishable 90% of the time which is not very significant in a statistical sense, Log and Mars' models give predictions which are distinguishable 19 times out of 20 which is significant and the predictions from Log and Moe's models are different at the 99% significance level.

One further point of note is that the three models all give the same predictions if equilibrium conditions are reached. Thus if one wants to compare their relative merits only values away from equilibrium conversions should be considered. By examination of table 3.1. this means that only runs at 365° C and 390° C should be compared i.e. the first 31 runs. The relevant analysis is given in table 3.4.

TABLE 3.4.

Model	S.S. over First 31 Runs	Ratio	$F_{31,31}$
Mars	232	Mars / Moe	1.57
Moe	135	Log / Mars	1.74
Log	369	Log / Moe	2.73

From Davies (32)

$$F_{31,31}\ (0.90) = 1.61 \qquad F_{31,31}\ (0.95) = 1.84 \qquad F_{31,31}\ (0.99) = 2.39$$

Thus once again Mars' and Moe's models are insignificantly different but both Mars' and Log models and Log and Moe's models are different, the Log model giving the worst predictions.

So far the models have considered deviations from the thermodynamic value of equilibrium conversion. However, both Mars and Moe (21, 22) in their papers gave expressions which approximate the equilibrium constant by an exponential form i.e.

$$K_T = A(KT) \exp\left(E(KT) / RT \right)$$
$$= \exp\left(E(KT) / RT - A'(KT) \right) \qquad 3.6.3.$$

Taking this approximation a step further, the constants $A'(KT)$ and $E(KT)$ were chosen so as to minimize the sum of squares of discrepancies between the predicted and actual conversions. Thus four constants were used to fit the best model, but as was mentioned earlier and can be seen from figures 3.1. and 3.2. only two of the constants are independent. If one of the parameters of both k and K_T is fixed, this specifies the optimum values of the remaining two parameters. For Mars' model this is shown in figure 3.5. The shaded portion indicates the 95% confidence limit. However, at another setting of $A'(k)$ or $A'(KT)$ the optimum values of the activation energies would change but the shape of the contours would stay the same. Figures 3.6. to 3.17. illustrate this point. Each figure shows the variation of the sum of squares of residuals with one parameter while the other three parameters are kept constant. The confidence limits calculated from 3.6.2. are also indicated.

The results are shown in the tables 3.5. and 3.6.

MARS' MODEL

LACK OF FIT AS A FUNCTION OF THE RATE AND EQUILIBRIUM CONSTANTS ACTIVATION ENERGIES

A'(K) = 34·0 A'(KT) = 4·55

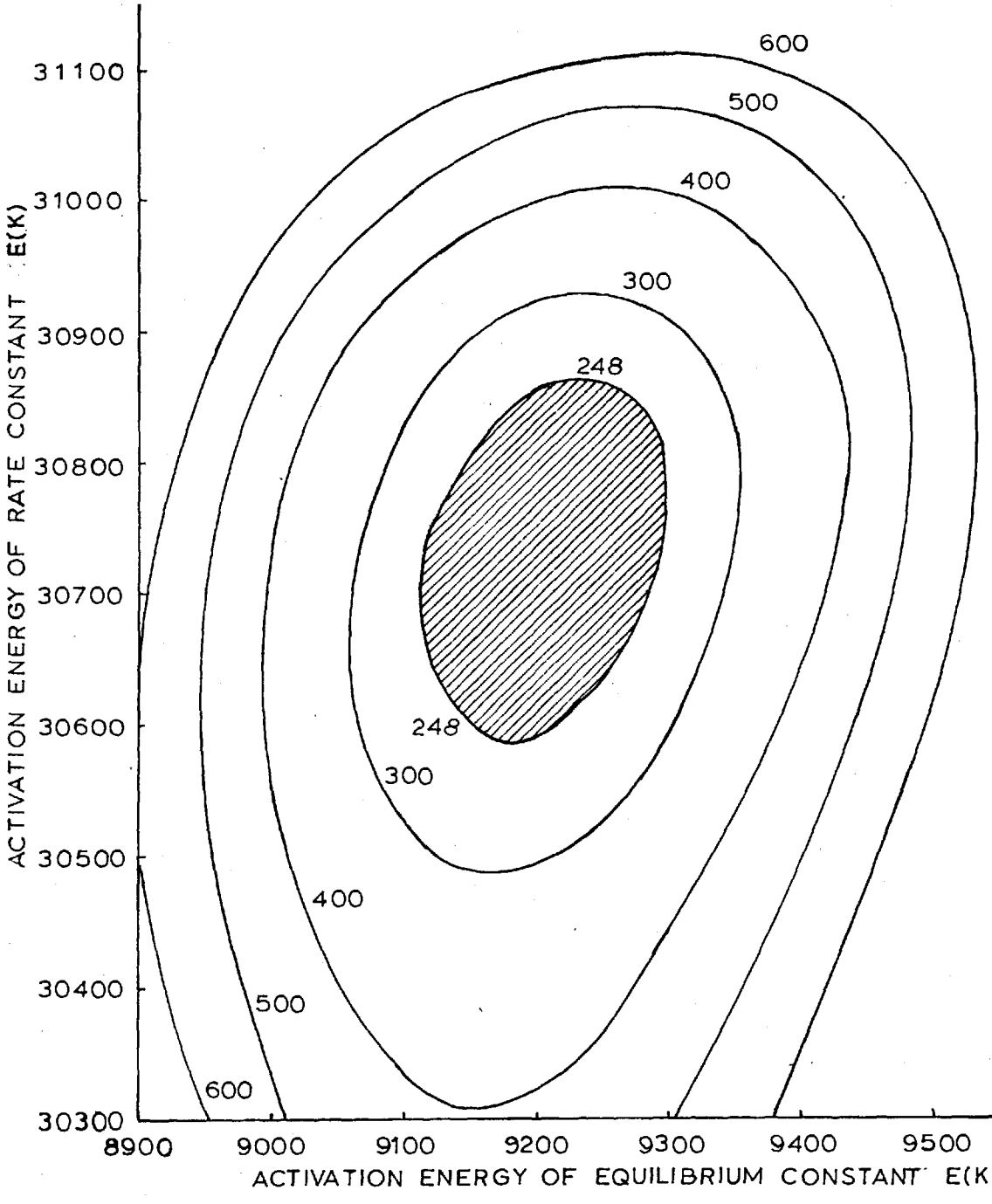

FIG.3.5.

MARS' KINETIC MODEL

EQUILIBRIUM EXPRESSION GIVEN BY 3.6.3.

A'(KT) = 4.55 E(KT) = 9200

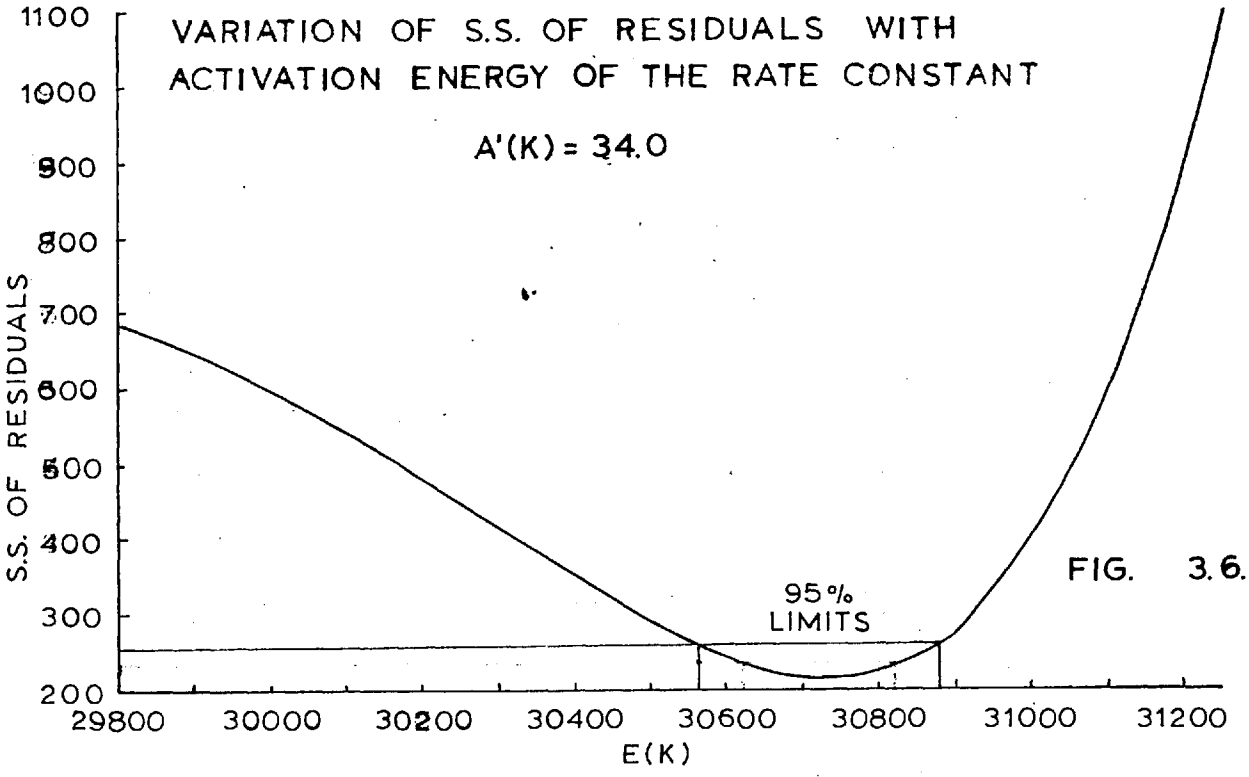

FIG. 3.6.

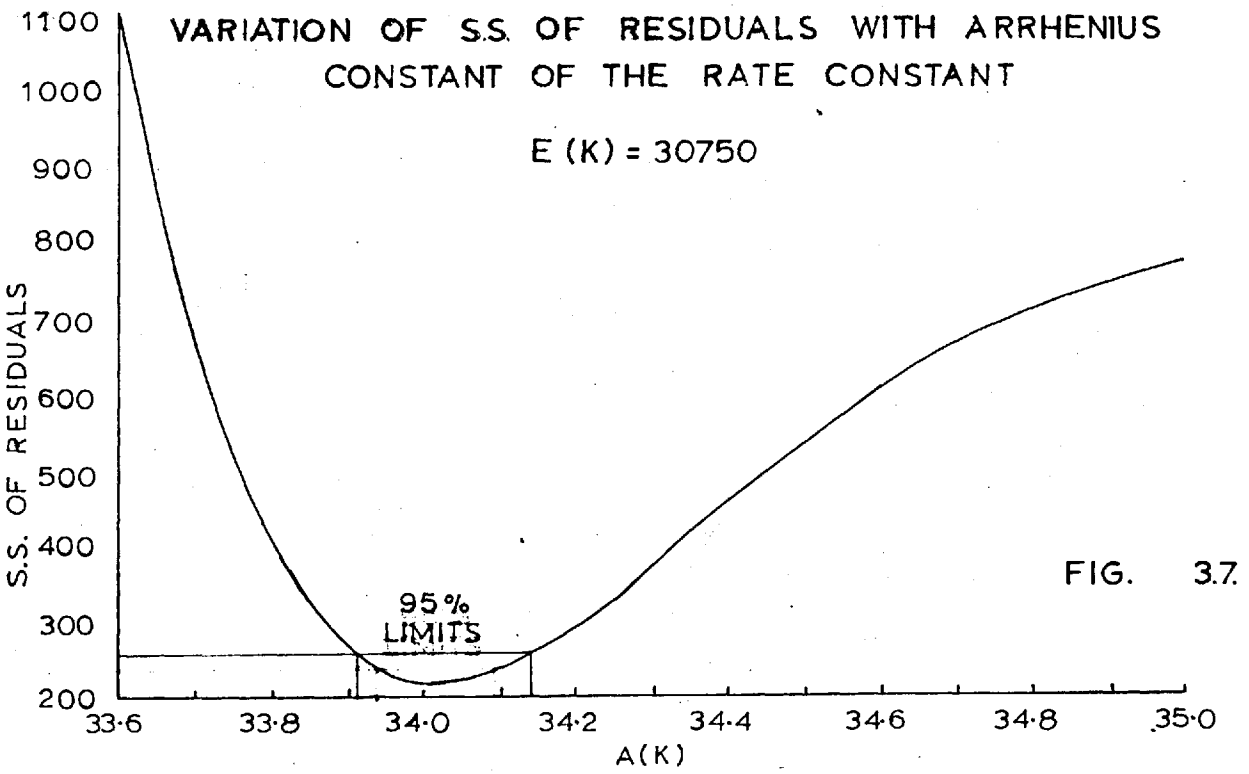

FIG. 3.7.

MOE'S KINETIC MODEL

EQUILIBRIUM EXPRESSION GIVEN BY 3.6.3.

A'(KT) = 4.55 E(KT) = 9300

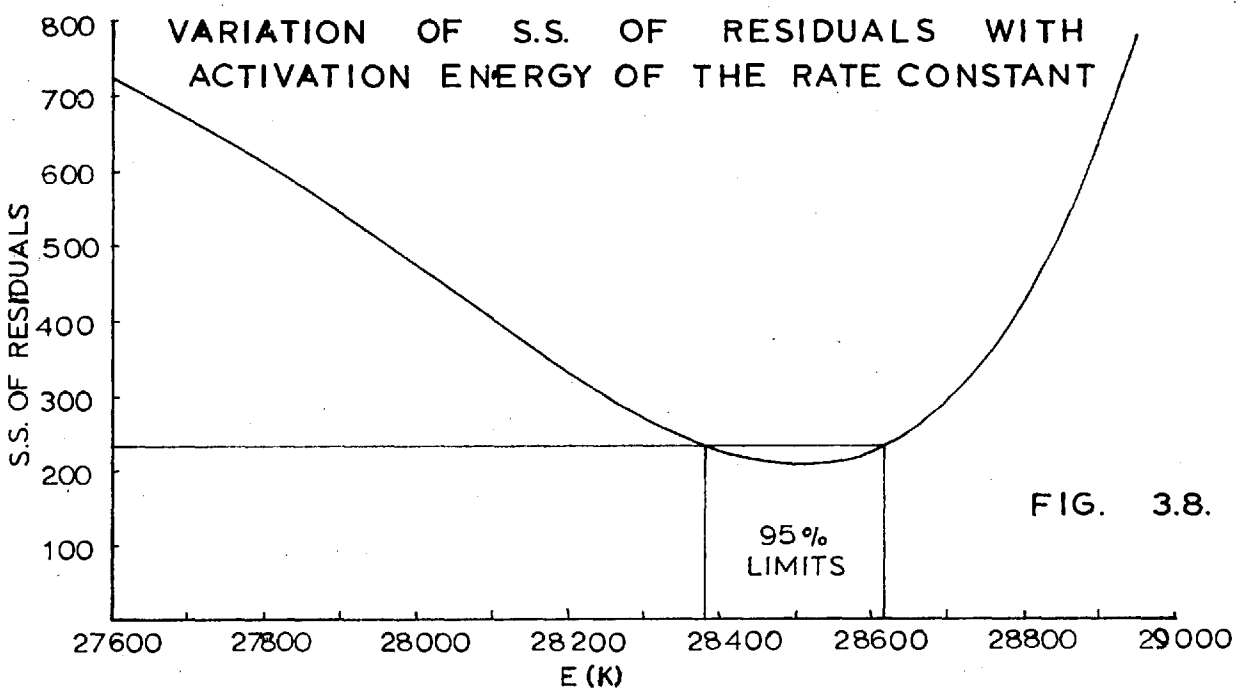

FIG. 3.8.

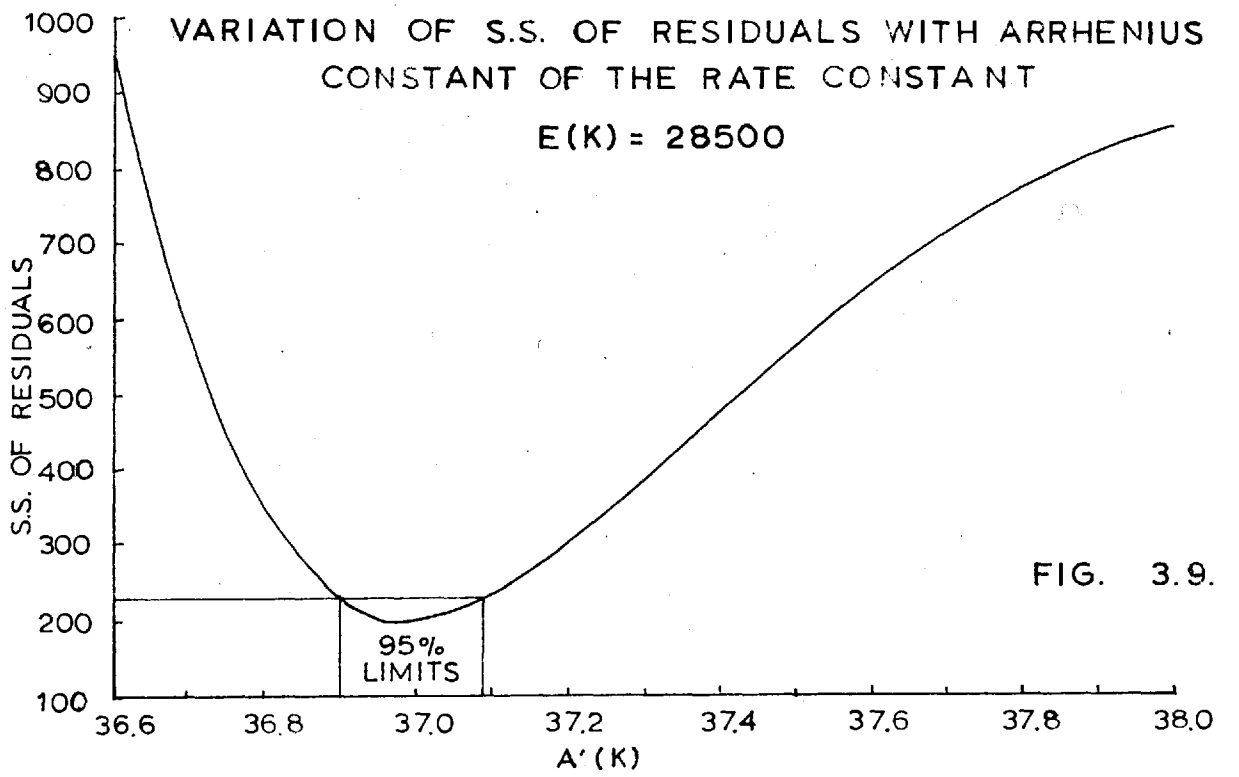

FIG. 3.9.

LOG KINETIC MODEL

EQUILIBRIUM EXPRESSION GIVEN BY 3.6.3.

A'(KT) = 4.55 E(KT) = 9150

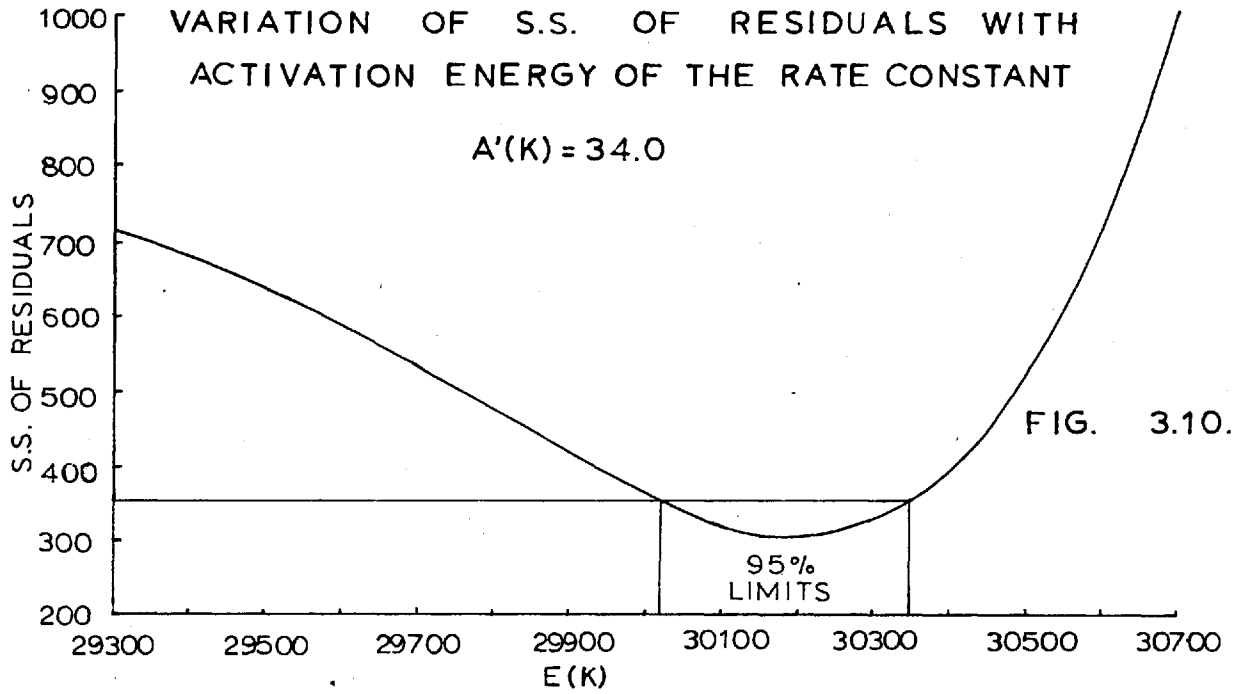

FIG. 3.10.

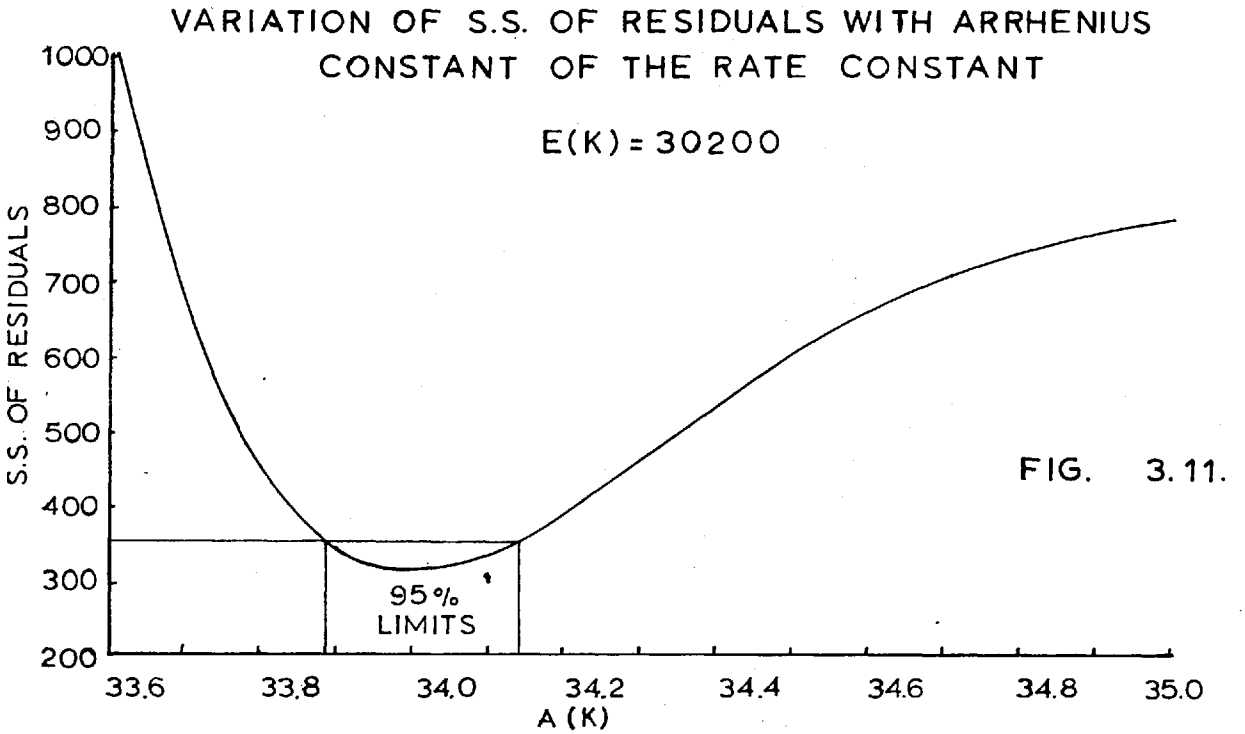

FIG. 3.11.

MARS' KINETIC MODEL
EQUILIBRIUM EXPRESSION GIVEN BY 3.6.3.
A'(K) = 34.0 E(K) = 30750

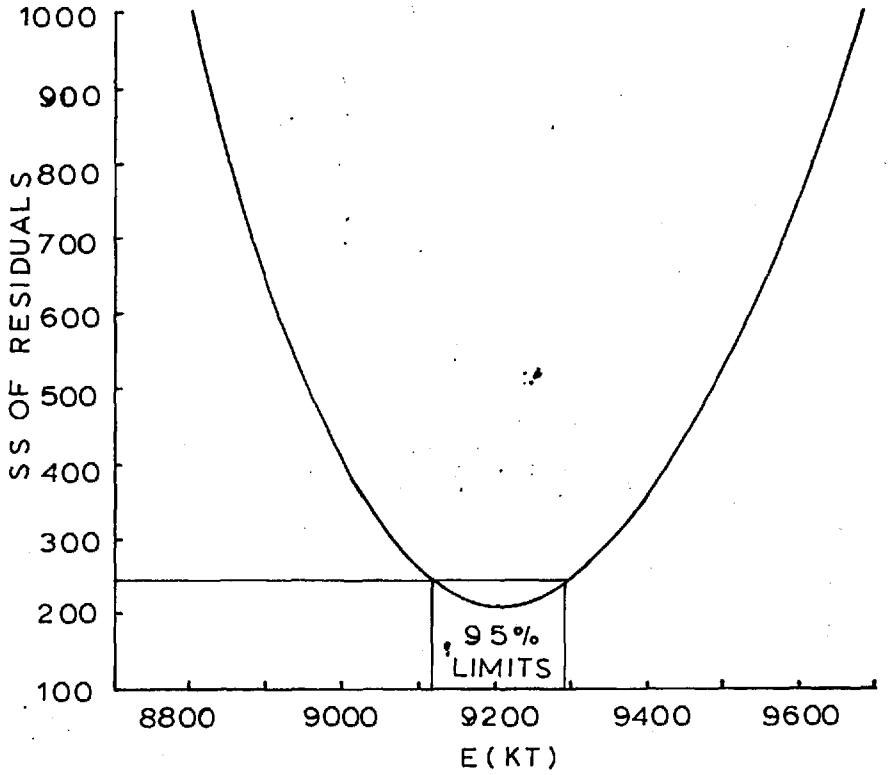

VARIATION OF THE S.S. OF RESIDUALS WITH ACTIVATION ENERGY OF THE EQUILIBRIUM EXPRESSION

A'(KT) = 4.55

FIG. 3.12

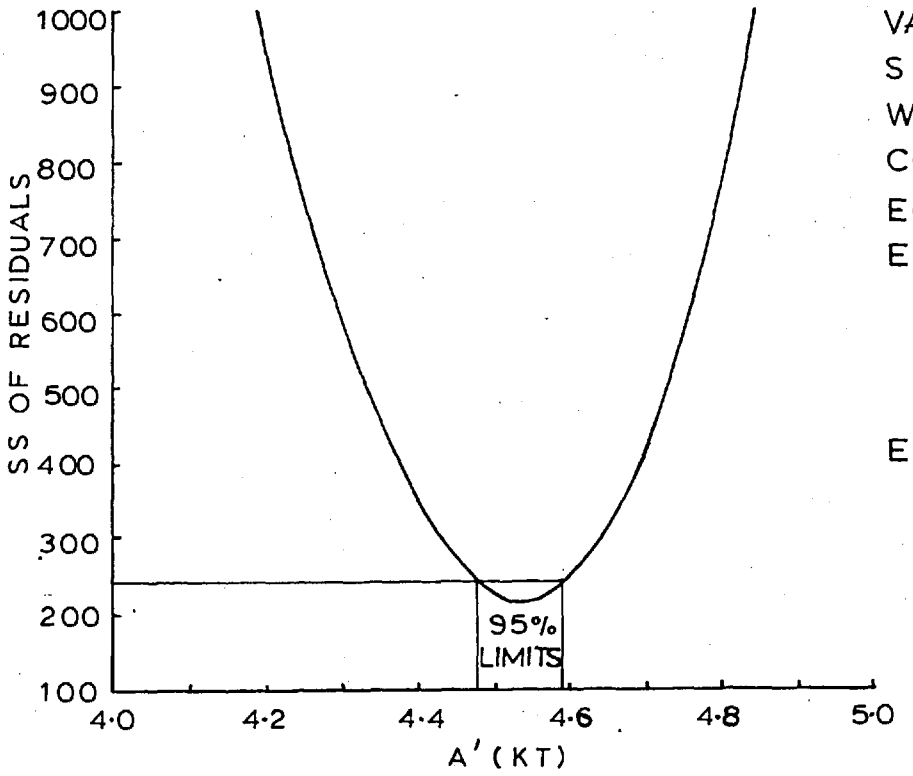

VARIATION OF THE SS OF RESIDUALS WITH ARRHENIUS CONSTANT OF THE EQUILIBRIUM EXPRESSION

E(KT) = 9200

FIG. 3.13

MOE'S KINETIC MODEL
EQUILIBRIUM EXPRESSION GIVEN BY 3.6.3.

A(K) = 37.0 E(K) = 28500

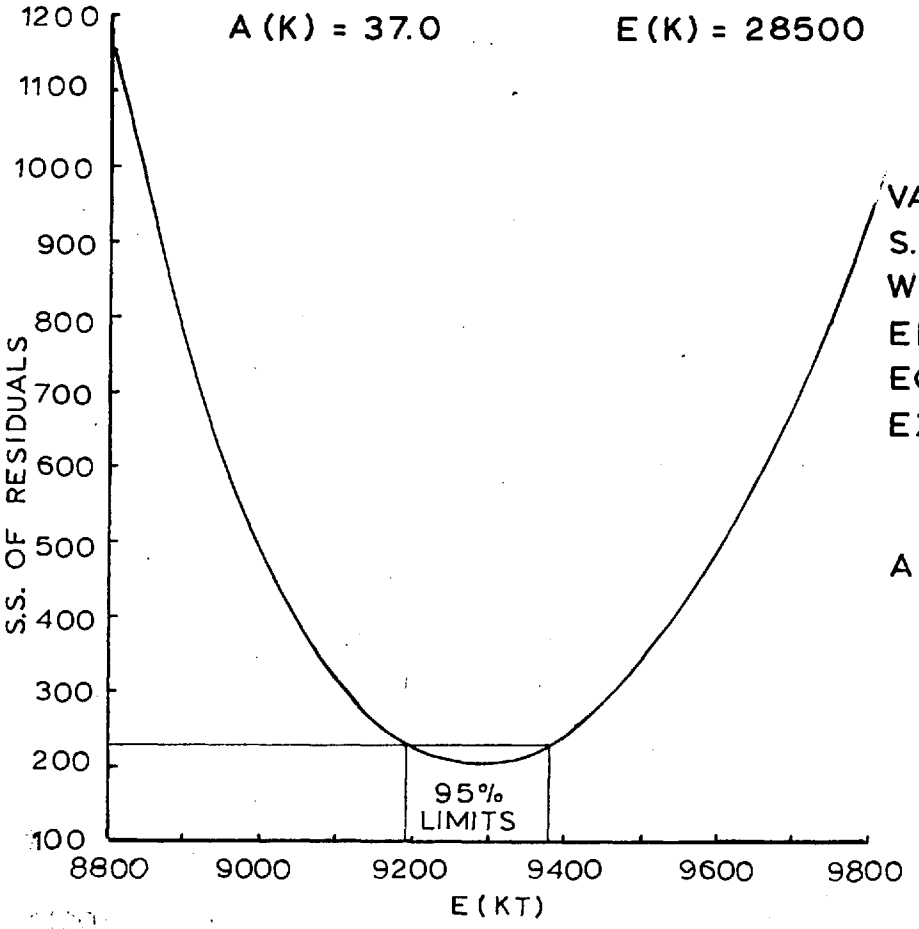

VARIATION OF THE S.S. OF RESIDUALS WITH ACTIVATION ENERGY OF THE EQUILIBRIUM EXPRESSION

A(KT) = 4.55

FIG. 3.14.

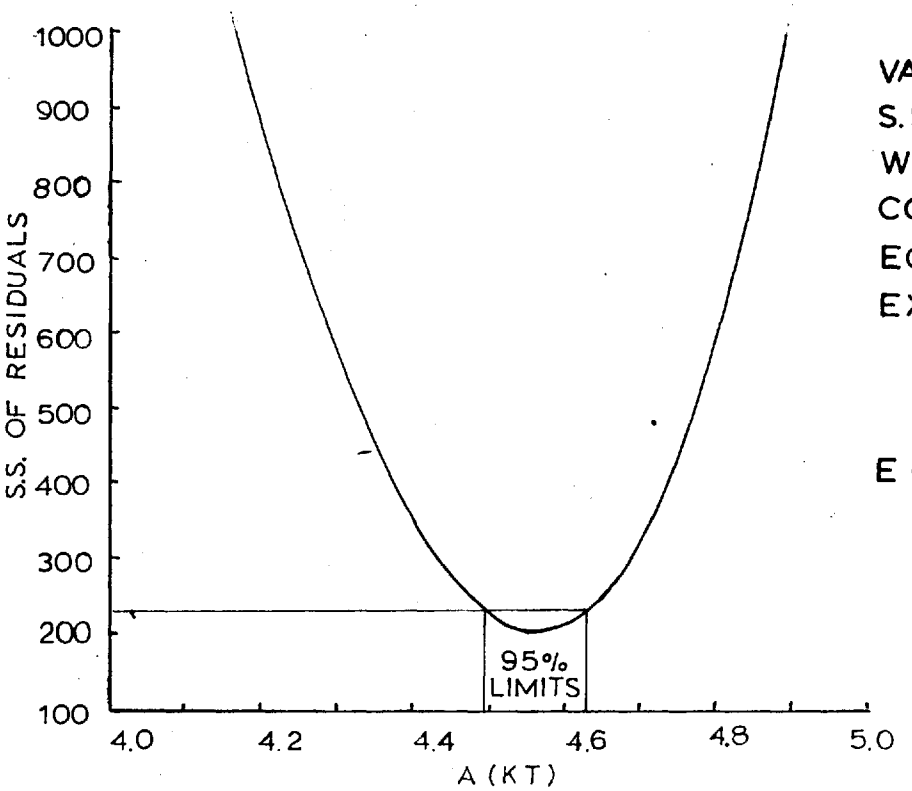

VARIATION OF THE S.S. OF RESIDUALS WITH ARRHENIUS CONSTANT OF THE EQUILIBRIUM EXPRESSION

E(KT) = 9300

FIG. 3.15.

LOG KINETIC MODEL

EQUILIBRIUM EXPESSION GIVEN BY 3.6.3.

A'(K) = 34.0 E(K) = 30200

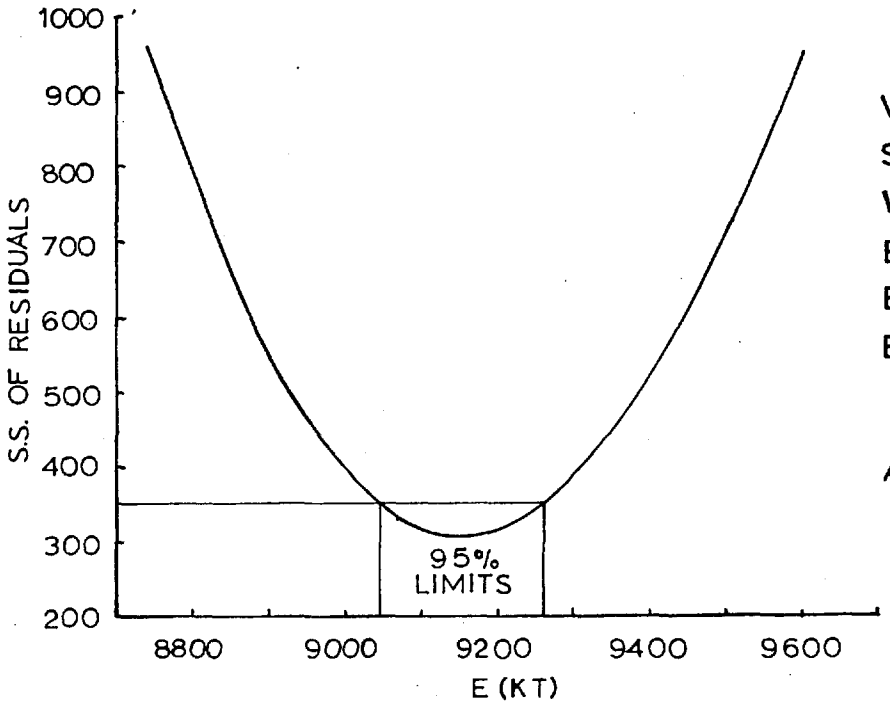

VARIATION OF THE S.S. OF RESIDUALS WITH ACTIVATION ENERGY OF THE EQUILIBRIUM EXPRESSION

A'(KT) = 4.55

FIG. 3.16.

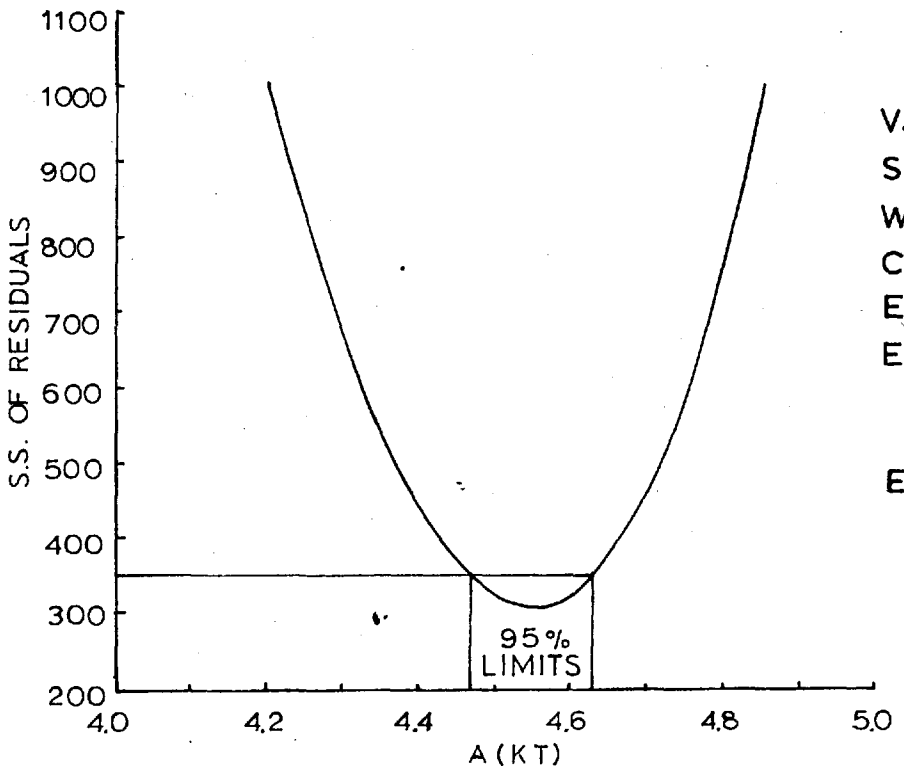

VARIATION OF THE S.S. OF RESIDUALS WITH ARRHENIUS CONSTANT OF THE EQUILIBRIUM EXPRESSION

E (KT) = 9150

FIG. 3.17.

TABLE 3.5.

Model	S.S. of Deviations with True Equilibrium Constant	S.S. of Deviations with Best Value of 4 Parameters	Fixed Parameters		Best Values	
			A'(k)	A'(KT)	E(k)	E(KT)
Mars	3o8	217	34.o	4.55	3o25o	92oo
Moe	225	2o1	37.o	4.55	285oo	93oo
Log	458	3o6	34.o	4.55	3o2oo	915o

TABLE 3.6.

Model	Confidence Limits			
	A'(k)	A'(KT)	E(k)	E(KT)
Mars	33.92 - 34.12	4.47 - 4.6o	3o585 - 3o86o	912o - 93oo
Moe	36.9o - 37.o9	4.49 - 4.63	2839o - 2863o	919o - 9375
Log	33.88 - 34.14	4.47 - 4.63	3oo15 - 3o345	9o4o - 926o

Analysing the results in the same way as those where the true equilibrium constant was used, it can be shown that the differences in prediction of the three models are insignificant at the 95% level. Thus one could in principle use any of the three to predict conversions. A point to notice is that the"equilibrium"conversion is now different for each model and thus one does not find points of identical predictions. Hence all the 75 runs are compared in order to distinguish between the models. The predicted contour surfaces for the three models are shown in figures3.18, 3.19, 3.2o. They are all seen to be rising ridge contours. Cuts through the contours at constant temperature and constant steam flow rate are shown in figures 3.21. and 3.22. Here the predictions of conversion on the basis of the three models are superimposed and the true conversions are also indicated. The three models are seen to give very similar predictions at high temperatures but differ considerably at the low ones.

CONVERSION RESPONSE SURFACE PREDICTED BY MARS' MODEL

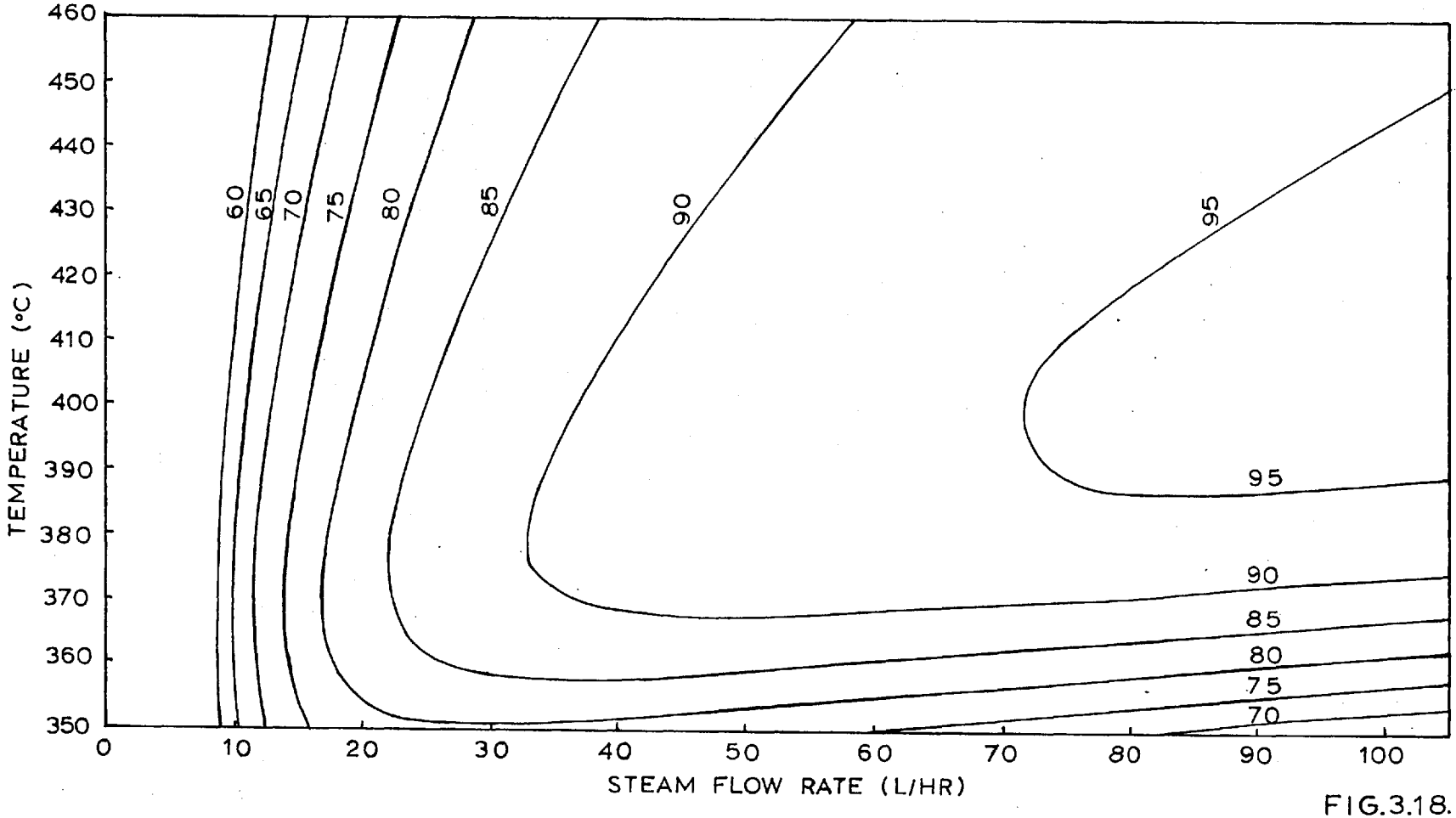

FIG.3.18.

CONVERSION RESPONSE SURFACE PREDICTED BY MOE'S MODEL

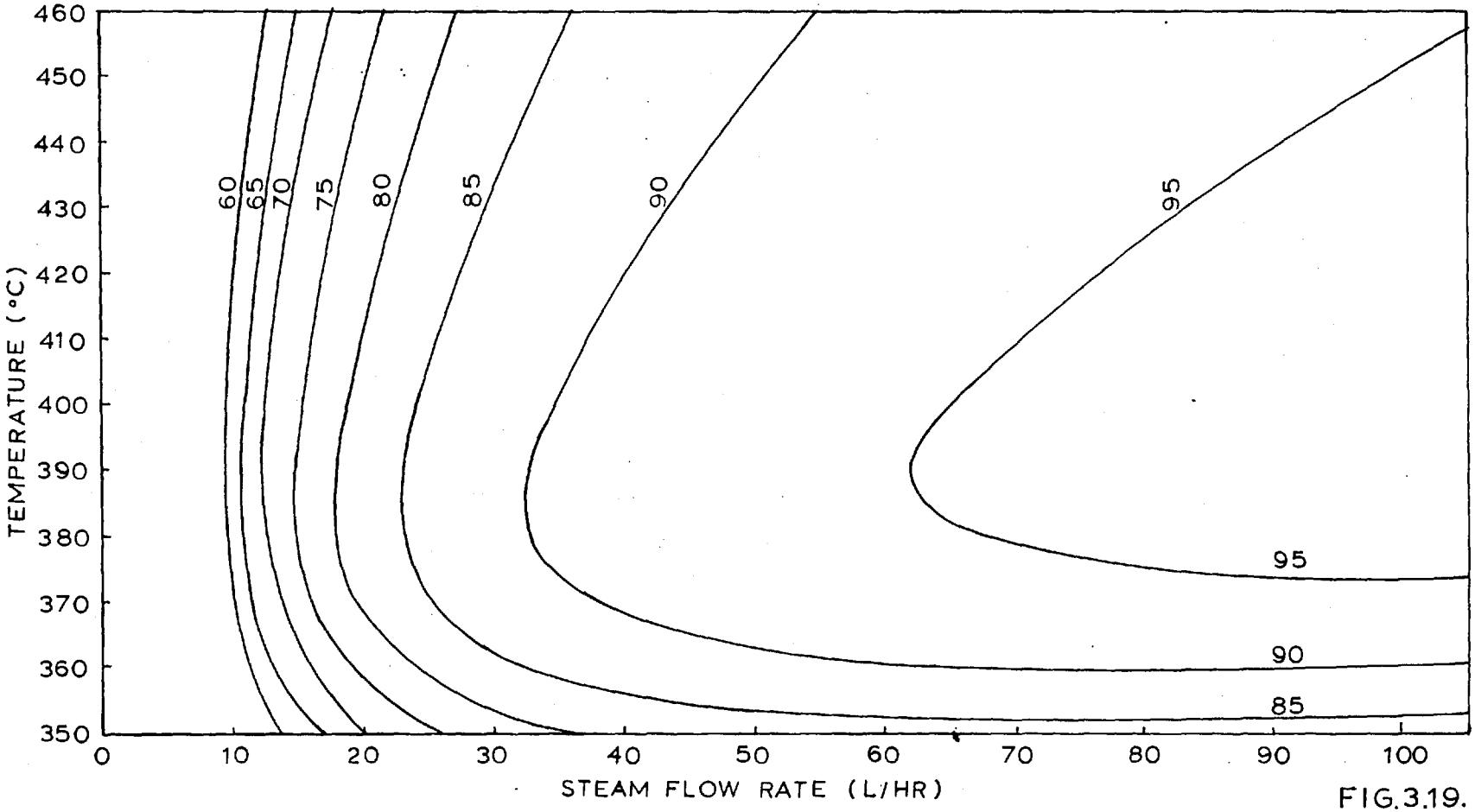

FIG.3.19.

CONVERSION RESPONSE SURFACE PREDICTED BY LOG MODEL

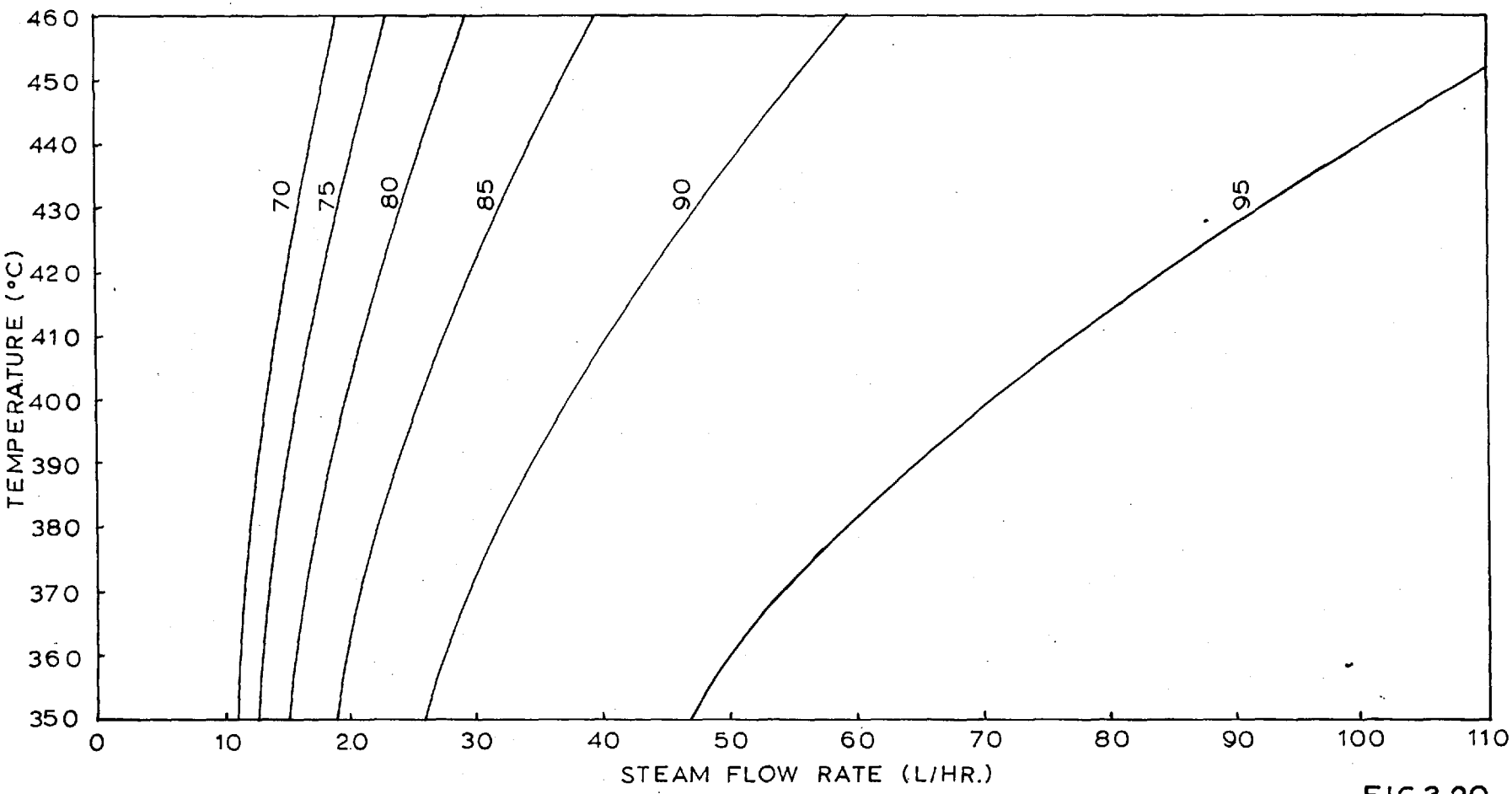

FIG.3.20.

VARIATION OF CONVERSION WITH TEMPERATURE AT 34 L/HR STEAM FLOW

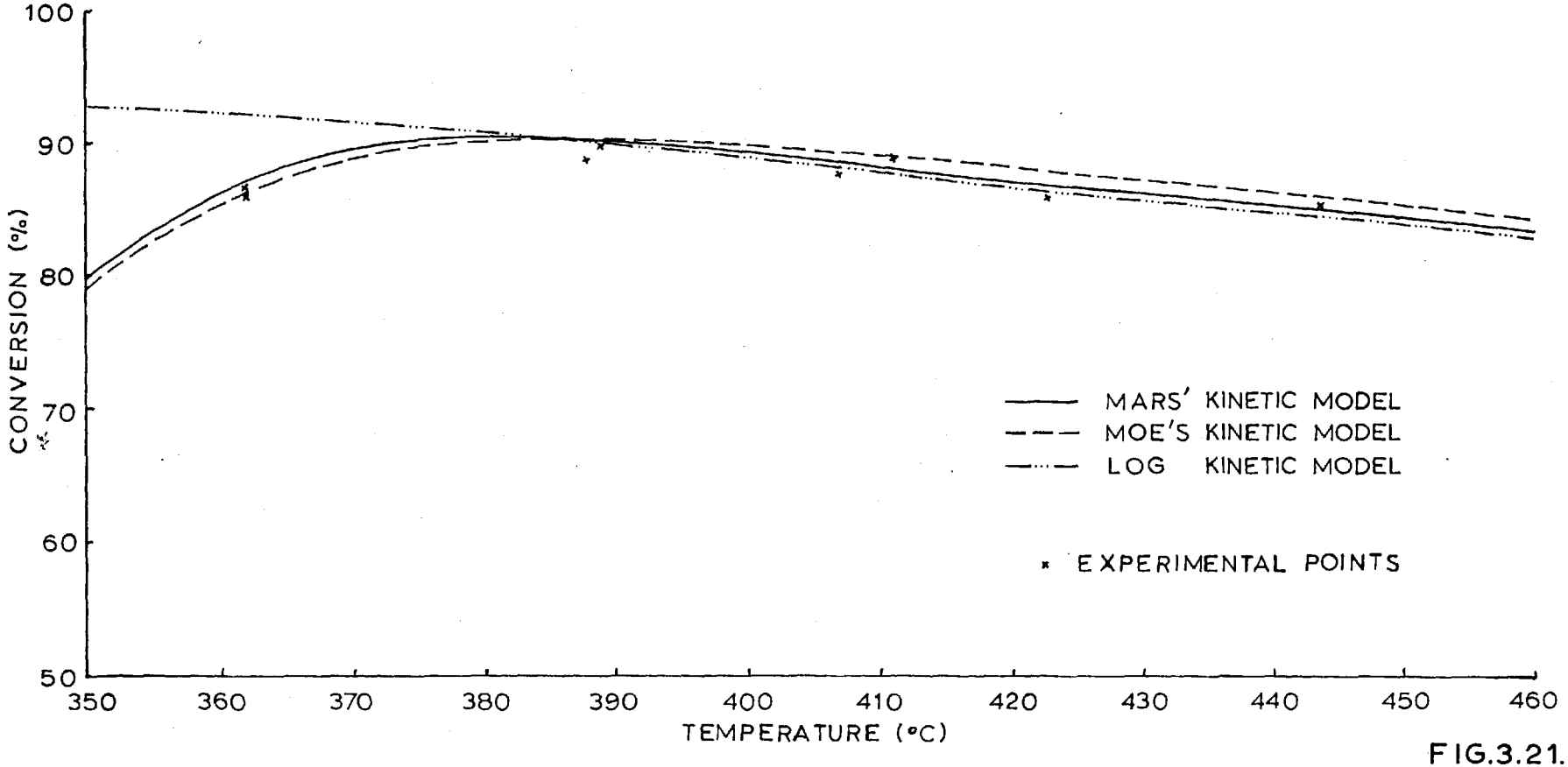

FIG.3.21.

VARIATION OF CONVERSION WITH STEAM FLOW RATE AT 405°C

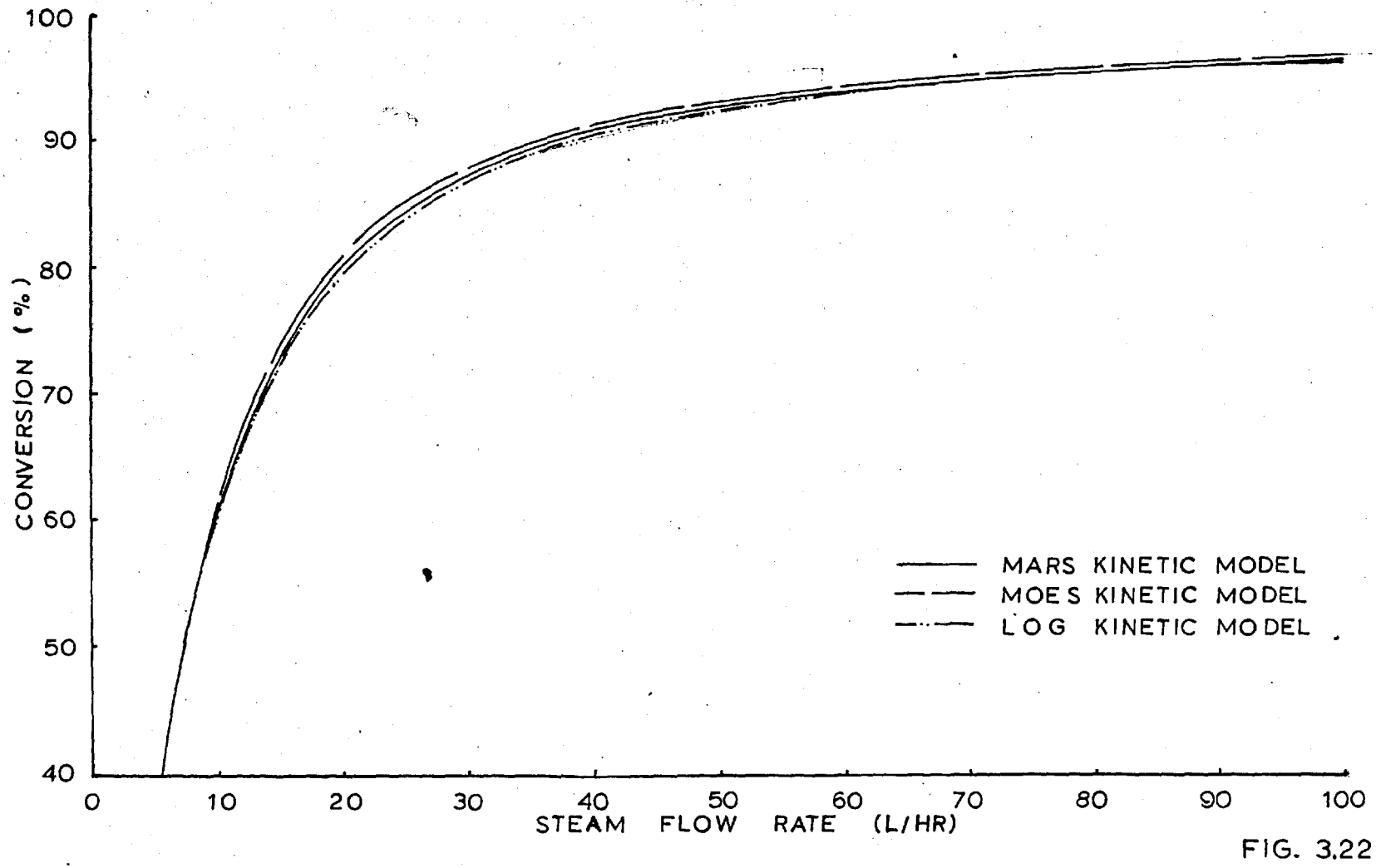

FIG. 3.22

Maximum values are seen to be present but the maxima are very flat.

Analysis of the results in table 3.1. shows that the use of the thermodynamic expression for the equilibrium constant in the models yields a high prediction for the conversions (the predicted conversion is higher than that observed, 61 times for Mars' model, 57 times for Moe's model and 62 for the Log model). However, if the parameters of K_T in 3.6.3. are also adjusted to their optimum values, this effect is lost and the normality approximations for the statistical analysis do apply.

Table 3.7. shows the sum of squares of the residuals at 365° and 390° C. The remaining squares of residuals are used to provide an estimate of variance of the predictions and thus the "F" statistic can be estimated.

TABLE 3.7.

Model	S.S. of 13 Residuals at 365° C	S.S. of 18 Residuals at 390° C	S.S. of Remaining 44 Residuals	$F_{13,\ 42}$	$F_{18,\ 42}$
Mars	124	31	62	6.45	1.37
Moe	101	36	64	5.10	1.31
Log	205	57	44	15.01	3.02

From tables (32)

$F_{13,42}(0.90) = 1.69 \qquad F_{13,42}(0.95) = 1.96 \qquad F_{13,42}(0.99) = 2.60$

This indicates that the discrepancy at 365° C is highly significant for all three models but that at 390° C there is no significant correlation for Mars' and Moe's model but there is for the Log model. It is also of interest that at temperatures above 390° C the Log model gives better predictions than the other two models, however, the difference is not significant.

Moe (22) found a correlation between the residuals and steam flow rate when fitting Mars' model to his experimental results. This correlation was reduced when fitting his own model. Table 3.8. shows the sum of squares of residuals for various flow rates of steam, using the best fitting models.

TABLE 3.8.

Model	Steam Flow Rates in l/hr					
	Less than 20	20 - 30	30 - 40	40 - 60	60 - 80	Greater than 80
Mars	119	49	11	5	16	18
Moe	77	27	22	21	37	17
Log	174	81	20	7	11	16

The results show that at low steam flow rates the estimates are widely out in the cases of all three models. However, the measurements of conversion below about 30 l/hr are expected to be less accurate than the others, because the analyser was used on the 0 - 20% scale as opposed to 0 - 2% scale for the other readings. Thus any small drift in the zero setting tended to introduce proportionally larger errors. Further the prediction by Mars' and Log models of the result of run 22 was a long way out, pointing to the fact that this measurement might be in error. Overall there is less correlation between steam flow and residuals in Moe's model than in the other cases but short of a thorough further examination the indications are that all three models are adequate as far as allowing for the steam flow is concerned.

The above analysis of the data obtained at the constant inlet gas composition shows that any of the three kinetic models quoted could be used to predict the conversion. The overall differences between them are insignificant

although each model has certain regions of operation which are better than those of the others. Thus as a final level of sophistication one could consider linear or other combinations of the models i.e.

$$\text{Conversion} = a\,(\text{Conv})_{\text{Mars}} + b\,(\text{Conv})_{\text{Moe}} + (1 - a - b)\,(\text{Conv})_{\text{Log}} \qquad 3.6.4.$$

Another way of approach would be to build a systematic model of the system on the lines suggested by Hunter and Mezaki (38). This is discussed more fully in the next section. However, no such model building has been done.

In practice Mars' model has been used in the computer simulation, because it is the simplest one to operate.

3.7. Determination of a General Model for the Water Gas Shift Reaction

The previous section has been concerned with finding the best model to fit the data obtained with a constant dry gas composition. The results obtained showed that all three models considered, fitted the data fairly well and could thus be used for the purposes of a computer simulation of the process. However, those results applied to a certain fixed gas composition and although of great interest to the project, were not general. In order to consider the usefulness of the models derived over a wide range of gas compositions, a fractional factorial experiment was designed and run. The values and ranges of the various factors considered are shown in table 3.9.

TABLE 3.9.

Factor	Units	Nomenclature	Mean	+ ve Level	- ve Level
Temperature	^{o}C	6	405	445	365
Steam	l/hr	1	45.0	70	20
Hydrogen	l/hr	2	21.8	29.0	14.2
Carbon monoxide	l/hr	3	9.85	13.65	6.0
Carbon dioxide	l/hr	4	3.9	7.9	0.0
Nitrogen	l/hr	5 = 1234	24.7	16.2	16.2

The range of values of the factors was chosen fairly arbitrarily in the case of the gas flow rates, the idea being to consider most of the compositions encountered in industrial reactors. As the process took several hours to settle down in steady state after a change in temperature the experiment was "blocked" in that variable. This means that the factorial was run at one level of the temperature and then it was replicated at the other level. The order in which the experiments were run was randomized by use of random numbers and the fraction used was specified by the defining relation I = + 12345. The settings of the factors, the order in which the runs were performed together with the results obtained for the conversion are shown in table 3.10. The centre point was replicated three times at each temperature in order to give an indication of the reproducibility of the results. The settings of the variables are often seen not to be at the exact levels defined by the factorial. This is because a change in gas flow rate altered the pressure at the saturator

TABLE 3.1o.

RESULTS OF THE FACTORIAL EXPERIMENT PERFORMED ON THE INLET GAS COMPOSITON

RUN NO	TEMP ^{o}C	STEAM FLOW (L/HR)	H_2 FLOW (L/HR)	CO FLOW (L/HR)	CO_2 FLOW (L/HR)	N_2 FLOW (L/HR)	TRUE CONV (%)	MARS' MODEL	MOE'S MODEL	LOG MODEL
1o	446	58.o	32.oo	16.65	1o.9o	35.3o	72.4o	- 7.4	- 6.9	- 7.7
18	447	19.2	29.2o	13.85	8.1o	16.4o	46.2o	- 7.2	- 7.o	- 7.4
7	445	68.8	14.5o	13.95	8.2o	16.5o	92.oo	1.8	1.6	1.6
13	447	15.2	15.4o	14.85	9.1o	33.4o	63.5o	11.2	11.6	9.o
9	448	7o.o	29.oo	6.oo	7.9o	16.2o	81.7o	- 2.7	- 2.8	- 2.8
6	447	15.2	3o.2o	7.2o	9.1o	33.5o	45.1o	5.2	5.6	5.1
4	448	68.4	14.6o	6.4o	8.3o	32.7o	92.2o	2.1	2.o	2.o
5	446	19.6	14.3o	6.1o	8.oo	16.3o	77.7o	9.6	9.6	9.6
14	447	7o.o	29.oo	13.65	o.oo	16.2o	91.8o	o.9	o.8	o.7
19	447	16.o	3o.oo	14.65	o.oo	33.3o	72.2o	13.5	14.2	12.6
2	445	66.5	14.7o	14.15	o.oo	32.8o	95.3o	2.1	2.o	1.9
3	446	2o.o	14.2o	13.65	o.oo	16.2o	73.3o	- 1.7	- 1.6	- 1.7
16	447	68.2	29.6o	6.6o	o.oo	32.9o	93.9o	1.4	1.3	1.2
12	446	2o.6	28.8o	5.8o	o.oo	16.oo	52.5o	-25.8	-25.7	-25.8
8	446	7o.o	14.2o	6.oo	o.oo	16.2o	95.5o	- o.4	- o.5	- o.5
1	447	2o.o	14.1o	5.9o	o.oo	32.2o	83.oo	- 2.3	- 2.1	- 2.3
15	447	44.2	22.oo	1o.o5	4.1o	24.9o	85.6o	o.3	o.3	o.2
17	447	43.8	22.1o	1o.15	4.2o	25.oo	86.8o	1.8	1.8	1.7
11	445	43.8	22.1o	1o.15	4.2o	25.oo	85.4o	o.2	o.3	o.1
2o	367	58.7	32.1o	16.15	1o.9o	35.oo	31.8o	- 5.2	- 4.6	- 4.5
35	366	2o.o	29.oo	13.65	7.9o	16.2o	25.6o	-16.4	- 7.3	-22.4
36	367	69.2	14.4o	13.85	8.1o	16.4o	43.3o	- 2.9	-13.3	- o.6
38	366	19.2	14.4o	13.85	8.1o	32.5o	36.7o	- 8.1	4.4	-13.2
31	367	69.2	29.2o	6.2o	8.1o	16.4o	37.8o	- 5.3	-14.7	- 3.1
3o	364	16.o	3o.oo	7.oo	8.9o	33.3o	27.6o	- 7.4	5.8	-11.5
24	365	66.o	15.2o	7.oo	8.9o	33.3o	42.5o	o.7	- 6.6	3.2
32	364	18.4	14.6o	6.4o	8.3o	16.6o	35.5o	-19.3	-11.1	-2o.4
28	366	7o.6	28.8o	13.45	o.oo	16.oo	56.7o	13.1	3.7	15.3
29	365	19.4	29.2o	13.85	o.oo	32.5o	43.3o	o.5	14.o	- 4.7
23	365	69.7	14.3o	13.75	o.oo	32.4o	6o.6o	17.8	9.6	2o.4
27	365	19.4	14.4o	13.85	o.oo	16.4o	5o.5o	- 6.9	1.8	-1o.6
33	366	69.4	29.2o	6.2o	o.oo	32.5o	67.2o	25.2	17.8	27.7
26	365	2o.6	28.8o	5.8o	o.oo	16.oo	53.3o	- 4.1	4.8	- 4.6
21	364	69.7	14.3o	6.1o	o.oo	16.3o	68.2o	19.6	3.3	22.9
22	365	19.7	14.3o	6.1o	o.oo	32.4o	61.oo	1.7	14.5	2.7
34	367	45.o	21.8o	9.85	3.9o	24.7o	47.6o	- 2.2	- 3.9	- o.5
37	366	45.8	21.6o	9.65	3.7o	24.5o	45.6o	- 3.3	- 5.6	- 1.4
25	366	45.8	21.6o	9.65	3.7o	24.5o	43.8o	- 5.1	- 7.4	- 3.2

VARIATION OF THE S.S. OF RESIDUALS WITH ACTIVATION ENERGY OF THE RATE CONSTANT THERMODYNAMIC VALUE OF EQUILIBRIUM CONSTANT

$A'(K)_{MARS} = 32{\cdot}0$ $A'(K)_{MOE} = 36{\cdot}5$ $A'(K)_{LOG} = 32\,4$

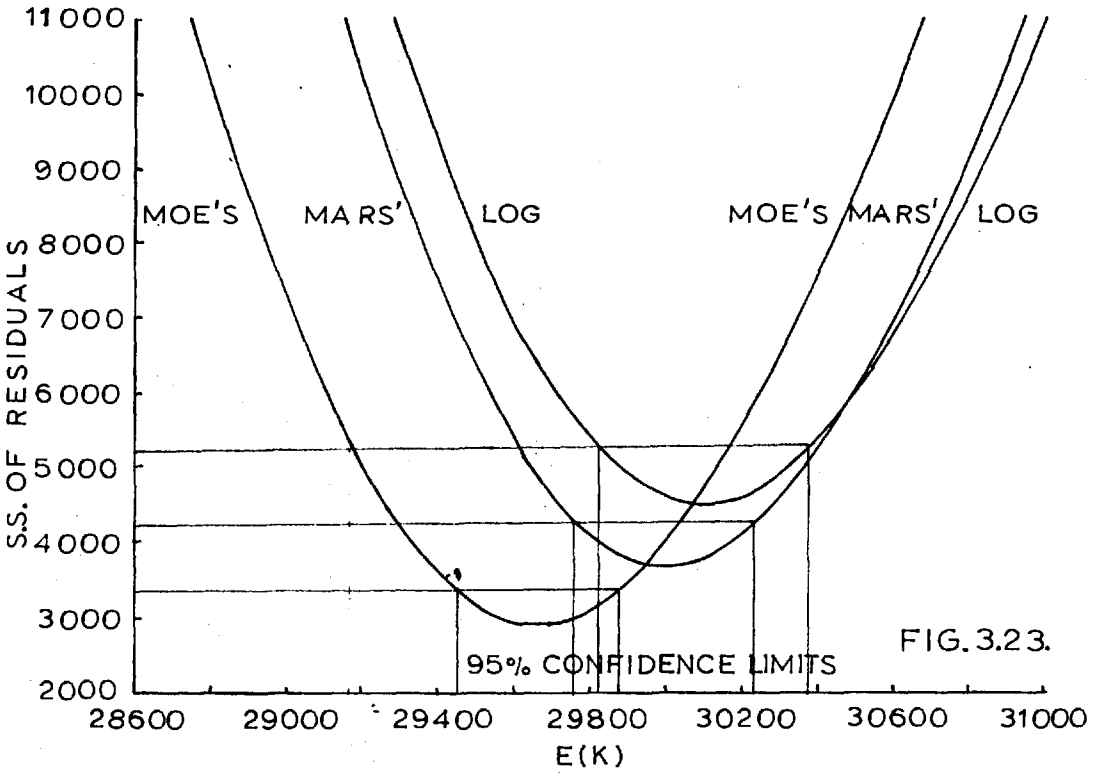

FIG. 3.23.

VARIATION OF THE S.S. OF RESIDUALS WITH ACTIVATION ENERGY OF THE EQUILIBRIUM CONSTANT EQUILIBRIUM EXPRESSION GIVEN BY 3.6.3.

$A'(K) = 32.0$	$A'(K) = 36.5$	$A'(K) = 32.4$
$E(K) = 30000$	$E(K) = 29660$	$E(K) = 30090$
$A'(KT) = 4.45$	$A'(KT) = 4.45$	$A'(KT) = 4.45$
MARS	MOE	LOG

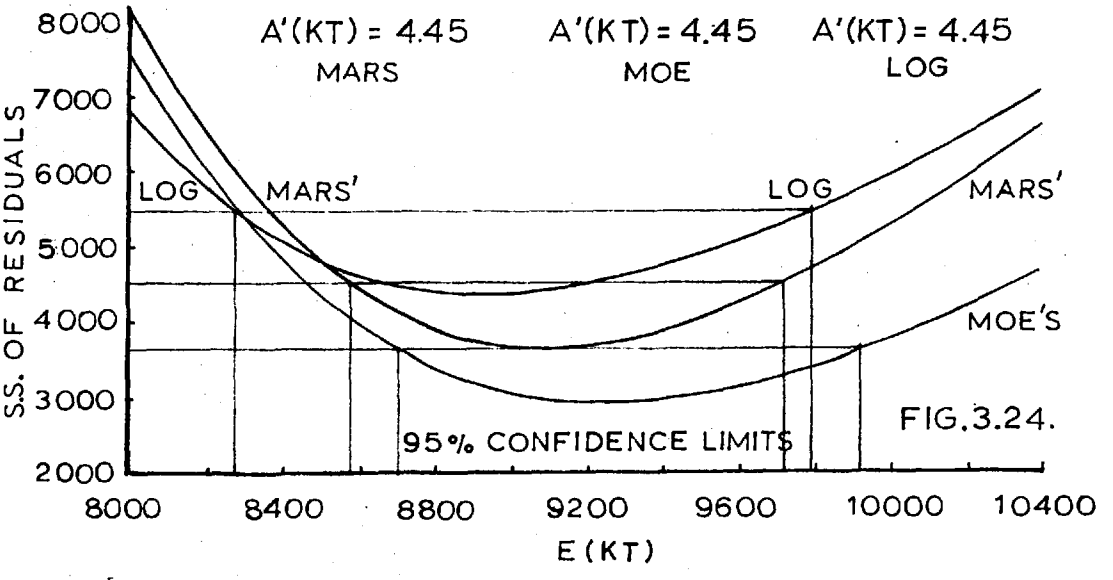

FIG. 3.24.

and thereby the calibration of the rotameters. This effect was not noticed till after the results had been obtained, and so the settings had to be adjusted. There was also a slight drift in temperature over a series of runs.

The results were analysed in an identical way to those in section 3.6. and the shapes of the curves obtained had the same characteristics as before. For that reason only two diagrams are presented. Figure 3.23. shows how the sum of squares of the discrepancies between observed and predicted percentage conversion varies with the activation energy of the rate constant for the case of the three models.

The results obtained when the thermodynamic expression has been used for the equilibrium constant are given in table 3.11.

TABLE 3.11.

Model	E (k)	A'(k)	S.S. of Deviations	Confidence Limits E (k)
Mars	30000	32.0	3672	29750 - 30240
Moe	29660	36.5	2910	29430 - 29890
Log	30090	32.4	4555	28810 - 30380

As before the models are also considered with an expression of the form 3.6.3. in place of the equilibrium constant. Thus in fact one is fitting four constants to the data. The relevant results are shown in table 3.12. The variation of the s.s. of discrepancies with the activation energy in the equilibrium expression is shown in figure 3.24.

TABLE 3.12.

Model	E (k)	A'(k)	E (KT)	A'(KT)	S.S. of Deviations
Mars	30000	32.0	9100	4.45	3629
Moe	29660	36.5	9250	4.45	2903
Log	30090	32.4	9000	4.45	4374

As the improvement in using 3.6.3. rather than the thermodynamic equilibrium constant i.e. 3.2.9., is very slight it was considered pointless to introduce yet another modification to the published models. Thus only the models using 3.2.9. for the equilibrium expression will be considered in the further discussion.

The sums of squares of deviations for all three models are very large. The estimated mean square error of the results based on the two lots of three repeated points is 2.38. Thus the estimated value for $F_{36,4}$ for each of the models could be found and the significance of the model obtained. The results are shown in table 3.13.

TABLE 3.13.

Model	$S.S._{min}$	$F_{36,4}$
Mars	3672	42.8
Moe	2910	33.9
Log	4555	53.0

From tables, (32) $F_{36,4}(95) = 5.75$ and $F_{36,4}(99) = 13.8$

From the above it can be seen that none of the models are very satisfactory. To determine whether the models are significantly different from one another one considers the ratios of the minimum sums of squares of the deviations and compares these with the relevant F statistic i.e. $F_{36,36}$. This is shown below;

Mars / Moe = 1.26 Log / Mars = 1.24 Log / Moe = 1.56

$F_{36,36}(0.90) = 1.54$ $F_{36,36}(0.95) = 1.75$

Thus there are no really significant differences between any of the three models. However, from the residuals' columns in table 3.10. it can be seen that the data at the high level of temperature gives very similar values for the residuals irrespective of the model used. This points to the system being at equilibrium. Thus in order to distinguish between the models, all of which describe deviations from the equilibrium value of conversion, one should consider only the results at the low temperature. This is shown below in table 3.14.

TABLE 3.14.

Model	S.S. of Residuals at 365° C	Ratio of Models	Estimate of $F_{19,19}$
Mars	2443	Mars / Moe	1.48
Moe	1655	Log / Mars	1.38
Log	3382	Log / Moe	2.04

$F_{19,19}(0.90) = 1.82$ $F_{19,19}(0.95) = 2.17$

The estimated values of the "F" ratio are seen to be less than the 95% significant level and so statistically speaking there is no conclusive evidence that the models are different.

TABLE 3.15.

Model	Value of Correlation Coefficient between Factors										
	1	2	3	4	5	6	12	13	14	15	16
Mars	0.35	-0.13	0.02	-0.30	0.27	0.03	0.22	0.23	-0.21	0.37	0.31
Moe	-0.13	-0.08	0.07	-0.29	0.44	-0.01	-0.14	-0.11	-0.40	0.05	-0.12
Log	0.44	-0.15	-0.04	-0.30	0.23	0.02	0.29	0.28	-0.15	0.43	0.39

Model	Value of Correlation Coefficient between Factors									
	23	24	25	26	34	35	36	45	46	56
Mars	-0.07	-0.33	0.11	-0.13	-0.28	0.16	0.04	-0.21	-0.25	0.27
Moe	0.00	-0.30	0.26	-0.10	-0.26	0.29	0.08	-0.15	-0.24	0.41
Log	-0.12	-0.33	0.07	-0.14	-0.29	0.09	0.02	-0.22	-0.25	0.22

The factors in the above are

1 flow rate of steam

2 flow rate of hydrogen

3 flow rate of carbon monoxide

4 flow rate of carbon dioxide

5 flow rate of nitrogen

6 temperature of the reactor

The next point of interest is that if the models are all inadequate, where is it that they fail. The lack of fit for the individual observations when using the three models is shown in the last three columns of table 3.10. As before the residuals are computed on the basis

(the observed readings - the predicted ones)

In order to determine the places of failure of the models, the residuals obtained for each model were tested for correlations with the settings of the factor levels and the results are shown in table 3.15. In order to have a firm basis for judging significant correlations, the correlations were normalized by the use of the following procedure (32).

$$\text{correlation of residuals with factor i} = \frac{\sum_{p=1}^{38}(\text{actual setting of i} - \text{mean setting of i})(\text{actual value of residual} - \text{mean value of residual})}{\sqrt{\sum_{p=1}^{38}(\text{actual setting of i} - \text{mean setting of i})^2 \sum_{p=1}^{38}(\text{actual value of residual} - \text{mean value of residual})^2}}$$

3.7.1.

The above correlation was denoted by symbol i. The correlation ij was similarly evaluated, but in this case a new column was first formed. This consisted of the products of the actual settings of factors i and j in the p^{th} run. The mean of this column was then obtained.

The significance of a given correlation was obtained from a standard table (table E in Davies (32)). This assumed that the residuals were normally distributed. For 38 degrees of freedom two quantities are significantly correlated at the 95% level if the value of the correlation coefficient exceeds 0.31. The corresponding values for 90% and for 99% levels are 0.26 and 0.37.

TABLE 3.16.

Level of Temperature	Model	Value of Correlation Coefficient between Factors										
		1	2	3	4	5	6	12	13	14	15	16
446° C	Mars	-0.05	-0.29	0.20	0.16	0.36	0.13	-0.17	-0.02	-0.04	0.02	-0.05
	Moe	-0.07	-0.28	0.21	0.16	0.37	0.14	-0.18	-0.03	-0.04	0.01	-0.07
	Log	-0.04	-0.29	0.18	0.15	0.35	0.13	-0.16	-0.01	-0.04	0.03	-0.04
365° C	Mars	0.64	-0.02	-0.11	-0.64	0.22	0.06	0.50	0.42	-0.33	0.63	0.64
	Moe	-0.21	0.11	0.02	-0.67	0.51	0.06	-0.12	-0.19	-0.72	0.06	-0.21
	Log	0.73	-0.06	-0.17	-0.59	0.17	-0.09	0.57	0.48	-0.23	0.69	0.73

Level of Temperature	Model	Value of Correlation Coefficient between Factors									
		23	24	25	26	34	35	36	45	46	56
446° C	Mars	-0.01	-0.02	0.10	-0.29	0.04	0.33	0.20	0.15	0.16	0.36
	Moe	0.01	-0.01	0.12	-0.27	0.05	0.35	0.21	0.16	0.16	0.37
	Log	-0.03	-0.03	0.10	-0.29	0.02	0.30	0.18	0.14	0.15	0.35
365° C	Mars	-0.11	-0.56	0.12	-0.02	-0.52	0.03	-0.11	-0.48	-0.64	0.22
	Moe	0.04	-0.55	0.40	0.11	-0.51	0.26	-0.02	-0.42	-0.67	0.51
	Log	-0.17	-0.53	0.06	-0.06	-0.50	-0.04	-0.17	-0.46	-0.59	0.16

The significant levels of the correlation coefficients with 19 degrees of freedom are

90% = 0.37 95% = 0.43 99% = 0.55

From table 3.15. it can be seen that for Mars' model the three of the most significant correlations involve the flow rate of steam. This was also noticed by Moe who attempted to correct for it by using his own model. In this respect he is seen to have succeeded. Moe's model however has highly significant positive correlations involving the flow rate of nitrogen, indicating that the time of passage of gas through the reactor is badly underestimated. Mars' model although an improvement, is still bad at allowing for the inert gas flow. Both models are equally bad at allowing for the flow rate of carbon dioxide. The Log model is inadequate at similar points to Mars' model and as it does not predict results significantly better than Mars' model, there does not seem to be a case for considering it any further.

Table 3.16. gives the values of the correlations if the results at the two temperatures are considered separately. From this it can be seen that at 446° C there are no significant correlations between the parameter settings and the residuals, indicating that the equilibrium form of the equations is fairly adequate. The results however point to the flow rate of nitrogen being incompletely described by the models. At the low level of the temperature the residuals show highly significant correlations with the steam flow rate for the cases of Mars' and Log models. This arises both in the single factor term and in the interactions. Moe's model does correct for this adequatly. The carbon dioxide is highly correlated with the residuals for all three models and for Moe's model the flow rate of nitrogen is also poorly described. Thus in conclusion all three models allow correctly for temperature, and the flow rate variations of hydrogen and carbon monoxide. Moe's model is a large improvement on Mars' model because it takes care of the steam flow variations. Thus for the feed gas originating from the

partial oxidation process, Moe's model would be very satisfactory. However, Moe's model describes inadequatly the flow rates of the inert gases and carbon dioxide. This is a big hinderance when the feed gas contains considerable quantities of these gases e.g. gas from steam cracking of heavy hydrocarbon oils. The Log model gives similar predictions to Mars' model, but is inferior and so does not seem to be any help in this respect either. The correction for nitrogen points to a different function from those used in order to allow for deviations from equilibrium conversion. A reason may be that the compensation for the deviation from plug flow is inadequate. In principle one could fit the constant determining the relative proportions of gas flowing at the inside and outside of the reactor, by a procedure similar to the fitting of the rate and equilibrium constant parameters. From table 3.16. it can be seen that at the low temperature there is a highly significant correlation between the residuals and nitrogen setting, but there is no such effect at the high temperature. This is explicable, because at the high temperature the system is at equilibrium and thus the conversion in both the inner and outer layers of the reactor is virtually the same, whereas at the low temperature the two are significantly different. If this compensation still proves to be inadequate and also to allow for the carbon dioxide flow, the best procedure would be to assume another kinetic model and develop it from the initial assumptions (33). Models like Moe's and Mars', where deviations from equilibrium conversion are considered, seem to be on the correct lines.

In the absence of any further analysis, Moe's kinetic model has been found to be the best one to use for predicting the performance of water gas shift reactors.

CHAPTER IV

Introduction

This chapter considers the dynamic simulation of the process as programmed in Mercury Autocode for the London University computer. The procedure was to superimpose dynamics onto Mars' steady state kinetic model. The transformation of the analysing and filtering operations performed on the analogue computer, into a form suitable for the digital computer is also derived. The experiments run to calibrate the model so as to predict experimental results, are described at the end of the chapter.

4.1. The Objective Function

The objective function (C) which has been optimized is

$$C = \text{conv}(S) - a.\ \text{steam flow rate}(W)$$

$$= S - aW - b \qquad 4.1.1.$$

In practice C corresponds to a very simple profit function being based On the fact that the supply of steam is not unlimited and thus costs money. Also for greater accuracy on the analogue computer a constant, b, was subtracted from the conversion term.

The optimisation experiments were run at around 405° C, the temperature being kept constant. The reason for choosing this temperature was that it was convenient to control and that Mars' model predicted the conversion satisfactorily. As can be seen from figures 3.18, 3.19 and 3.2o the conversion response curves with respect to steam flow do not change shape to any great extent with change in temperature. In particular the maximum is a very flat

one, and this is undesirable for the exploratory studies as described in this thesis. Hence the use of a cost function. Curves showing variation of objective function with steam flow and temperature are shown in figures 4.1. and 4.2. The objective function is in fact

$$C = 0.30 \ (S - 0.4 W - 53.3) \qquad 4.1.2.$$

the 0.30 factor being present for scaling purposes. The dotted curves show what the objective function would be if the steam flow measurement was in error by 5 l/hr in both positive and negative directions. From this it can be seen that the value at the maximum is very sensitive to the accuracy with which the steam flow is measured. However, the position of the maximum stays constant despite any steam measurement errors.

So far the steady state case has been described. In practice there is a delay between the adjustment of the valve controlling the flow of steam, the actual steam flow and conversion. This is due both to the finite time of passage of gas from one part of the system to another - i.e. pure time lag - and also to dynamic or capacitance lag of the system. For this reason it is necessary to delay the steam flow measurement so that a particular measured flow of steam corresponds to its resultant conversion. This is a trivial matter to achieve on a digital computer, but not on the analogue computer.

As the delay between steam and conversion was about 30 seconds - a large proportion of this was due to the delay in the infra red analyser - and the frequency of operation was around 1 cycle/100 secs, this meant that the phase shift required was about 110° i.e. 1.9 radians. A convenient way to introduce such a delay to an accuracy of 1° is by means of a 1st order Padé approximation (30) However, there was insufficient equipment available on the analogue computer,

VARIATION OF OBJECTIVE FUNCTION-0.3(S-0.4W-53.3) WITH FLOW RATE OF STEAM AT 405°C

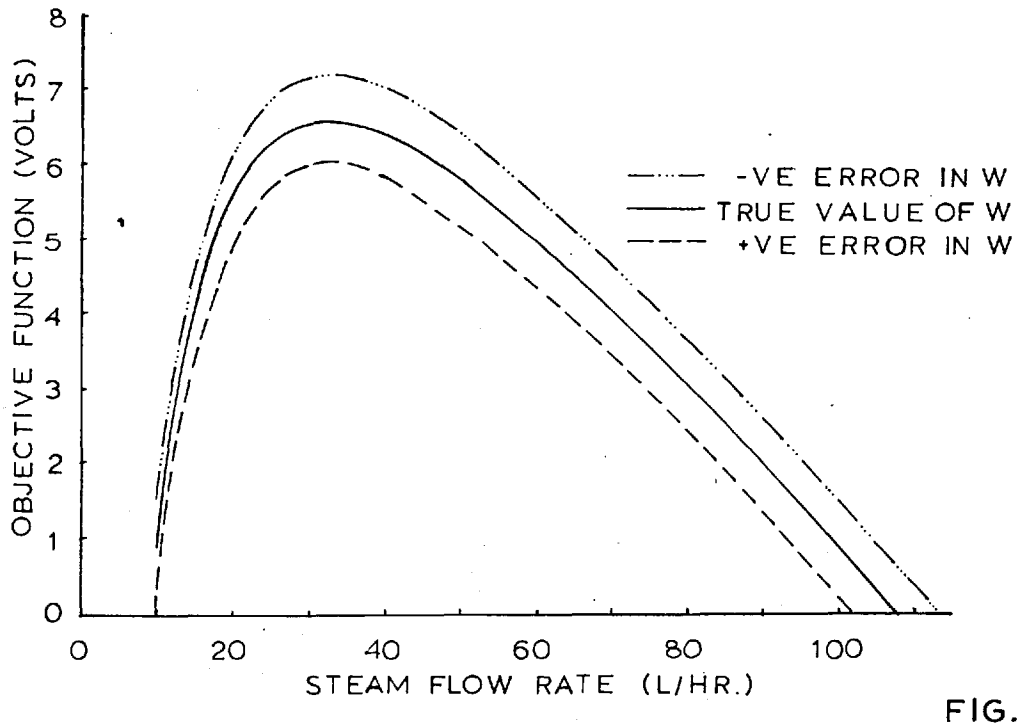

FIG.4.1.

THE EFFECT OF 5°C CHANGE IN TEMPERATURE

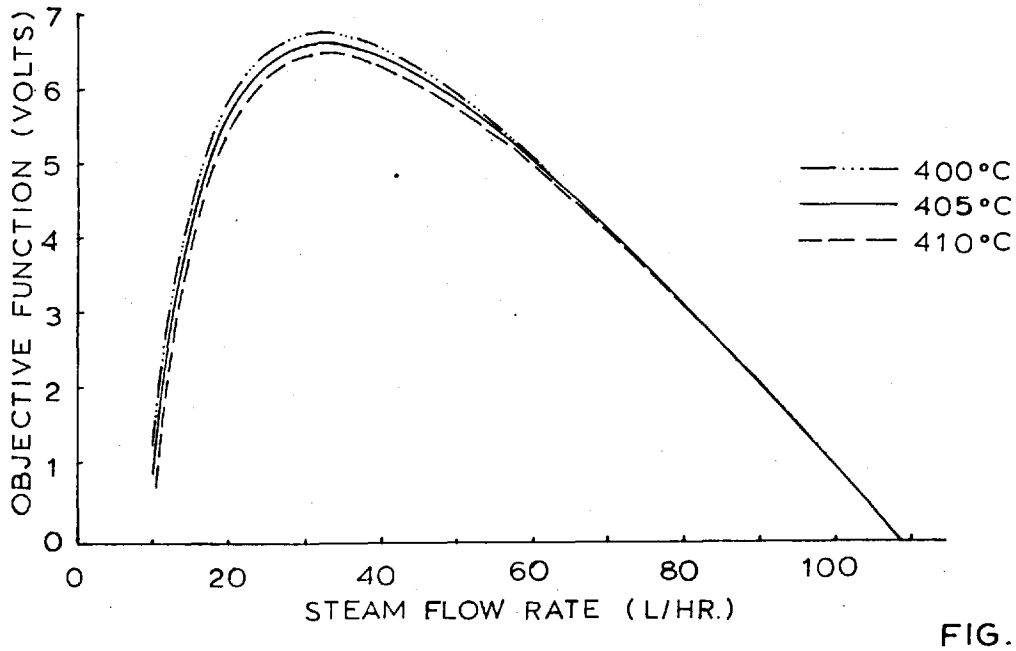

FIG.4.2.

to set up this circuit - it requires 4 amplifiers and 3 integrator networks. Thus a compromise was achieved using a less accurate circuit. The approximation used was

$$e^{-\tau p} = -\frac{p-\frac{2}{\tau}}{p+\frac{2}{\tau}} = 1 - \tau p + \frac{(\tau p)^2}{2} - \frac{(\tau p)^3}{4} \qquad 4.1.3.$$

where τ is a time constant.

The resultant gain introduced was

$$g = \text{Mod}\left(-\frac{i\omega-\frac{2}{\tau}}{i\omega+\frac{2}{\tau}}\right) = \text{Mod}\left(\frac{\frac{4}{\tau^2}-\omega^2-\frac{4i\omega}{\tau}}{\frac{4}{\tau^2}+\omega^2}\right) = 1$$

which has the required characteristics. The phase shift

$$= \tan^{-1}\left(-\frac{\frac{4\omega}{\tau}}{\frac{4}{\tau^2}-\omega^2}\right) \qquad 4.1.4.$$

The circuit is shown in figure 10. The delay altered with the position of operation on the response surface because the time of passage of gas changed with the flow of steam. Thus complete correspondence between conversion and steam flow rate was not attained. In the digital simulation the delay obtained in the analogue circuit was calculated from 4.1.4., as both the time constant, τ, and frequency of operation were known. The reason why the approximation was somewhat unsatisfactory at the frequency used was because $\frac{2}{\tau}$ and ω were of similar magnitudes and thus a small drift in frequency altered the delay by a significant amount.

The problem of delaying signals contained in the objective function is expected to be a difficult one when applying the technique to an industrial process. Here maybe ten or more individual measurements will be needed to specify the objective function and the dynamic relationships between these signals will tend to be highly complex. However, it is essential that the various measurements are at least approximately in phase otherwise it is likely that the optimiser will drive the system to wrong operating conditions or even make the system unstable. If the former happens even the "best" empirically found phase shift may not optimize the system very satisfactorily.

4.2. Simulation of the Process Dynamics

The dynamics were simulated by assuming that the system can be adequately described by two stage exponential dynamics and time lag. As was mentioned by Box and Jenkins (31), the theory can easily be extended to the case of multistage exponential dynamics. Thus the response $Y(t)$ to a forcing function $X(t)$ is assumed to be given by

$$(1 + T_1'D) (1 + T_2'D) \; Y(t) = gX (t - \tau') \quad \text{or}$$

$$Y + (T_1' + T_2') \frac{dY}{dt} + T_1' T_2' \frac{d^2Y}{dt^2} = g X (t - \tau') \qquad 4.2.1.$$

where T_1 and T_2 are the time constants of the two exponential stages

τ' is the time delay between Y and X and

g is the steady state gain of the system or in other words the effect which a unit change in $X(t)$ has on $Y(t)$.

In what follows the two stage exponential dynamics are considered first and

the dead time is accounted for later. Differencing of 4.2.1. gives

$$\left(1 + \frac{T_1'}{\Delta t}\Delta\right)\left(1 + \frac{T_2'}{\Delta t}\Delta\right) y_{p+1} = g\, x_p \qquad 4.2.2.$$

where x_p and y_p are the <u>changes</u> occurring in the forcing function and response during the interval between time $p-1$ and p whose length is Δt secs.

Let

$$T_i = \frac{T_i'}{\Delta t}$$

By expanding and rearranging 4.2.2.

$$y_{p+1} = \frac{(1+T_1)+(1+T_2)}{(1+T_1)\ (1+T_2)}\, y_p - \frac{T_1T_2}{(1+T_1)(1+T_2)}\, y_{p-1} + \frac{g x_p}{(1+T_1)(1+T_2)}$$

$$= \delta_1 y_p - \delta_2 y_{p-1} + (1 - \delta_1 + \delta_2)\, g\, x_p \qquad 4.2.3.$$

where

$$\delta_1 = \frac{(1+T_1)+(1+T_2)}{(1+T_1)\ (1+T_2)} = 1 - \frac{1}{1+T_1} + 1 - \frac{1}{1+T_2}$$

$$\delta_2 = \frac{T_1T_2}{(1+T_1)\ (1+T_2)} = \left(1 - \frac{1}{1+T_1}\right)\left(1 - \frac{1}{1+T_2}\right) \qquad 4.2.4.$$

In order to allow for pure delay in the system one can consider that the change which occurs in the response (Y) at time $(p+1)$ is the result of a change in the forcing function (X) several intervals, say j, previously.

Thus a more general form of 4.2.3. is

$$y_{p+1} = \delta_1 y_p - \delta_2 y_{p-1} + (1 - \delta_1 + \delta_2)\, g\, x_{p-j} \qquad 4.2.5.$$

Also one can consider that the result of a change in X will not appear after a whole number (j) of time intervals i.e. that the change takes ($j + \lambda$) time intervals to appear, where λ is a fraction whose value lies between o and 1. Thus

$$y_{p+1} = \delta_1 y_p - \delta_2 y_{p-1} + (1 - \delta_1 + \delta_2)\, g\left\{(1 - \lambda)\, x_{p-j} + \lambda x_{p-j-1}\right\} \qquad 4.2.6.$$

A final degree of sophistication is obtained if the gain g is assumed to vary with position of operation on the response surface. This implies the existence of a steady state model which in our case is available. A variable gain is essential for any system which cannot be represented linearly e.g. a reactor where chemical reaction takes place. In fact it was found that it is far more satisfactory to consider the potential response at time p - j, due to changes in the forcing function at that time rather than multiply the corresponding gain by the change in the forcing function. The latter method tends to introduce errors which continually amplify themselves i.e. for a maximum, the predicted curve once above the true curve will diverge from the true curve until after the optimum has been reached. The former method brings down the predicted curve to the true curve at each calculating stage.

In the computer simulation, the dynamics between the change in valve position and conversion were considered with a variable gain of the form just described i.e.

$$s_{p+1} = \delta_1 s_p - \delta_2 s_{p-1} + (1 - \delta_1 + \delta_2) \left\{(1 - \lambda)\, (\bar{s}_o)_{p-1} + \lambda (\bar{s}_o)_{p-j-1}\right\} \qquad 4.2.7.$$

and the dynamics between change in valve position (v) and change in the flow rate of steam (w) as

$$w_{p+1} = \delta_1' w_p - \delta_2' w_{p-1} + (1 - \delta_1 + \delta_2)\ g\left((1 - \lambda')\ v_{p-j'} + \lambda'\ v_{p-j-1} \right) \quad 4.2.8.$$

where the gain, g, is a constant.

Keeping the gain constant in 4.2.8. is a reasonable assumption, for the valve was specified as linear with respect to steam flow rate. In practice non linearity did occur at small flow rates but it was not considered worthwhile to allow for this.

It is worth noting that the form of the constants δ_1 and δ_2 in 4.2.4. is an approximation and this is demonstrated below.

For the sake of clarity consider the first order system

$$(1 + TD)\ Y(t) = X(t) \qquad 4.2.9.$$

The response of $Y(t)$ to a step change in $X(t)$ is

$$Y(t) = Y(o) + g\ x\ (1 - e^{-\frac{t}{T}}) \qquad 4.2.1o.$$

where $Y(o)$ is the initial value of $Y(t)$ and

x is the size of the step change.

If 4.2.9. is differenced and also one considers the <u>changes</u> in $Y(t)$ and $X(t)$ then

$$y_p + \frac{T}{\Delta t} (y_p - y_{p-1}) = x_{p-j}$$

and the response to a step change in $X(t)$ is thus given by

$$y_p + \frac{T_i}{\Delta t} (y_p - y_{p-1}) = 0$$

or

$$\frac{y_p}{y_{p-1}} = \frac{\frac{T}{\Delta t}}{1 + \frac{T}{\Delta t}} = \frac{1}{1 + \frac{\Delta t}{T}} \qquad 4.2.11.$$

The corresponding ratio of changes in $Y(t)$ when calculated from 4.2.1o. has the value

$$\frac{y_p}{y_{p-1}} = e^{-\frac{\Delta t}{T}} \qquad 4.2.12.$$

4.2.11. and 4.2.12. should be exactly equal which in general is seen not to be the case. However, if Δt is small compared to T then expanding 4.2.11. gives

$$\frac{1}{1+\frac{\Delta t}{T}} = 1 - \frac{\Delta t}{T} + \left(\frac{\Delta t}{T}\right)^2$$

and similarly 4.2.12. is

$$e^{-\frac{\Delta t}{T}} = 1 - \frac{\Delta t}{T} + \tfrac{1}{2}\left(\frac{\Delta t}{T}\right)^2$$

The above two are thus equivalent for small ratios of $\frac{\Delta t}{T}$. Extending the above to a two stage exponential system, the values of δ_1 and δ_2 in 4.2.4. should become

$$\delta_1 = \left(1 - e^{-\frac{\Delta t}{T_1}}\right) + \left(1 - e^{-\frac{\Delta t}{T_2}}\right)$$

$$\delta_2 = \left(1 - e^{-\frac{\Delta t}{T_1}}\right)\left(1 - e^{-\frac{\Delta t}{T_2}}\right) \qquad 4.2.13.$$

The response to a sinusoidal perturbation of the function $y = x^2$ was compared using the two sets of expressions for the δ's. It was found that when a cycle of the input sine wave was divided into 5o points, 4.2.13. gave an answer of o.782 for the attenuation of the signal and 4.2.4. a value of o.742. The attenuation calculated from the transfer function (4.5.2.) was

found to be o.781. Similar results were obtained at other frequencies investigated (15o and 5o secs/cycle). Thus in the digital simulation the δ's are calculated using 4.2.13.

Equations 4.2.7. and 4.2.8. can be expressed in an equivalent block diagram form i.e. for the case of conversion

$$\xrightarrow{V} \boxed{S_o = S(V)} \xrightarrow{S_o} \boxed{\frac{e^{-(j+\lambda)\Delta t}}{(1+T'_1 p)(1+T'_2 p)}} \longrightarrow S(t) \qquad \text{or}$$

$$1 + (T'_1 + T'_2)\frac{dS}{dt} + T'_1 T'_2 \frac{d^2S}{dt^2} = S(t - (j+\lambda)\Delta t) \qquad 4.2.14.$$

4.3. The High Pass Filter

In order to amplify the effect of the perturbation in the objective function the signal is passed through a high pass filter. This is an analogue computing device which transmits only the high frequency components of a signal and thus effectively filters out the direct current or steady state component. However, at the same time the required perturbation signal is attenuated and shifted in phase, this being particularly true at the slow perturbation frequencies used. The filter is necessary because otherwise the perturbation signal would be lost in the much larger steady state component. The transfer function of a high pass filter is

$$T(p) = \frac{p\tau}{1 + p\tau}$$

where τ is the time constant.

The corresponding analogue block diagram is shown in figure 1o (chapter 2). This is straight forward to set up on the analogue computer but unlike the case of the

delay it is harder to program on the digital computer. If C is the true objective function signal and C' is the filtered signal then

$$\frac{C'}{C} = \frac{p\tau}{1 + p\tau} \quad \text{or} \qquad 4.3.1.$$

$$C' + \tau \frac{d C'}{d t} = \tau \frac{d C}{d t}$$

In the differenced form

$$\frac{C'_{p+1} + C'_p}{2} + \frac{\tau}{\Delta t} (C'_{p+1} - C'_p) = \frac{\tau}{\Delta t} (C_{p+1} - C_p) \qquad 4.3.2.$$

where Δt is the sampling interval.

Rearranging 4.3.2. gives

$$C'_{p+1} = \frac{\frac{\tau}{\Delta t} - \frac{1}{2}}{\frac{\tau}{\Delta t} + \frac{1}{2}} C'_p + \frac{\frac{\tau}{\Delta t}}{\frac{\tau}{\Delta t} + \frac{1}{2}} (C_{p+1} - C_p)$$

$$= a C'_p + \frac{1 + a}{2} (C_{p+1} - C_p) \qquad 4.3.3.$$

where

$$a = \frac{\frac{\tau}{\Delta t} - \frac{1}{2}}{\frac{\tau}{\Delta t} + \frac{1}{2}} \qquad 4.3.4.$$

If the time interval, Δt, is small compared with time constant, τ, $a \longrightarrow 1$ and the change in the filtered signal, between the time p and $p + 1$ is the same as the change in the unfiltered signal which is as would be expected intuitively.

4.4. The Sample-Hold Operations

The signal from the high pass filter is correlated with a phase shifted input signal and then integrated over one cycle. On the plant the phase shift was altered by adjusting the relative position of the shaft on which the sin-cos potentiometer was mounted and the shaft carrying the swash plate which varied the air pressure signal. The magnet used to generate a signal for integrating over a cycle - i.e. to activate the sample-hold circuit described in figure 1o - was mounted on this shaft and so the signal was always integrated starting at the same point in the cycle. In practice this corresponded very closely to a cosine wave. In the digital simulation the above was achieved by varying the starting position of the count on the total number of points in such a way that the sum of the phase shift angle expressed as a number of intervals and the initial value of the count was a constant. The integration over a cycle was simulated by dividing a cycle into 5o intervals and integrating by Simpson's rule. The result was then stored, a facility not available on the analogue computer. Initially several numbers of points per cycle were tried out on the simple model $y = x^2$ and the dynamics were described with increasing accuracy as the number of points used per cycle was increased. However, the more points were used, the greater was the time required on the computer and thus 5o points/cycle was chosen as a compromise. 2o points per cycle in fact over-estimated the attenuation of the input signal by about o.7% but the phase shift was in error by two intervals. With 5o points/cycle the attenuation was out by less then o.2% and the phase shift predicted the correct number of intervals.

It can be seen in figure 1o that amplifier 4 has diodes limiting both the positive and negative signals coming out of the correlating multiplier

This was found to be very useful, if not essential, to keep the process stable during large changes both due to the action of the optimiser and noise. When a change in the valve position was required by the optimiser, the system in certain circumstances received a large signal in the wrong direction due to the non correspondence of dynamics in the objective function. By limiting this signal, stability was retained. The setting of the diodes was fixed at an arbitrary level which worked satisfactorily. The influence of the magnitude of this level on the performance of the optimiser might well be something for further investigation for the diodes limited to a certain extent the speed of approach to the optimum.

In the operations performed, the gain of the system was considered to be the constant by which the cumulative change of the valve was multiplied. This corresponds to a form of integral control which was appropriate for the discrete values of slope available from the sample and hold system.

4.5. Determination of Constants for the Simulated Model

4.5.1. Objective Function

The constants for the objective function were found by trial and error, so as to have the objective function described as accurately as possible in the available $\pm$ 10 volt range on the analogue computer. The above applied to the constant substracted from the conversion (53.3) and also to the multiplying factor of 0.30. The multiplying constant of 0.4 for the steam flow rate was fixed so that the position of the optimum was at a convenient value of the flow rate of steam.

The delay between steam and conversion in the objective function was again found empirically. The value used for $2/\tau$ was 0.057 which corresponds to a

time constant of 35.1 secs. In fact due to an error in the settings of constants in figure 1o the transfer function of the delay circuit was

$$T(i\omega) = -\frac{1}{2o}\ \frac{i\omega - 19\ \frac{2}{\tau}}{i\omega - \frac{2}{\tau}}$$

This unlike 4.1.3. produced an attenuated steam signal. However the delay obtained was larger than that from 4.1.3. for a given value of the time constant τ. In fact with $\frac{2}{\tau}$ set to o.o57, the delay at the frequencies used was about 2.2 radians i.e. 128 degrees.

4.5.2. The Steam and Conversion Time Constants

There are three basic ways of determining time constants of a given system - response to a step change, impulse response and response to sinusoidal variations at different frequencies. For this work the last method was used. On open loop the valve controlling the flow rate of steam was perturbed sinusoidally by means of the sine wave generator. The amplitude of the perturbation was fixed at 1 psi on a valve operating in a signal range of 3 - 15 psi. Electrical signals corresponding to the perturbation fed into the valve, flow of steam and conversion were plotted simultaneously on the four channel recorder. The frequencies were varied in the range 2oo to 17 seconds per cycle and the mean value of the valve setting about which the perturbation was performed, was kept fixed. The ranges of steam and conversion corresponding to the change of valve position at steady state were noted at the operating point and the amplitudes obtained were divided by the steady state amplitudes to get the "gains". The phase shift angles were obtained by simple measurement of the distances between the

ILLUSTRATION OF METHOD FOR DETERMINATION OF DELAY

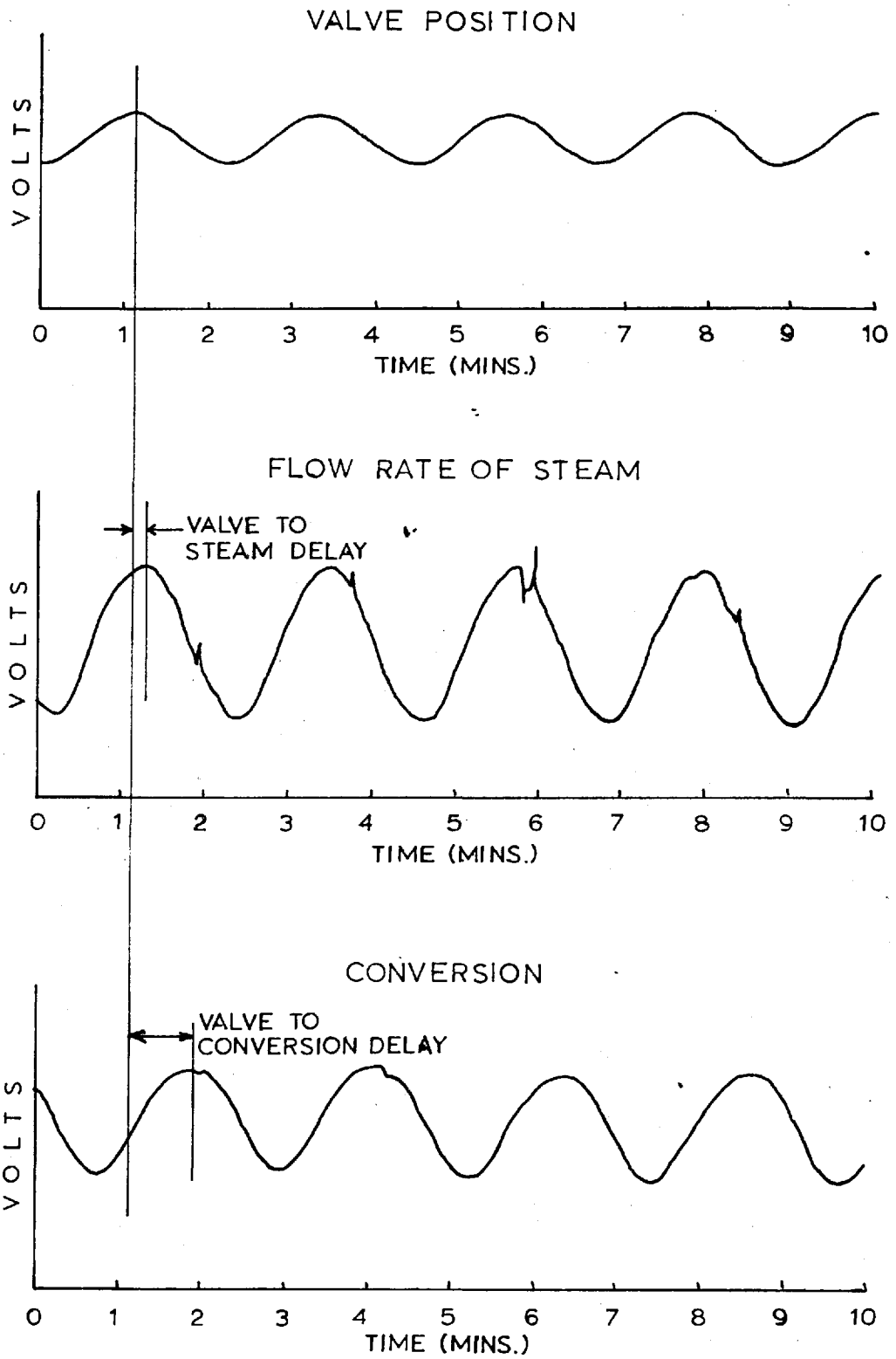

FIG.4.3

TABLE 4.1.

FREQUENCY			VALVE TO STEAM							VALVE TO CONVERSION						
RUN NO	RADS/ SEC	SECS/ CYCLE	PRED GAIN OBS GAIN		PRED P.S. DEGS OBS DELAY SECS		D-V LAG SECS PRED DELAY SECS		P.S. DEGS	OBS GAIN PRED GAIN		OBS DELAY SECS PRED P.S. DEGS		PRED DELAY SECS D-V LAG SECS		P.S. DEGS
1	195	o.o32	1.oo	o.96	9.5	22	12.1	-2.6	21	o.89	o.94	48.4	29	15.6	32.8	29
18	19o	o.o33	o.99	o.96	9.9	23	12.1	-2.2	22	1.oo	o.94	44.1	3o	15.6	28.5	3o
16	135	o.o47	o.98	o.93	9.o	32	11.9	-2.9	29	o.95	o.88	43.2	41	15.3	27.9	4o
1o	113	o.o56	o.89	o.9o	1o.9	38	11.7	-o.8	4o	o.97	o.83	48.o	48	15.1	32.9	49
2	1oo	o.o63	o.84	o.87	9.9	42	11.6	-1.7	44	o.81	o.8o	47.9	54	14.8	33.1	55
14	97	o.o65	o.95	o.86	11.4	43	11.6	-o.2	49	o.96	o.79	41.3	55	14.7	26.6	48
9	84	o.o75	o.84	o.83	9.5	49	11.4	-1.9	48	o.85	o.74	46.6	62	14.5	32.1	6o
17	79	o.o8o	o.83	o.81	8.5	52	11.3	-2.8	47	o.81	o.71	4o.3	65	14.3	26.o	55
6	71	o.o88	o.76	o.77	9.9	57	11.2	-2.3	58	o.65	o.67	46.1	71	13.9	32.2	68
8	6o	o.1o5	o.68	o.71	8.1	65	1o.9	-2.8	58	o.54	o.59	43.8	8o	13.3	3o.5	67
2o	55	o.114	o.71	o.67	7.1	7o	1o.7	-2.2	67	o.56	o.54	39.3	85	13.o	26.3	73
11	55	o.115	o.73	o.67	8.5	7o	1o.7	-3.6	57	o.66	o.54	39.4	85	13.o	26.4	45
3	49	o.128	o.6o	o.62	9.o	76	1o.4	-1.4	78	o.31	o.49	44.1	92	12.4	31.7	85
12	45	o.14o	o.65	o.58	7.6	81	1o.1	-2.4	75	o.42	o.45	38.4	97	12.o	26.4	81
21	45	o.141	o.6o	o.57	8.o	82	1o.o	-2.o	79	o.47	o.44	4o.3	97	12.o	28.3	98
7	41	o.153	o.52	o.53	8.6	87	9.8	-1.2	9o	o.23	o.4o	44.7	1o2	11.6	33.1	1o6
22	39	o.163	o.53	o.5o	7.6	9o	9.6	-2.o	87	o.36	o.37	37.9	1o5	11.3	26.6	9o
5	36	o.177	o.46	o.46	7.1	94	9.3	-2.2	88	o.23	o.33	45.7	11o	1o.8	34.9	133
23	32	o.199	o.38	o.4o	6.6	1o1	8.9	-2.3	95	o.21	o.28	38.4	116	1o.1	28.3	116
15	29	o.217	o.39	o.36	6.6	1o6	8.5	-2.3	1o3	o.19	o.25	4o.8	12o	9.7	31.1	155
4	25	o.251	o.26	o.3o	8.1	114	7.9	o.2	14o	o.19	o.2o	41.4	127	8.8	32.6	127
24	24	o.262	o.25	o.28	5.2	116	7.8	-2.6	1o4	o.19	o.19	37.9	129	8.6	29.3	144
25	24	o.262	o.26	o.28	7.6	116	7.8	-o.2	14o	o.2o	o.19	37.9	129	8.6	28.7	144
13	21	o.292	o.2o	o.24	6.2	121	7.3	-1.1	136	o.18	o.15	36.5	134	8.o	28.6	142
19	17	o.37o	o.1o	o.16	4.8	132	6.3	1.5	138	o.17	o.1o	39.8	143	6.7	33.1	222

peaks on the three curves. This is shown in figure 4.3. The results obtained are shown in table 4.1.

The results were analysed by means of Bode plots where the logarithm to base 10 of the gain and the true phase shift angle were plotted against the logarithm to base 10 of the frequency. The best curves through these points were drawn by eye. From the gain figure it was found that the system can satisfactorily be described by 2 stage exponential dynamics and estimates of the relevant time constants were obtained by drawing tangents to the curves at slopes of -1 and -2. The intercept of the former tangent with the $\log_{10} \omega$ axis at $\log_{10} G = 0$ corresponded to the reciprocal of the time constant of one of the exponential stages. The other time constant was obtained from the projection to the frequency axis of the intercept between the two tangents of slope -1 and -2. Again the time constant in seconds was the reciprocal of the relevant frequency measured in radians/sec. Having obtained this first estimate, the best time constants for predicting the data were found using the technique described for fitting constants to the kinetic models in 3.6.

The transfer function of a two stage exponential system is

$$T(i\omega) = \frac{1}{(1 + i\omega T_1')(1 + i\omega T_2')} \qquad 4.5.1.$$

$$\text{the gain} = \text{Mod}\left|T(i\omega)\right|$$

$$= \frac{1}{\sqrt{(1 + (\omega T_1')^2)(1 + (\omega T_2')^2)}} \qquad 4.5.2.$$

and the phase shift

$$= \tan^{-1}\left\{-\frac{\omega T_1' + \omega T_2'}{1 - (\omega T_1')(\omega T_2')}\right\}$$

VARIATION OF THE S.S. OF RESIDUALS OF GAIN WITH THE TIME CONSTANTS REPRESENTING TWO STAGE EXPONENTIAL DYNAMICS

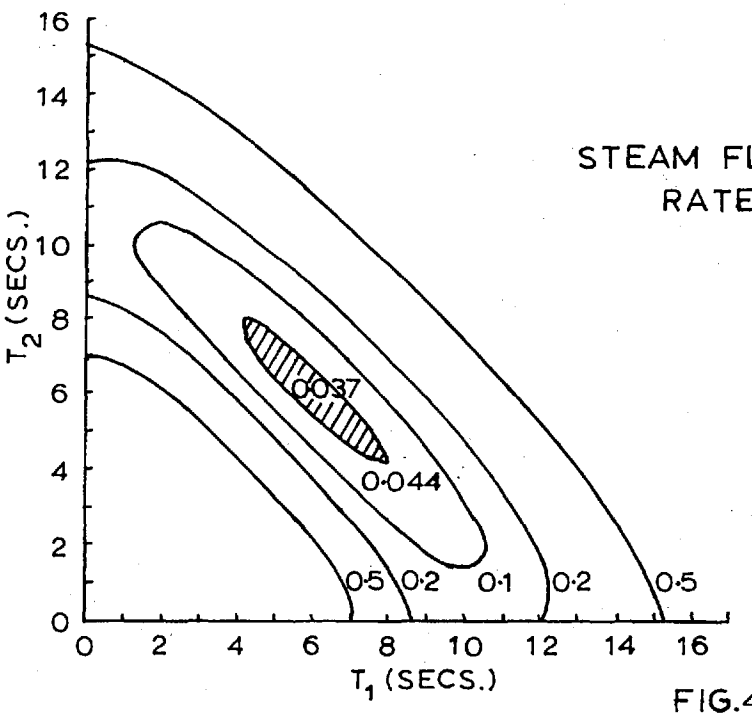

FIG.4.4.

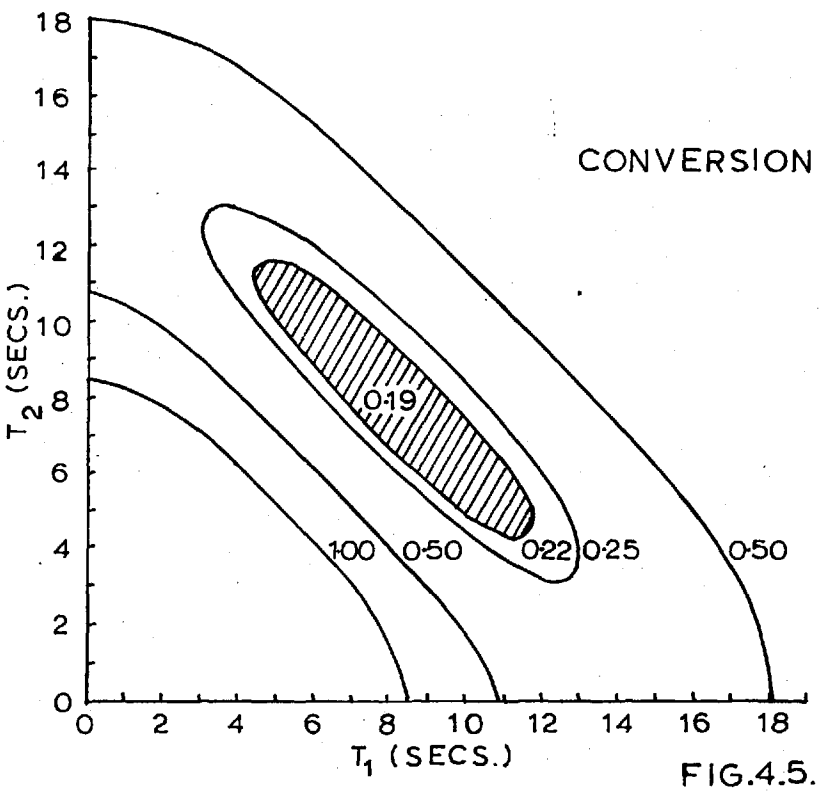

FIG.4.5.

VARIATION OF GAIN WITH FREQUENCY
BODE PLOT

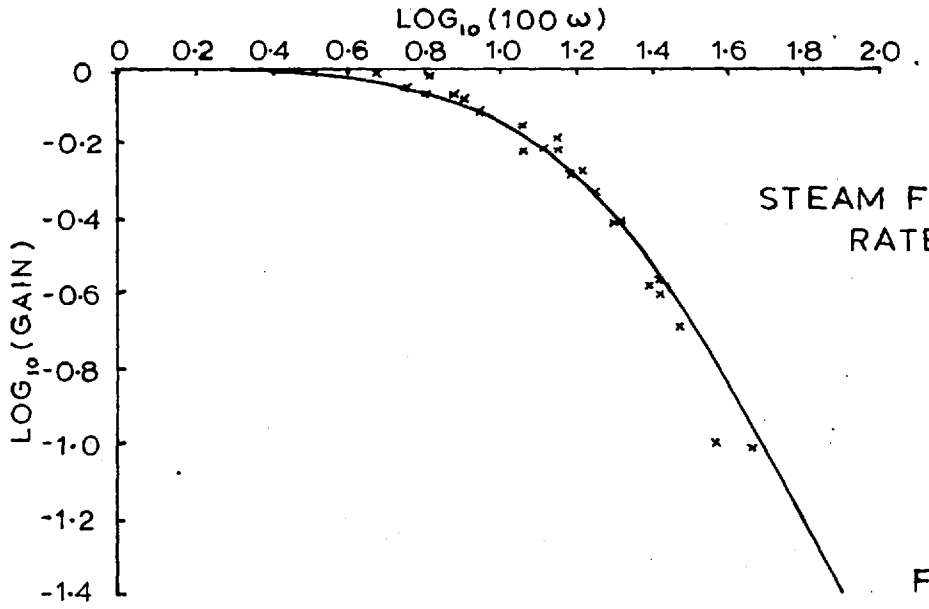

FIG. 4.6.

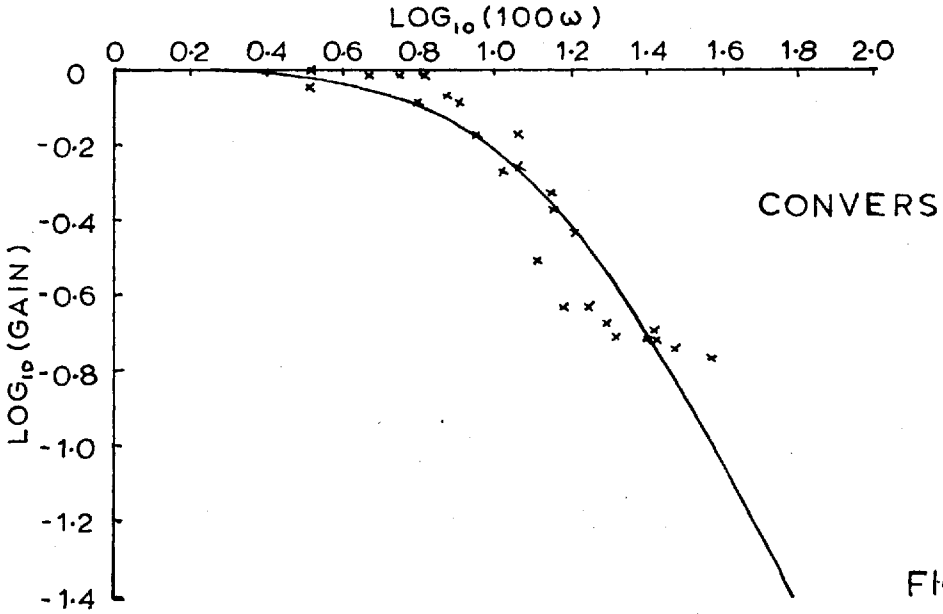

FIG. 4.7.

VARIATION OF PHASE SHIFT ANGLE WITH FREQUENCY

BODE PLOT

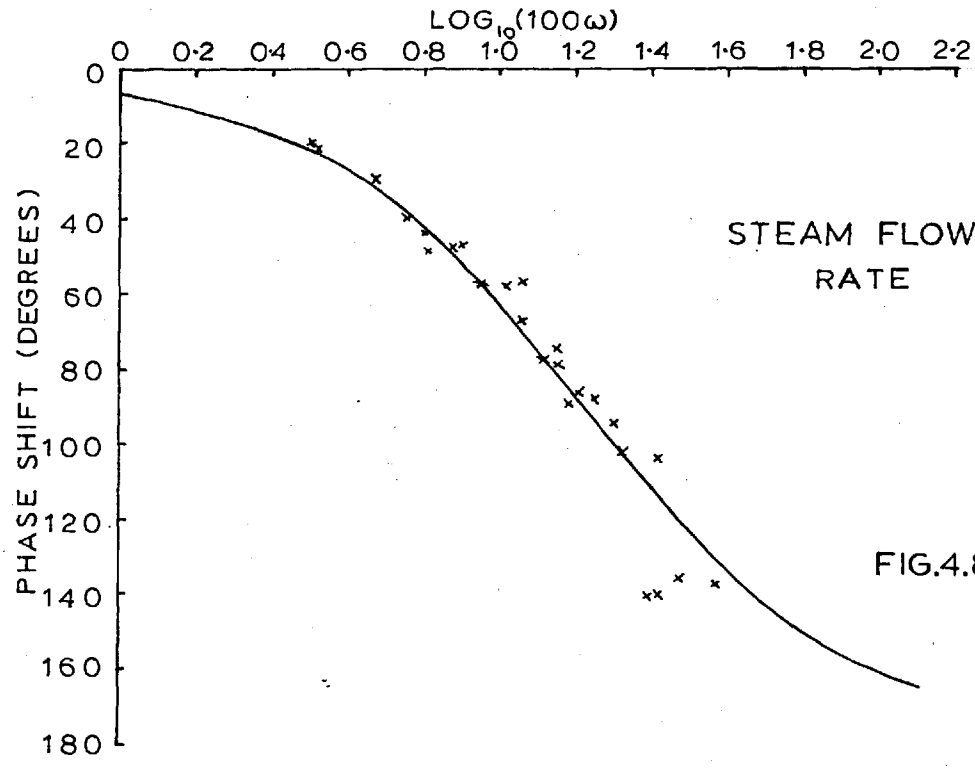

FIG.4.8.

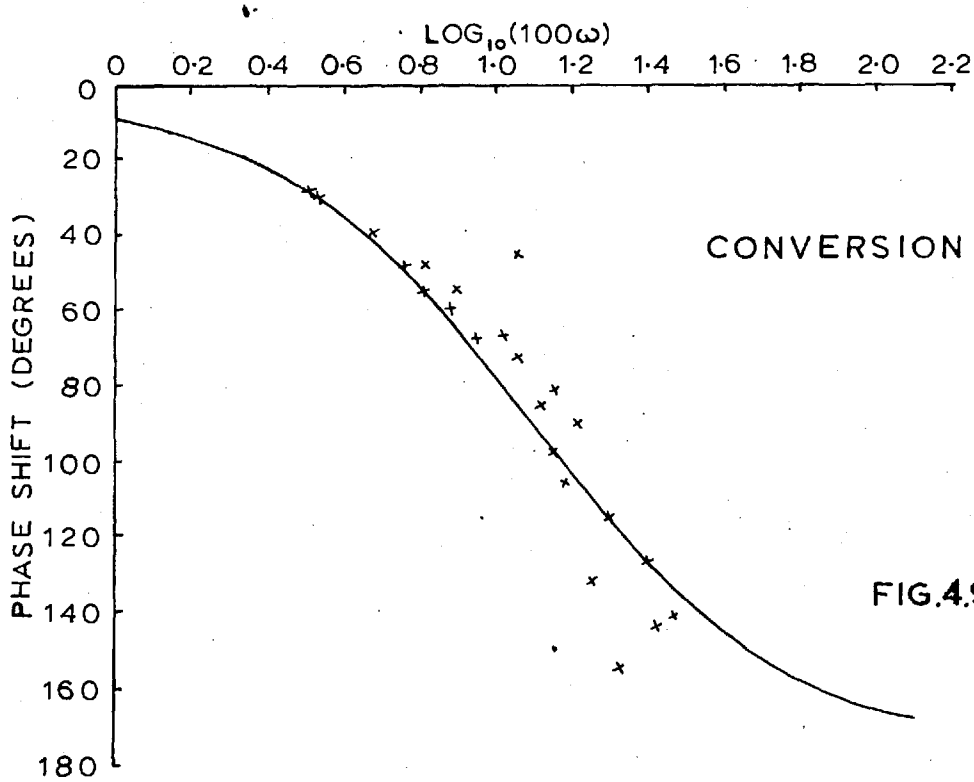

FIG.4.9.

The sum of squares of discrepancies between the actual gains and gains predicted from 4.5.2. were plotted on a grid of values of the two time constants T_1 and T_2. The diagrams for steam and conversion are shown in figures 4.4. and 4.5. From these the best constants with 95% confidence limits were found to be;

steam:	T_1 = 6.1 secs/rad	T_2 = 6.1 secs/rad	confidence limits 4.2 - 8.0 secs/rad
conversion:	T_1 = 8.0 secs/rad	T_2 = 8.0 secs/rad	confidence limits 4.4 - 11.7 secs/rad

Using these values the predicted gain plots were drawn - figures 4.6. and 4.7. These are seen to correspond very well to the true data obtained. In the high frequency part of the conversion plot it can be seen that the $\log_{10}$ G curve apparently tails off to a constant value. This however has not been considered significant because such behaviour would indicate that the gain at those frequencies increased rapidly, in order to compensate for the effect of the steep drop due to the steam flow rate. This is unlikely to have a true physical significance. Also at the higher frequencies the output became noisy and it was difficult to obtain good estimates of signal amplitudes, because small measurement errors produced large percentage changes in the estimated values.

Also using the best time constants, the phase shift angles due to dynamics of the system as opposed to dead time, could be predicted. These predictions which are shown in figures 4.8. and 4.9. were then converted into time delays by multiplying by the corresponding periods in secs/cycle and then subtracting from the time delays measured from the recorder chart. The mean levels of these

values gave the delays in the system which were

steam = - 1.7 secs conversion = 3o.5 secs

with a standard error of

steam = $\pm$ o.9 secs conversion = $\pm$ 1.6 secs

The above indicates that there is a negative delay between the valve and the steam measuring orifice, a situation which has no physical meaning. What is far more likely is that the pen recording the steam flow rate was not correctly lined up with the pen recording the valve position. This is particularly so as a 1 mm error in the lining up would correspond to 4.7 secs. Such an error would result in readings being always biased in the same direction. It would also explain why the mean of conversion in runs 1 to 1o was higher than that in runs 11 to 25 - the recorder chart was changed in between. In the circumstances the steam delay was given a value of 2 secs which was estimated as the time passage of gas from valve to measuring orifice.

4.5.3. High Pass Filter

The constant in the high pass filter was chosen to be about 7.5 secs on an empirical basis. This was further investigated as described in chapter 5.

4.5.4. The Frequency of Operation

From the Bode diagrams of gain vs frequency, the operating frequency was taken such that the attenuation produced was not "unduly large". It would be expected that increase in frequency would improve the performance of the optimiser, especially if a correction is made only once per cycle. On the other hand fast perturbations introduce large attenuations of the output signal, thereby reducing the optimizing efficiency. The problem is what attenuations should one tolerate, which is a point for further investigation. In the

circumstances a period of 1 cycle/95 secs was used, and this was kept constant throughout all the work except for drifts due to the sine wave generator. A better way would be to choose a frequency which maximizes the $\frac{\text{signal}}{\text{noise}}$ ratio. However to achieve this, one requires data, concerning the noise characteristics of the process and this data was not available at the time.

4.5.5. Amplitude of Operation.

This was further investigated in chapter 5. The range used was 0.5 - 7.5 psi on the valve which corresponded to 1.1 to 6.2 l/hr of steam.

4.5.6. The Gain of the Signal Fed Back

In theory the best gain would probably be such that the system reaches its best operating condition in one step. However, if the estimate of slope of the response surface were erroneous, the system would then become unstable. Too small a gain on the other hand slows down the optimisation. A compromise is investigated in chapter 5. The gain set up on the computer ranged from 0.10 to 0.36.

4.6. Conclusion

This chapter has described the systematic way in which a model of the process has been built for a digital computer. First Mars' kinetic model, derived in chapter 3, predicted the steady state response of the system as a function of the changes in temperature and steam flow at constant gas composition. Then dynamics were superimposed onto this model to predict the dynamic behaviour of the process and the required constants were determined experimentally.

Finally the procedure employed on the on-line analogue computer in order to analyze the output signal, was transposed into digital terms.

The resulting dynamic model could now be used to predict the behaviour of the process under various operating conditions. In this way experimental time could be saved because only the best region of operation need be investigated experimentally. The agreement between the model and results obtained experimentally is described in the next chapter.

CHAPTER V

A number of optimiser parameters are available for adjustment to maximize the optimiser performance. The best settings of these parameters will largely depend on the nature of the process, the noise in the process and also the form of the objective function chosen for optimisation. In this chapter various objectives for optimisation are discussed as well as their influence on the different optimiser parameters. Experimental results are compared with those predicted by the digital computer simulation and finally the computer model is used to generate information concerning the best optimiser parameters to use.

5.1. Objectives for Optimisation

Any investigation of the effects of optimiser parameters requires an objective function which is to be optimised. As was stated in chapter 4, this has been chosen as a simple profit function, suitably scaled for operation on the analogue computer. However, the function described is an instantaneous quantity and it is its average value over a period of time, which is of interest. Several objectives could be chosen and these are described below.

a) One could consider the time taken by the system to reach the optimum position after a disturbance. On this basis one could explore the way in which the optimiser parameters influence and minimize this time. However, this would not distinguish between a case where the system very quickly reached a position slightly offset from the optimum and then took a long time to climb to the best position and the case where the system climbed steadily to the optimum in the same time as before. Thus a more realistic objective would be to consider

b) the loss in the objective function in reaching the optimum. The

disadvantage here is that the objective function does not consider what happens to the system once the optimum has been reached. For example, the input signal amplitude which should have a large value in order to reach the optimum quickly, is required to be small at the optimum in order to avoid the losses due to the perturbation. Another objective which could be of interest is

c) the loss in the objective function while the system oscillates about the optimum value. Here, however, no account is taken of the time required to reach the optimum after a displacement. Thus the best objective to optimize seems to be some combination of the loss resulting from the climb to the optimum and also the loss at the optimum. Different times over which one considers the loss would give different weights to the climbing part and to the operation at the optimum. In fact the shorter the time the more weight is given to the effect of disturbances. Two times were considered

d) loss in 2o minutes

e) loss in 6o minutes

The two times were chosen by inspection of the results obtained - table 5.1. Other times would have resulted in different optimum settings of the optimiser parameters. The above two objectives correspond to

d) a system with noise occurring very frequently and

e) a system operating mostly at its optimum value.

In order to standardize the results of d) and e), they have been considered as the loss over the relevant period of time expressed as a percentage of the potential value of the objective function which would occur if the system reached the optimum in one step, starting at the current operating point, and

did not oscillate about the optimum value, i.e.

$$\frac{\int_0^T (P_{max} - P) \, dt}{(P_{max} - P_{in}) T} \quad \text{loo \%}$$

where P is the value of the objective function at time t

and P_{max} and P_{in} are its maximum and initial values respectively.

This formulation reduces the effect of various uncontrollable drifts occurring in the system, which alter slightly both the starting position and the position and value of the optimum. For similar reasons, objective b) was standardized by

$$\frac{\int_0^T (P_{max} - P) \, dt}{P_{max} - P_{in}}$$

and objective c) by

$$\frac{\int_0^T (P_{max} - P) \, dt}{P_{max}} \quad \text{loo \%}$$

5.2. The Optimiser Parameters Investigated

5.2.1. The Gain of the System

This was defined as the factor by which the estimate of the slope was multiplied before the signal was fed back as an adjustment to the valve position. The slope was obtained by integrating over a complete cycle and the valve

position was changed in proportion to this slope. The gain was altered by pot 16 in the analogue computer circuit (figure 1o). In fact as the correlating multiplier signal was integrated over a full cycle, the slope thus estimated contained a constant, whose value was the period of the perturbation, as well as the amplitude of the perturbation signal - (1.3.3.). Thus in this chapter the gain is considered as a product of the perturbation period and the setting of pot 16.

5.2.2. The Amplitude of the Perturbation Signal

This was a pneumatic signal fed into the valve controlling the steam flow rate and it was adjustable by a dial on the sine wave generator. The set up had the large disadvantage that the amplitude could not be controlled very exactly and one was thus limited with the size of amplitudes investigated. A more satisfactory way would have been to generate the sine wave on the analogue computer, but there was insufficient equipment available.

5.2.3. The Phase Shift

This was introduced to compensate for the dynamic delays in the process. As was mentioned before, it was altered by adjusting the relative position of the shaft on which the sin-cos potentiometer was mounted and the shaft carrying the swash plate which varied the air pressure signal. A dial calibrated in degrees was available on the sine wave generator.

5.2.4. The Constant of the High Pass Filter.

This determined the speed with which the filter could follow changes in the system and also introduced an attenuation into the perturbation of the objective function signal. Its value was altered by pot 13 in figure 1o.

5.2.5. The Period of the Perturbation

This was kept constant throughout in order to reduce the amount of experimentation. Changes in the frequency of perturbation influence all the other parameters. If the frequency is increased, the amplitude of the output signal from the process is reduced for a given input amplitude. The gain is also reduced due to a reduction in the period. The phase shift angle is increased but this increase is automatically compensated by the delay circuit. The high pass filter on the other hand increases the size of the output amplitude. In fact for a given time constant of the high pass filter there is an optimum frequency of operation, if the objective is to minimize the attenuation of the input signal amplitude. The period was set up on the sine wave generator and was found to drift by several seconds during a day. This was hard to compensate because at the periods used the frequency was very sensitive to small changes in the dial setting.

5.3. The Experiments Performed.

A half replicate 2^{4-1} factorial experiment was run on the four optimiser parameters described in the last section. Each run was started with the reactor at 405^{o}C, a fixed gas flow rate and composition and a steam flow rate of 60 l/hr. The results obtained are shown in table 5.1. Three replicates of the centre point were also run to give an estimate of the reproducibility of the results. The runs were performed in a random order shown in column 1 of the table.

Unlike the factorial experiment performed to compare the kinetic models in chapter 3, the settings of the parameters could be reproduced very well, except the setting of the signal amplitude. In the runs, the frequency is seen to have drifted around by about $\pm$ 4%, a factor which has been disregarded

TABLE 5.1.

2^{4-1} FACTORIAL EXPERIMENT FOR THE OPTIMISATION OF THE OPTIMISER PARAMETERS

RUN NO	GAIN (γ)	AMPLITUDE (a) 1/hr	PHASE SHIFT (θ) degs	HIGH PASS FILTER CONST (τ) degs	PERTURBATION PERIOD secs	γa	$\frac{\gamma}{a}$	TIME TO REACH MAX mins	STD LOSS TO REACH MAX secs	%-LOSS AT MAX	%-LOSS IN 20 MIN	%-LOSS IN 1 HOUR
10	29.7	4.0	114	10	99	119	7.4	6.9	138	7.7	32.9	20.2
6	9.7	5.4	114	6	97	52	1.8	62.9	602	8.1	56.2	52.0
7	30.0	1.4	114	6	100	42	21.4	58.8	590	3.9	73.2	41.6
11	9.2	1.4	114	10	92	13	6.6	70.7	710	3.3	78.2	48.2
8	29.7	4.6	94	6	99	137	6.5	13.4	153	5.1	34.5	20.1
2	9.7	4.9	94	10	97	48	2.0	26.6	290	7.8	50.0	29.4
4	28.5	1.1	94	10	95	31	25.9	11.3	152	6.4	28.0	18.3
5	9.5	1.4	94	6	95	13	6.8	101.8	1125	3.7	82.6	63.8
1	19.6	2.9	104	7.5	98	57	6.8	23.8	301	5.4	55.1	28.4
3	19.4	2.6	104	7.5	97	50	7.5	20.0	234	4.9	49.4	24.0
9	19.6	3.2	104	7.5	98	63	6.1	20.0	231	4.8	46.2	22.2

in the analysis, but has been included in the gain. Further the temperature in the reactor fell by as much as 5° C during an optimisation run and thus a mean value was taken. As the temperature control was based on a thermocouple measuring the temperature at entry to the catalyst bed, the fall in temperature was probably the result of there being less monoxide converted at the maximum of the objective function than at the starting position of 60 l/hr steam flow.

The experimental results obtained were analysed in terms of each of the five objectives described in 5.1. The effects of the optimiser parameters together with their significance levels are presented in table 5.2. Discussion of these results is given below.

5.4. Analysis in Terms of Time Required to Reach the Maximum

From the table 5.2. it can be seen that at the operating point there are three highly significant effects: gain (γ), amplitude (a) and $\gamma a + \Theta \tau$ as well as the high pass filter constant (τ), which is significant, but only at the 95 % level. The factorial experiment in fact indicates that both the gain and amplitude are some distance from the optimum value and they should be increased in magnitude, which is as expected intuitively. The fastest approach to the maximum will be expected to occur with as large a gain and amplitude as possible, subject to stability restrictions. As was mentioned earlier (1.3.3.), the slope estimated by the computer includes the amplitude of the perturbation signal and as this slope is multiplied by the gain, one would expect a large correlation between γ and a. Further, in the experiment it was the setting of pot 13 in figure 10 which was changed linearly at the two levels of the factorial. This setting corresponded to the reciprocal of the high pass filter

TABLE 5.2.

ANALYSIS OF THE RESULTS IN TABLE 5.1.

SOURCE OF VARIATION	OBJECTIVE FUNCTION									
	TIME TO REACH MAXIMUM		LOSS IN REACHING MAX		LOSS AT MAXIMUM		LOSS IN 2o MINUTES		LOSS IN 1 HOUR	
	EFFECT	MEAN SQUARE	EFFECT	MEAN SQUARE	EFFECT	MEAN SQUARE	EFFECT	MEAN SQUARE	EFFECT	MEAN SQUARE
GAIN (γ)	- 42.9	184o	- 426	181500	o.o5	o.oo	- 24.6	6o5	- 23.3	543
AMPL (a)	- 34.2	117o	- 348	121100	2.85	8.12	- 22.1	488	- 12.5	156
PHASE SHIFT (θ)	8.3	69	12o	1440o	1.1o	1.21	- 14.3	2o5	- 15.3	234
H.P.F. CONST (τ)	11.5	132	8o	64oo	o.oo	o.oo	11.3	128	7.6	58
$\gamma a + \theta\tau$	- 29.4	864	- 297	882oo	- 1.6o	2.56	5.4	29	- 2.7	7
$\gamma\theta + a\tau$	9.o	81	129	166oo	o.o5	o.oo	1o.4	1o8	4.1	17
$\gamma\tau + a\theta$	3.1	9	68	46oo	1.4o	1.96	- 9.o	81	3.7	14
AVERAGE	44.o	194o	44o	193600	5.75	33.o6	1o8.9	1186o	73.4	5388
ESTIMATED VARIANCE		4.81		1567		o.1o		2o.3		1o.2
S.S. AT 95% SIGNIFICANCE LEVEL		89		29ooo		1.85		376		189
S.S. AT 99% SIGNIFICANCE LEVEL		474		1542oo		9.85		2ooo		1oo5

constant and as the results indicate that the reciprocal value should be reduced, it means that the value of the high pass filter time constant should in fact be increased. In so doing the attenuation of the amplitude of the input signal will be decreased. In the circumstances it is a little surprising that the effect $a\tau + \gamma\theta$ is not more significant, the reason may be that $\gamma\theta$ is working in the opposite sense to $a\tau$ and also that the operating point is a long way from the optimum.

5.5. Analysis in Terms of Loss in Reaching the Optimum

The results here are very similar to those in the last section. This is because the climb to the maximum was fairly steady, i.e. in none of the runs did the system approach quickly a value near the maximum and then take a long time actually to reach the optimum value. As before, the gain and amplitude together with their interaction are the three highly significant effects, which are as would be expected. In this case the effect of the high pass filter constant has been slightly reduced but this is not very important as it is still significant at the 90 % level. Also all this really means is that for this particular objective function the high pass filter constant is nearer to its best value than in the last case. In both the cases the phase shift angle is very close to its optimum value.

5.6. Analysis in Terms of Percentage Loss at the Maximum

The effects significant at the 95 % level are the amplitude, a, and the two sets of interactions $\gamma a + \theta\tau$ and $\gamma\tau + a\theta$. In this case the most important change from the two objectives so far considered is that neither the gain nor the high pass filter constant have any effect at all, meaning that

they are either at their optimum values or more likely, especially in the former case, do not really influence the loss at the maximum. Obviously the amplitude of the input signal is of the utmost importance. This can be seen from 1.3.3. for the case of a parabola in the absence of noise, where the loss at the optimum is proportional to the square of the amplitude. The results indicate that the amplitude should in fact be reduced considerably, the limit really being such that the perturbation signal is just distinguishable from the noise in the system. The large interaction terms indicate that the operating point about which the factorial experiment was performed, is close to the optimum value of the three other parameters.

5.7. Analysis in Terms of Percentage Loss in 20 Minutes

The only two significant effects here are the gain and amplitude. This indicates that the position of operation is some distance from the optimum position and so the interaction effects are negligible. This has been found to be the case, as is brought out by the experiments described later in this chapter. The time constant of the high pass filter and phase shift are close to their best values, but both of them should be marginally increased. The amplitude and gain on the other hand should be increased considerably. A large gain and amplitude is required here, as in 20 minutes the process spends most of the time in climbing to the maximum and thus the loss at the maximum due to the large amplitude is not so important.

5.8. Analysis in Terms of Percentage Loss in 60 Minutes

This objective gives far more weight to the loss at the maximum than the last one. The most important effect here is the gain, which determines the

speed with which the system reaches the maximum and this gain should be increased. The results already considered, indicate that the amplitude of the perturbation signal should be increased in order to reduce the loss to reach the maximum but it should be reduced in order to decrease the percentage loss at the optimum. Thus for the present objective function i.e. percentage loss in 60 minutes the operational setting of the amplitude is not a bad compromise. In fact the amplitude should be marginally increased in order to speed up the attainment of the maximum, which is not reached in 60 minutes during runs 5, 6 and 11. The phase shift should also be increased, which is a little surprising, as neither the loss to the maximum nor the loss at the maximum was influenced by the phase shift. An incorrect phase shift would in fact attenuate the value of the predicted slope and also move the position at which the slope was zero. This would be particularly true if the delay in the steam flow did not correspond exactly to the conversion calculated.

After this initial set of experiments had been run and the results had been analysed it was decided to investigate further the objective "percentage loss in 20 minutes." The reason for this was that with a better choice of optimiser parameters, the system was expected to reach the optimum value in the time chosen as well as to oscillate about the optimum, thus giving a realistic objective to optimize. Also it meant that experiments could be run off fairly rapidly, both on the plant and in the computer simulation. Finally in order to reduce the number of experiments the phase shift and high pass filter constant were fixed at the best values found and only the influence of gain and amplitude on the objective function was investigated. The results are shown in table 5.3.

The experimental procedure was to specify as closely as possible a grid in the γa and $\frac{\gamma}{a}$ plane. The reason for this way of presentation is that

TABLE 5.3.

RUN NO	% LOSS	GAIN (ɣ)	AMP (a)	ɣ a	ɣ / a
1	42.4	14.1	4.1	58	3.4
2	36.3	17.6	3.7	65	4.8
3	42.7	23.5	3.3	78	7.1
4	61.4	18.3	2.4	44	7.6
5	58.7	18.6	3.3	61	5.6
6	34.o	23.4	4.1	96	5.7
7	32.o	28.2	4.1	116	6.9
8	33.8	24.5	5.7	14o	4.3
9	31.7	29.1	3.1	9o	9.4
1o	33.o	23.9	4.1	98	5.8
11	34.8	28.2	3.5	99	8.1
12	unstable	33.5	4.3	144	7.8
13	4o.o	27.4	2.4	66	11.4
14	37.9	22.8	2.2	5o	1o.4
15	44.6	14.3	5.3	76	2.7
16	31.2	28.5	5.5	157	5.2
17	37.1	28.5	2.6	74	11.o
18	29.7	32.4	4.4	143	7.4
19	33.8	27.6	3.5	97	7.9
2o	31.2	27.4	3.3	9o	8.3
21	3o.o	31.3	3.9	122	8.o
22	31.6	23.6	6.o	142	3.9
23	3o.5	22.9	6.2	142	3.7
24	unstable	31.6	2.8	82	11.3
25	unstable	33.8	4.3	145	7.9
26	unstable	31.6	6.2	196	5.1
27	51.3	18.o	5.9	1o6	3.1

DIAGRAM OF A TYPICAL OPTIMISATION RUN

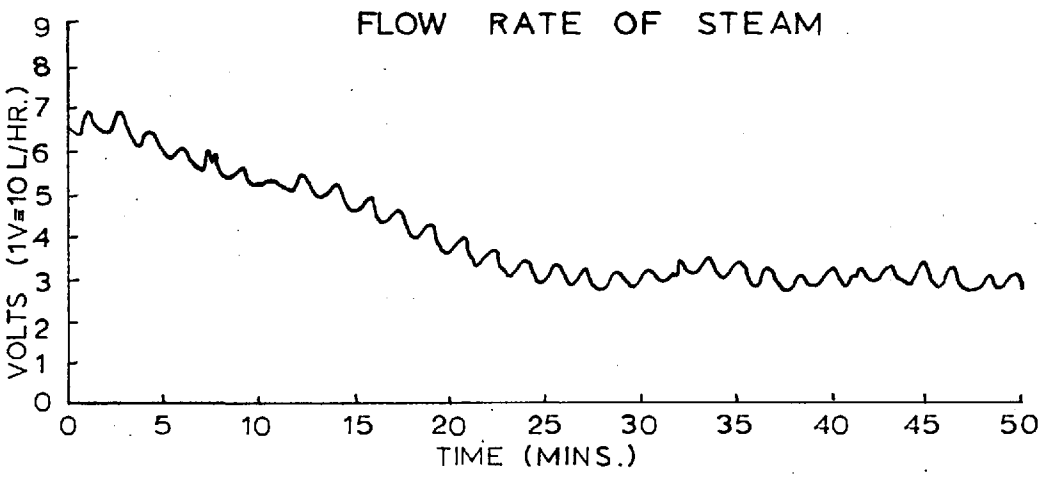

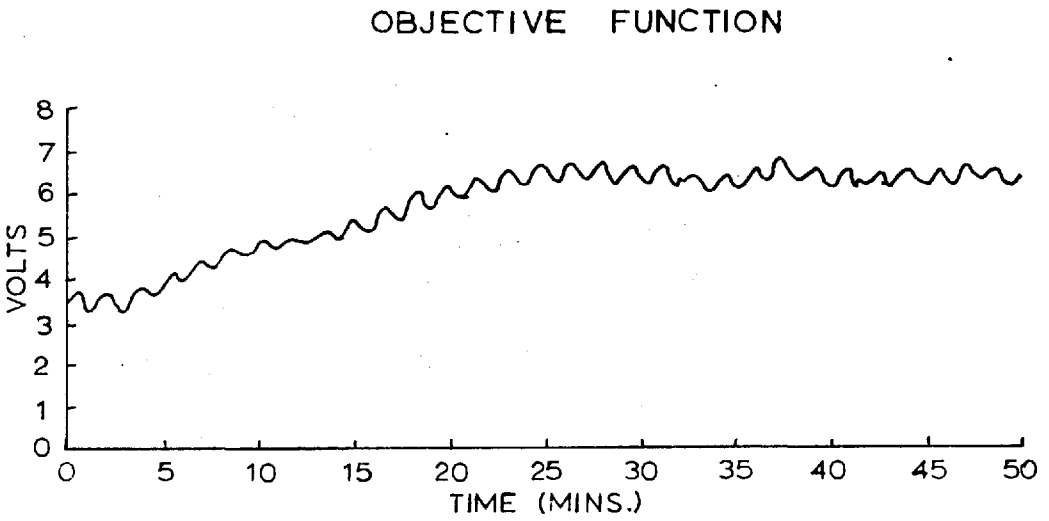

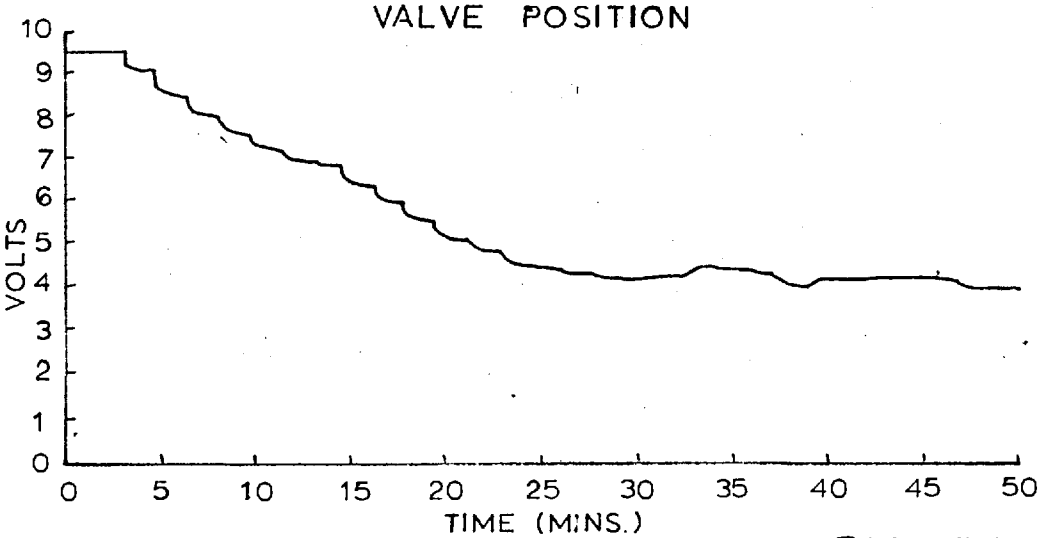

FIG. 5.1.

VARIATION OF THE %AGE LOSS IN 20 MINUTES WITH GAIN AND AMPLITUDE

HIGH PASS FILTER CONST. = 10 SECS.
PHASE SHIFT ANGLE = 94 DEGS.

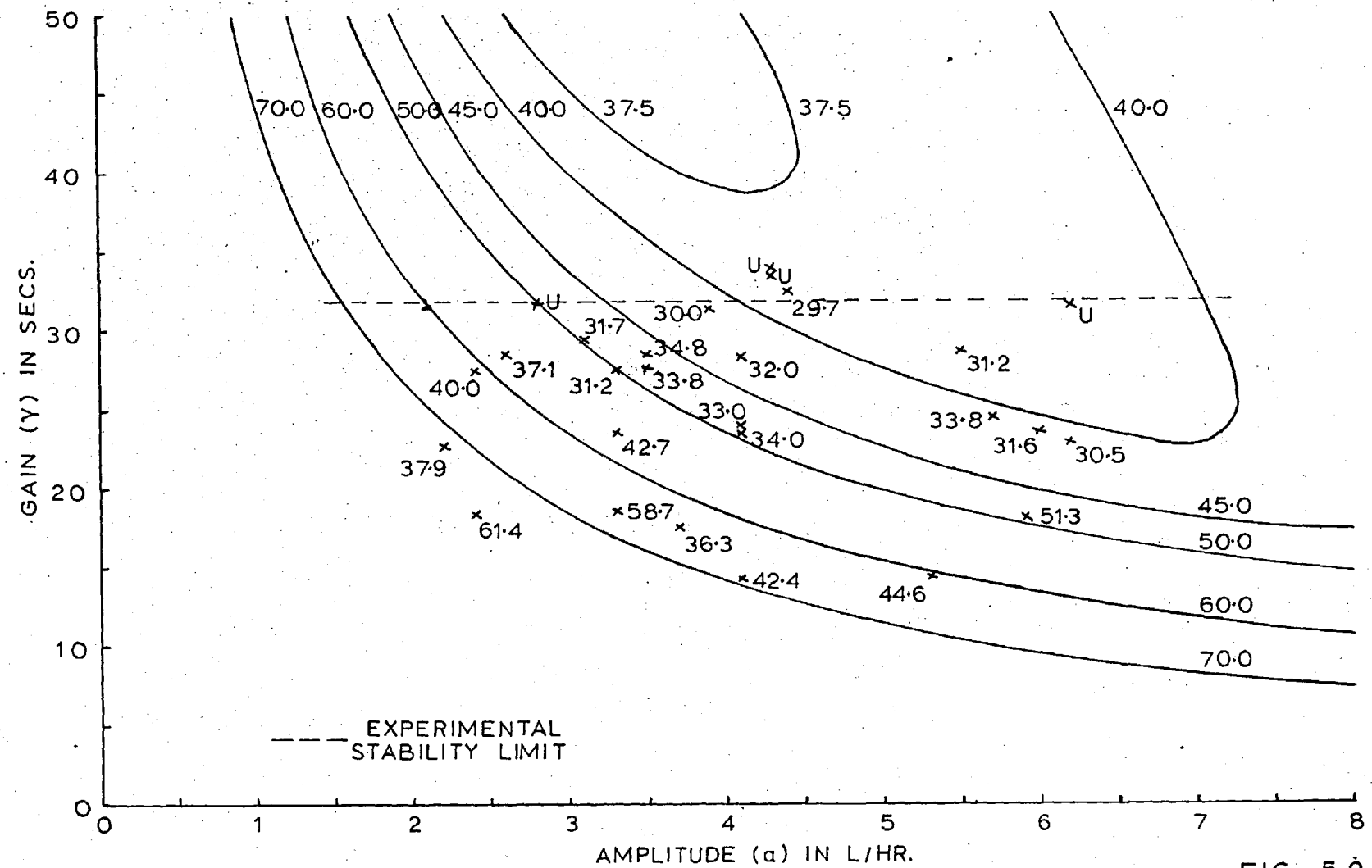

FIG. 5.2.

VARIATION OF THE %AGE LOSS IN 20 MINUTES WITH γa AND γ/a

HIGH PASS FILTER CONST = 10 SECS.
PHASE SHIFT ANGLE = 94 DEGS.

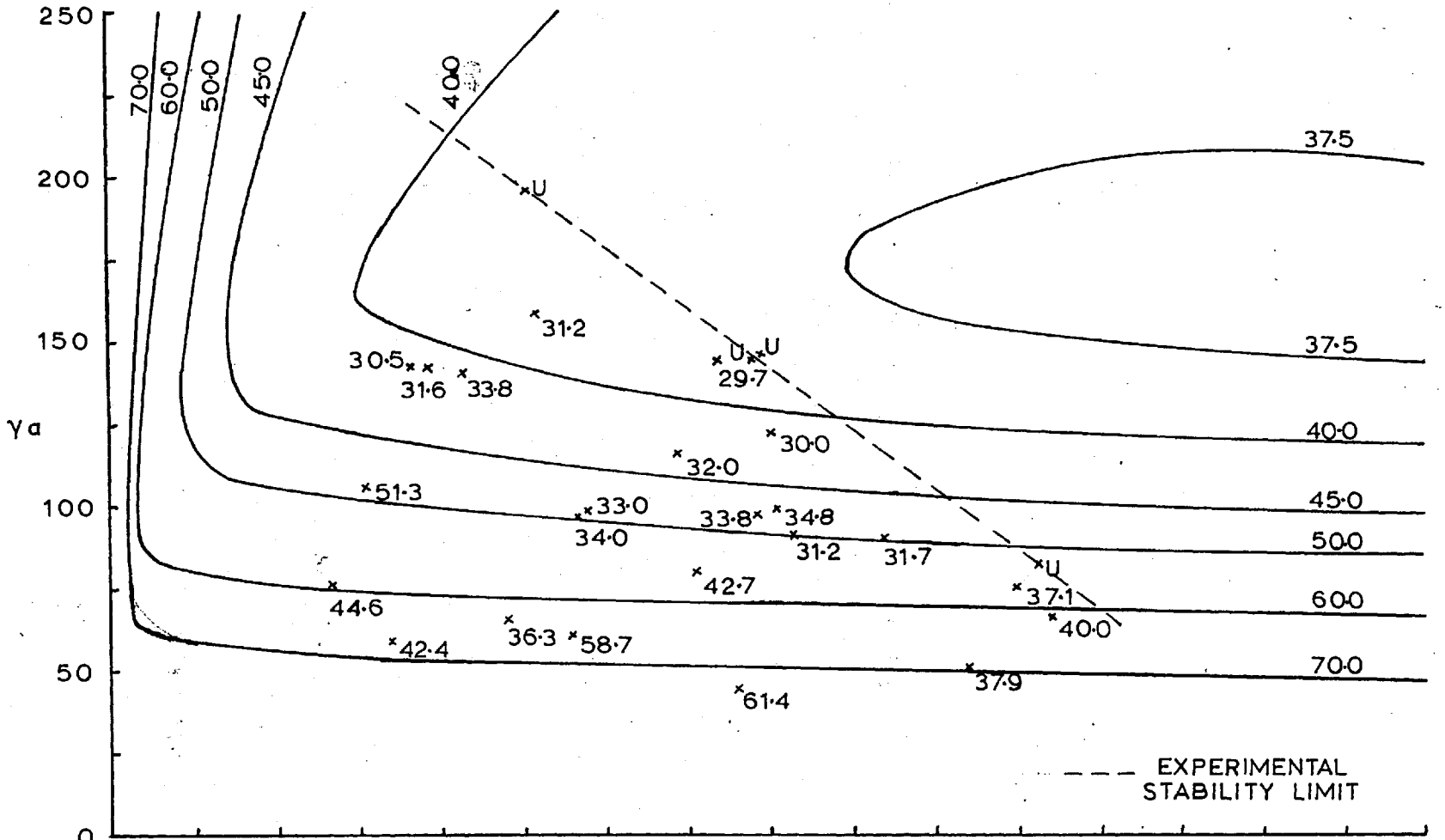

FIG. 5.3.

effectively γ_a controls the time taken to reach the optimum, while $\frac{\gamma}{a}$ describes the amplification of the noise in the system. Although the settings in terms of the dial position on the sine wave generator were such, that a factorial climb to the optimum was performed, when the pressure settings of the valve were converted to the corresponding steam amplitudes, the factorial scheme was badly distorted. Despite this the optimum region of operation was reached.

The experiments showed that good choice of operating conditions was at a combination of large values of both γ_a and $\frac{\gamma}{a}$. The limit on the magnitude was the stability criterion, for in the range of investigation the system became unstable at gains higher than 32, irrespective of the perturbation amplitude - the gain in question is the setting of pot 16 multiplied by a constant whose value is the perturbation period. The low level of the amplitude setting was limited by the crude calibration of the amplitude control dial on the sine wave generator and thus lack of reproducibility of results. The best parameter values obtained corresponding to a minimum loss of 29.7% were $\gamma_a = 143$, $\frac{\gamma}{a} = 7.4$. The results were also plotted in terms of γ and a (figure 5.2) and as was mentioned earlier the boundary of the stable region occurred when the gain γ had a limit value of 32.

5.9. The Digital Simulation

The process was simulated on the London University Atlas computer in a way described in chapter 4. Initially the 11 runs of the factorial experiment shown in table 5.1. were simulated, without considering the delay circuit used in practice. Thus the conversion signal was matched exactly with the corresponding steam flow signal and the delay circuit was assumed not to attenuate the amplitude of the steam flow signal. The results obtained for the objective, %-loss in 20 minutes, are shown in column 3 of table 5.4.

TABLE 5.4.

2^{4-1} FACTORIAL EXPERIMENT AS SHOWN IN TABLE 5.1.

COMPARISON OF OBSERVED AND PREDICTED RESULTS FOR THE OBJECTIVE

PERCENTAGE LOSS IN 20 MINUTES

Run No	Percentage Loss in 20 Minutes						
	Observed	Predicted		Source of Variation	Effect Based on Results from Column (i)		
		True θ Incorrect λ	Incorrect θ True λ				
	(1)	(2)	(3)		(1)	(2)	(3)
10	32.9	45.8	21.5	Gain (γ)	- 24.6	- 12.7	- 11.4
6	56.2	70.0	42.2	Ampl (a)	- 22.1	- 14.9	- 14.1
7	73.2	66.6	43.3	Phase (θ) Shift	- 14.3	1.0	- 1.5
11	78.2	75.0	50.9	H.P.F. (τ) Const.	11.3	- 2.8	- 2.0
8	34.5	49.2	29.0	$\gamma a + \theta\tau$	5.4	- 4.8	- 4.5
2	50.0	60.0	40.0	$\gamma\theta + a\tau$	10.4	- 3.9	- 2.8
4	28.0	68.4	44.5	$\gamma\tau + a\theta$	- 9.0	2.8	- 1.1
5	82.6	75.3	50.5	Average	108.9	63.7	40.2
1	55.1	62.9	39.0	Estimated Variance	20.3	5.3	2.4
3	49.4	66.0	40.5	S.S. at 95% Sig. Level	376	98	45
9	46.4	61.5	37.4	S.S. at 99% Sig. Level	2000	522	237

The above runs were recomputed using a discrete form of the delay circuit (4.5.1.). The results in this case were however very different from those observed on the real plant. In particular, the optimiser moved by a maximum distance of only 7.4 l/hr of steam over a period of 36 cycles i.e. almost 1 hour of real time. The direction of movement depended primarily on the value of the phase shift angle and when this was at the high level, i.e. 114 degrees, the optimiser moved in the wrong direction. Thus a further set of simulated results was investigated, with the phase shift angles reduced by 90 degrees for each of the 11 runs. Some of the results thus obtained are shown in column 4 of table 5.4. The analysis of the three lots of results is also shown in table 5.4. From this it can be seen, that although the predictions are numerically considerably different from the observed results, the two significant effects i.e. gain ($\aleph$) and amplitude (a), are correctly reproduced in both the simulations. The standard error between the observed results and those predicted by the two methods described, is 17.2 and 19.5% respectively. Thus there exists a doubt whether the phase shift angles recorded were in fact correct, or whether through a wrong connection on the control panel they were apparently 90 degrees out of phase. As no possibility existed to perform more practical experiments, from which one could decide on the true set up, no further work was done on this part of the results. This was thought not to be a major setback because in either case the significant effects were correctly predicted and also the runs at constant value of phase shift angle, high pass filter constant and frequency were available to check the effectiveness of the simulation. In any case the interest in the results was mostly qualitative, because although the optimum settings of the optimiser parameters are expected to vary from plant to plant, the form of the dependance of the objective function on these

parameters should remain constant.

5.10. The Experiments at Constant Phase Shift Angle and High Pass Filter Constant

Here the period of the perturbation was fixed at 92.3 secs/cycle. This was convenient for computational purposes, because 13 complete cycles corresponded to 20 minutes of real time. Further the temperature was fixed at 405°C. The phase relations between the conversion and steam flow rate signals in the objective function were matched exactly, without simulating the analogue computer delay expression. This reduced the importance of the exact specification of the phase shift angle. As in the experiments both the phase shift angle and the time constant of the high pass filter were kept constant at the best values found on the plant. The results obtained are shown as contour lines in figures 5.2. and 5.3.

The simulation gives higher losses than the experimental results but the effects of variations in the parameter settings are similar. In particular the simulation confirms the experimentally obtained best operating region. The experimental instability occurring in the process when the gain was greater than 32, has not been reproduced, probably because the simulation was noise free - in the experiments the process was considered unstable when the steam valve was shut off by the controller. With sufficiently high gains (e.g. $\gamma = 150$ when $a = 2$) the simulated results did become unstable, but this is of no practical interest. According to the simulation the contours of γa vs $\frac{\gamma}{a}$ close, but they are considerably elongated along the $\frac{\gamma}{a}$ axis. In fact below a certain value of γa (about 150 1/hr) and above a $\frac{\gamma}{a}$ of about 10 $(1/hr)^{-1}$ the performance of the noise free system depends approximately only on the value of γa, which is similar to the findings of Hammond and Duckenfield (34). At low values of $\frac{\gamma}{a}$

and δa, the contours are very closely bunched together because at zero gain or amplitude the loss is 100% due to the system effectively operating on open loop.

The discrepancy between the predicted and the observed results may be due to one of several causes. Thus some non-linear process components like the variation of the steam amplitude with position, for a given pressure signal fed into the valve, were not exactly simulated. However a far more sensitive effect on the objective function was the difficulty in judging the value at the maximum due to dynamic effects and noise. Further the calibration of the transducer measuring the flow of steam into the reactor tended to drift, despite the temperature at the orifice remaining reasonably constant (the size of the drift was about $5^{\circ}C$ at $200^{\circ}C$ during the course of an optimising run). As the steam flow was obtained by difference, this meant that the signal used in calculating the objective function could be out by anything up to 10 l/hr of steam, which would alter the value of the percentage loss by several percent. It could also account for large variations in values between adjacent points. This effect of the drift in the calibration has not been simulated at all, as it was not measurable - if it had been, an allowance would have been made for it.

The simulation showed an interesting trend whereby the optimum value of the steam flow rate depended on the amplitude of the perturbation. Thus at amplitudes less than 5 l/hr the final position was 25.4 l/hr of steam. At 8 l/hr the position had become 25.9 l/hr and at $a = 22.6$ l/hr the position was 30 l/hr. This behaviour is partly due to the unsymmetrical nature of the response surface - see figure 4.1. It results in the system finding a position at which the losses on each side of the optimum due to the straddling, are

equal. However this cannot be the full explanation. At 405°C the steady state optimum of the profit objective function occurs at a steam flow rate of 32 l/hr and in some of the runs the simulated system was seen to settle at a position distant by more than one perturbation amplitude from 32 l/hr. Thus another effect must be present and it is probably the "transfer at the optimum" mentioned by Box and Chanmugan (12). This effect arises in our case, because in computing the objective function, two quantities with independent dynamics are subtracted. As a result the Laplace coefficients, p, occur in the numerator as well as the denominator i.e. on the basis of the theory of linear systems the overall transfer function contains both zeros and poles. As is shown in 5.11., this means that with a given phase shift angle, even if it is the optimum one, the slope of the response curve is not necessarily zero at the optimum. In particular, for the case of the simulated runs described in this section, where the conversion and steam flow signals are exactly matched in phase, the bias to the slope is given by:

$$0.4\ (1 - \frac{\nu_2}{\nu_1}) = -\ 0.042$$

which corresponds to the optimum occurring at a steam flow rate of about 27.8 l/hr.

Thus in conclusion, transfer at the maximum together with the non-symmetrical nature of the response surface at the maximum, can account for the variation with the perturbation amplitude of the position of steam flow, corresponding to the maximum of the profit objective function.

5.11. Derivation of an Expression for Transfer at the Maximum

Let

θ_i = delay in the system due to finite time of passage

ϕ_i = delay in the system due to dynamics

λ = compensation for delay between steam and conversion signals

λ_h = phase shift due to the high pass filter

ψ = phase shift applied to the input signal before correlating with the output signal

ν_i = gain due to the dynamics of the system

ν_h = gain due to the high pass filter

For the purpose of the derivation, the value of conversion at time t resulting from a sinusoidal perturbation of the steam flow rate, is represented by a first order Taylor expansion about the steady state value i.e.

$$\text{conversion } (S) = \text{s.s. conversion } (S_o) + \frac{\partial}{\partial W}(\text{conversion})_{\text{s.s.}} \nu_1 \, a \cos(\omega t + \theta_1 + \phi_1)$$

$$= S_o + \left(\frac{\partial S}{\partial W}\right)_o \nu_1 \, a \cos(\omega t + \theta_1 + \phi_1) \qquad 5.11.1.$$

Thus the value of the objective function, C, is

$$C = S_o + \left(\frac{\partial S}{\partial W}\right)_o \nu_1 \, a \cos(\omega t + \theta_1 + \phi_1)$$

$$- 0.4\, W_o - 0.4\, \nu_2 \, a \cos(\omega t + \theta_2 + \phi_2 + \lambda) - 53.3 \qquad 5.11.2$$

and the signal at the outlet from the high pass filter is

$$C' = \nu_h \left\{ \left(\frac{\partial S}{\partial W}\right)_o \nu_1 \, a \cos(\omega t + \theta_1 + \phi_1 + \lambda_h) - 0.4\, \nu_2 \, a \cos(\omega t + \theta_2 + \phi_2 + \lambda + \lambda_h) \right\} \qquad 5.11.3.$$

The signal from the high pass filter is correlated with the phase shifted

input signal and is then integrated over one cycle i.e.

$$\int_{\frac{2\pi n}{\omega}}^{\frac{2\pi(n+1)}{\omega}} C' \cos(\omega t + \psi)\, dt = \nu_h \nu_1 a \frac{\pi}{\omega} \cos(\theta_1 + \phi_1 + \lambda_h - \psi) \left\{ \left(\frac{\partial S}{\partial W}\right)_o - 0.4 + 0.4 \left(1 - \frac{\nu_2 \cos(\theta_2 + \phi_2 + \lambda + \lambda_h - \psi)}{\nu_1 \cos(\theta_1 + \phi_1 + \lambda_h - \psi)} \right) \right\} \qquad 5.11.4.$$

The steady state slope of the objective function at a steam flow rate, W_o, is

$$\left(\frac{\partial S}{\partial W}\right)_o - 0.4$$

∴ the output from the integrator is seen to be proportional to the steady state slope, biassed by the factor

$$0.4 \left(1 - \frac{\nu_2 \cos(\theta_2 + \phi_2 + \lambda + \lambda_h - \psi)}{\nu_1 \cos(\theta_1 + \phi_1 + \lambda_h - \psi)} \right) \qquad 5.11.5.$$

5.11.5. has a finite value providing $\nu_1 \cos(\theta_1 + \phi_1 + \lambda_h - \psi)$ is non-zero and also

$$\nu_2 \cos(\theta_2 + \phi_2 + \lambda + \lambda_h - \psi) \neq \nu_1 \cos(\theta_1 + \phi_1 + \lambda_h - \psi) \qquad 5.11.6.$$

Under the operating conditions the various parameters in 5.11.5. had the following values:

$\nu_1 = 0.80$ (0.76) $\nu_2 = 0.87$ (0.84)

$\theta_1 = 1.92$ (2.13) $\theta_2 = 0.13$ (0.14)

$\phi_1 = 0.97$ (1.02) $\phi_2 = 0.73$ (0.81)

$\lambda = 2.25$ (2.20)

$\lambda_h = 2.15$ (2.18)

$\psi = 1.64$

In the above, all the angles are expressed in radians. The first number refers to

a period of 100 s/c and the number in brackets to a period of 90 s/c. The corresponding values for the bias in the slope are: - 0.001 and - 0.044 respectively.

The results show that the optimiser climbs to a position at which the slope is + 0.001 and + 0.044 at the two frequencies considered. Thus at a period of 100 s/c there is effectively no transfer at the maximum, but at 90 s/c the apparent optimum occurs at a steam flow rate of 27.5 l/hr. As the above was not considered until after the practical experiments had been completed, no compensation was allowed for this transfer at the maximum.

5.12. Conclusions

The experimental study has demonstrated the satisfactory performance of an on line perturbation optimiser. A number of practical points have resulted, in particular the need for careful phase matching of the components of the objective function. This can be a serious obstacle in applying the method to an industrial process, where the objective function may contain a large number of components, each with different dynamic characteristics. Unless the matching is good and an allowance is made for transfer at the maximum, it can easily happen that the optimiser will not find a turning point in the allowable region of operation, despite the existence of such an optimum position. Thus in practice one does need to know a fair amount about the properties of any but the simplest system, before the optimiser can be made to work satisfactorily.

Once the phase matching between the components of an objective function has been performed, the most important control parameters investigated were the gain and amplitude of the perturbation signal. For the case where it is desired to

minimize the percentage loss of the profit objective function over a period of 20 minutes, the optimum gain should be maximized subject to the system remaining stable. This boundary occurred when the gain had a value of 32 and it did not depend on the amplitude of the perturbation signal. The best combination was $\gamma_a = 143$ and $\frac{\gamma}{a} = 7.4$, which corresponded to a loss of 29.7%.

The digital simulation correctly predicted trends in the optimiser performance with respect to the optimiser parameters. However the numerical correspondence between the observed and predicted results was somewhat disappointing. The reason for this may well be the noise characteristics of the process, which were not simulated on the digital computer.

CHAPTER VI

6.1. Conclusions

6.1.1. Kinetic Models for the Water Gas Shift Reaction

It was found that for the fixed composition gas used in the optimisation runs, any of the three kinetic models considered - Mars', Moe's or Log - predicted adequately the conversion, Moe's model being marginally the most satisfactory. The relevant standard errors based on 90% conversion were $\pm$ 1.90%, $\pm$ 1.83% and $\pm$ 2.23%.

When the gas composition and reaction temperature were varied over a wide range of conditions using a factorial scheme, all the models predicted correctly the variation of conversion with temperature and the flows of carbon monoxide and hydrogen. Moe's model alone predicted correctly the influence of steam flow on conversion but none of the models could account for the variation of conversion with flow rate of carbon dioxide or the inert nitrogen. This meant that the standard errors obtained were much higher than for the case of fixed composition gas. The respective standard errors for the three models based as before on 90% conversion were: $\pm$ 11.5%, $\pm$ 9.9% and $\pm$ 14.7%. Thus in the absence of further information, it was concluded that Moe's model provides the most satisfactory description of the kinetics of water gas shift reaction. The importance of this part of the work lies mostly in the method of analysis and presentation of results, which has not been widely used.

If the inlet gas stream contains significant amounts of carbon dioxide or inert gases and if these are expected to change over a period of time, then Moe's model should be adapted. The action taken would depend on whether the kinetic model is to be used in optimisation of a plant or for design purposes.

In the former case the best procedure would be to take Moe's model or even the simpler Mars' model, and to update the rate constant, k(T), so as to obtain a local fit of the model to the observed results. This is satisfactory as the gas compositions would be unlikely to change appreciably between optimizing runs. If, however, the model is used for design purposes, then the model must account for all expected gas compositions and so the basic assumptions from which the model was derived should be reexamined. Another approach is to multiply the conversion predicted from Moe's model by an empirically determined factor which is a function of the individual gas flows and temperature. The form of this correction can be found by considering the possible reaction mechanisms in which the catalyst acts as the active medium i.e. using the Hougen-Watson approach (35).

The experimental results further showed that there is a close correlation between the estimates of the activation energy and the Arrhenius constant in the rate constant expressions of the type 3.~~1-3~~ 6.1. This arises because the operating temperatures are limited to lie within the range 350 - 460°C. Thus the percent variation of the reciprocal temperature is small and the data is effectively ill conditioned for the regression. This point is often overlooked by experimenters when results are quoted in literature. The presentation of results using the Log likelihood function method brings out such correlations very clearly.

The reactor used was made of copper and this metal is known to catalyze the shift reaction to a certain extent which of course is all to the good in industrial reactors. This, however, should not alter the conclusions concerning the reaction kinetics. The magnitude of the Arrhenius constant would be

changed if the reactor were made of a non-catalyzing material, e.g. silica, but in any case this constant must be fitted empirically, as must also the activation energy, which for the shift reaction has no real significance without the relevant Arrhenius constant.

The catalyst used was the ICI high temperature catalyst. By now low temperature catalysts, operating at temperatures 100 - 150°C lower than the other, have been developed and are starting to be used in industry. This results in large saving of heat and thereby production costs. It is difficult to predict which kinetic models will apply for this type of catalyst, as the mechanism of the catalysis may well be substantially different from the high temperature case. However, what chapter 3 has shown is a method to use in order to test the suitability of different kinetic models which describe the shift reaction performed over a given catalyst.

6.2.2. The On-Line Optimisation

The experimental results for the on-line optimisation demonstrated the feasibility of using the perturbation method in practical cases. So far very little practical work has been done on perturbation systems although a lot of computer simulation results are quoted in literature. The practical results show that the system takes about 17 times its time constant to reach the maximum, which at the frequencies used, corresponds to six or seven cycles. The time constant here is defined as the sum of the dead time and capacitance lags. The above result is much less than the results from computer simulations quoted in literature (34). The optimiser performance in the face of controlled noise input into the system has not been investigated.

The applicability of the optimisation scheme lies in an intermediate region between the case of very slow disturbances relative to the time constant of the process, where the steady state experimentation of Evolutionary Operation can be used, and the case where the noise is high frequency and thus the system is always in a dynamic state. In the latter case the slope estimated from the perturbation has no practical meaning and thus the method breaks down. The limits of the region depend on the dynamic characteristics of the system. The main use of the adaptive scheme is in fact in cases where no model of the process is available mostly due to the lack of suitable instrumentation on the given plant and the prohibitive costs of installing it or else because the parameters of the model are unknown. In such cases, when the optimum conditions are changing slowly due to causes like catalyst decay, metal corrosion, feed stratification, there is no constant set point available for conventional control. Thus the adaptive scheme is very suitable, because in the simplest case it needs only one adjustable independent input variable and the resulting objective function measurement, in order to control the plant in some optimum fashion. If several measurable and adjustable variables are available, then the two or three variables which have the greatest influence on the objective function should be used in order to compensate for the changes in the process whose effect only can be measured. The perturbation technique can also be used in conjunction with feed forward optimisation schemes in order to compensate for the effects which have not been included in the process model. A fact to note is that continuous or at any rate frequent measurements of product quality are essential for the success of the optimisation.

Several practical points have come out of the experiments. Firstly

it is fairly hard to match exactly in time two separate signals measured at different points in the process, because the flow rates of fluids in the process change the phase relationships. This matching, however, is essential otherwise it can happen, that no optimum is obtained. Where a profit function on a typical industrial plant consists of several measurements, their phase matching will require some careful calibration i.e. one should allow for the variation of the time of passage with flow rates.

Connected with the above is the possibility that the estimate of the slope is not zero at the true maximum of the objective function, due to the special form of the transfer function of the system. In this case if prior knowledge is available, the slope estimate can be compensated by a biassing factor, so that the system does tend to a maximum value and once reached, stops there. This biassing factor could well be an updatable quantity.

In the analogue computer circuit a diode limiter has been incorporated. This was found to be very useful in order to keep the system stable when using high gains. In these circumstances the correction steps tended to be large and created instability due to the large dynamic effects. The diode limiters kept the size of steps within limits so that instability was prevented. In some cases, however, as the diode bias was always kept at the same constant level, the limits were still too wide and the system became unstable. The influence of the variation of the size of the limits on stability is something which might well be further investigated.

6.1.3. The Off-Line Simulation of the Process

The simulation of the process in order to predict regions for best experimental investigation proved fairly successful. The predicted and

experimentally obtained values differed a little, but this was very likely due to the unsatisfactory performance of the steam measuring instrument. The signal corresponding to the total flow of dry gas and steam had to be calibrated with nitrogen and the result extrapolated, which from the analysis of the practical results does not seem to have been a very satisfactory procedure. Further the condensation of steam to different levels in the limbs of the tubes connecting the orifice tappings to the pressure chambers of the transducer, introduced systematic errors and altered the transducer calibration. This purely practical point apart, the simulation predicted the correct trends.

The method used to simulate dynamics by superposition onto the steady state model, can have very wide applications especially in industrially used models for feed forward control. The complexity of the dynamics can be adjusted at will starting initially with a one stage exponential system and no delay and increasing the complexity when and if required. The use of non-linear least squares method of data fitting is again very useful.

A point found concerning the above procedure, which was not considered by Box and Jenkins, is that in the forcing function it is much better to take thedifferences between actually predicted steady state values of the objective function at time $(p - j)$ and $(p - j - 1)$, rather than multiply the steady state gain by the change in the independent variable over the corresponding time interval. In cases when the steady state model is not available, then of course a constant gain is best used. Another point is that the optimum dynamic parameters change with the position of operation, this being particularly true of delays. Thus in an ideal case the variation of these parameters with the settings of the variables should be simulated. This has not been done,

but is expected not to be particularly difficult to achieve on a digital computer.

Thus in conclusion the work has demonstrated experimentally the feasibility of using a perturbation method to optimize the performance of a water gas shift reactor. The use of a computer simulation to predict good investigation regions for the optimiser parameters was also shown to be satisfactory and useful. The method used in fact amounted to the flow of information between an on-line and off-line computer in order to investigate optimiser performance in the most efficient manner.

6.2. Suggestions for Further Work

The experiments performed investigated the variation of a single objective function with gain and amplitude of the perturbation signal at constant values of the other optimiser parameters. The point of interest was the shape of the contours obtained, because the actual values of the objective function will differ considerably from plant to plant. The effects of frequency of the perturbation signal, the phase shift angle, as well as the high pass filter constant, should similarly be investigated, the region of interest around the optimum settings being first found from the off-line digital computer simulation of the process. The point of interest again will not be so much the actual optimal values of the settings but the shape of the contours i.e. whether one has to be very careful about fixing the settings. The next stage would be to investigate the problems connected with optimisation in two perturbed variables, which in the case of the project would best be the steam flow rate and the reactor temperature. Here the problem is to find the best ratios of frequencies

to use and to carry out the perturbation in terms of canonical variables rather than the process ones. It is also interesting that the form of the objective function used in the one variable study, has an optimum with respect to temperature, which is at around 380°C. At this stage the optimiser optimisation becomes a problem in ten variables. The process can still be simulated by a mathematical model using the same procedure as before but the change in objective function will now consist of two sets of expressions each containing different dynamic constants. The total change is the sum of the two.

After the two variable investigations the system can be adapted so that controlled noise can be fed into one or more of the inlet gas flows e.g. hydrogen or nitrogen and the variation of the best optimiser settings investigated with different forms of the noise. In particular the quantity of interest would be the ratio of the frequency of noise input, to the perturbation frequency if the noise took a form of step or ramp functions.

A further extension of the work would be to investigate the practical difficulties connected with having feed forward optimisation as well as the feed back adaptive scheme. For this purpose a small digital computer - e.g. one containing 4096 words - could be linked up with the analogue computer. This would also provide experience concerning the use of hybrid computers where the digital part performs some of the arithmetical calculations as well as the logic. The expected difficulty there would involve the flow of information between the digital and analogue computers.

Finally, operation in more than two variables could be investigated, in particular from the point of view of improvement in the optimisation, compared with the one and two variable cases. Here also a complex objective function involving dynamic relationships between several constituents could be investigated as a step before trying out the method on a full scale industrial plant.

BIBLIOGRAPHY

1) Box G.E.P. and Wilson K.B. On the experimental attainment of optimum conditions. J.R. Stat. Soc. B. 13 (1951) 1

2) Box G.E.P. and Hunter J.S. The 2^{k-p} fractional factorial designs. Technometrics 3 (1961) 311 and 449

3) Arnold D.S., Box G.E.P., Erikson E.E., Hunter J.S., Nelli J.R., Pike F.P. The application of statistical procedures to the flooding capacity of a pulse column. North Carolina State College Dept. of Chem. Eng. Progress report 3 under contract AT (40-1) - 1320

4) Box G.E.P. The exploration and exploitation of response surfaces; some general considerations and examples. Biometrics 10 (1954) 16

5) Box G.E.P. and Youle P.V. The exploration and exploitation of response surfaces; an example of the link between the fitted surface and the basic mechanism of the system. Biometrics 11 (1955) 287

6) Hunter J.S. Some applications of statistics to experimentation. C. E. P. Symposium Series 31, 56 (1960) 10

7) Koehler T. Evolutionary operation, some actual examples. Proc. 2nd Stevens Symposium on Statistical Methods. New York (1958)

8) Box G.E.P. Evolutionary operation: A method for increasing industrial productivity. J. Applied Statistics 6 (1957) 3

9) Box G.E.P and Hunter J.S. Condensed calculations for Evolutionary operation programs. Technometrics 1 (1959) 77

10) White B. The Quarie optimal controller. Instruments and Automation 29 (1956) 2212

11) Draper C.S. and Li Y.T. Principles of optimalising control systems. A.S.M.E. special publication series. Sept. 1951

12) Box G.E.P. and Chanmugan J. Adaptive optimisation of continuous processes. Ind. Eng. Chem. Fundamentals 1 (1962) 2

13) Jenkins G.M. Adaptive optimisation of chemical reactors using sine wave probes. Paper read to Inst. of Chem. Engrs. Loughborough Feb. 1964

14) Kuehn D.R. and Davison H. Computer control - mathematics of control C. E. P. 57 (1961) 44

15) Eckman D.P. and Lefkowitz I. Application and analysis of a computer control system. J. Basic Eng. 81 (1959) 569

16) Williams T.J. Progress in chemical process control in America: Computers instrumentation and applications. Trans. Inst. Chem. Eng. 41 (1963) 326

17) Stelling O. and Krusenstierna Evaluating kinetic data for technical purposes. Acta Chemica Scandinavica 12 (1958) 502

18) Hulburt H.M. and Srinivasan C.D. Design of experiments on the kinetics of the water gas shift reaction. A.I. Ch. E. J. 7 (1961) 143

19) Bohlbro H. Kinetics of the water gas shift conversion of atmospheric pressure. Acta Chemica Scandinavica 15 (1961) 502

20) Hoogschagen J. Diffusion in porous catalysts and adsorbents. Ind. Eng. Chem. 47 (1955) 906

21) Mars P. Factors governing the behaviour of the adiabatic water gas shift reactor. Chem. Eng. Sci. 14 (1961) 375

22) Moe J.M. Design of water gas shift reactors. C.E.P. 58 (1962) 33

23) Bartholome E. and Krabetz B. Zur numerischen Berechnung von Optimaltemperaturen. Zeitschrift fuer Electrochemie 65 (1961) 223

24) Rietema K. The role of chemical reaction engineering in process research and scaling up. Chem. Eng. Sci. 14 (1961) 3

25) Glasstone S. Thermodynamics for chemists. Van Nostrand Co. Inc. New York 1956

26) Box G.E.P. Fitting of empirical data. University of Wisconsin M.R.C. Technical Summary Report. No 151. May 1960

27) Kenney J.F. and Keeping E.S. Mathematics for statistics Part 2 2nd Ed. Van Nostrand 1951

28) Paratella A. and Sorgato I. Fluodynamische Erscheinungen bei der katalytischen CO Konvertierung. Third European Symposium on "Chemical Reaction Engineering." Sept. 1964

29) Goursat E. Differential equations Vol. 2 Part 2 Ginn and Co. Translated by Hedrick and Dunkel p. 216

30) Rogers A.E. and Conolly T.W. Analog computation in engineering design McGraw Hill 1st Ed. 1960

31) Box G.E.P. and Jenkins G.M. Further contributions to adaptive quality control. Statistics in Physical Sciences 1 (1964) 943

32) Davies O.L. Design and analysis of industrial experiments 1st Ed. Oliver and Boyd. London 1954

33) Hunter W. G. and Mezaki R. A model building technique for chemical engineering kinetics. A.I.Ch.E.J. 10 (1964) 315

34) Hammond P. H. and Duckenfield H.J. Automatic optimisation by continuous perturbation of parameters. Automatica 1 (1963) 147

35) Hougen O. A. and Watson K. M. Chemical process principles Part III J. Wiley and Sons New York 1950